BOTSWANA UNIVERSITY OF AGRICULTURE & NATURAL RESOURCES

Integrating GIS and remote sensing in estimation of soil loss using the SLEMSA and RUSLE models: **A case study of Taung Watershed, Ramotswa Agricultural District**

A dissertation submitted to the Department of Agricultural & Biosystems Engineering in partial fulfillment of the requirement for the degree of Master of Science (MSc) in

Agricultural Engineering (Land Use Planning) stream

By

Motshereganyi Sylvester Moesi

(ID: 201300155)

July 2021

Main Supervisor: Prof. R. Tsheko

Co - Supervisors:

Prof. B. Kayombo

Mr. E. Setlhabi

CERTIFICATION

Main Supervisor's Name and Signature Date

Co-Supervisor's Name and Signature Date

Co-Supervisor's Name and Signature Date

Head of Department's Name and Signature Date

APPROVAL

Main Supervisor's Name and Signature	Date
Co-Supervisor's Name and Signature	Date
Co-Supervisor's Name and Signature	Date
Head of Department's Name and Signature	Date
Dean of Faculty's Name and Signature	Date

STATEMENT OF ORIGINALITY

The work contained in this dissertation was compiled by the author at the Botswana University of Agriculture & Natural Resources between January 2019 and August 2021. It is original except where the references are made and it will not be submitted for the award of any other degree or diploma of any other University.

Author's Name and signature Date

ACKNOWLEDGEMENTS

I will start with my main supervisor and co-supervisors Prof R. Tsheko, Prof B. Kayombo and Mr. E. Setlhabi. Thank you very much for your unreserved support, help, advice, guidance, comments and dedication from beginning to end and also for the critical review of the MSc draft report. I highly acknowledge your efforts. I would like to thank my best friend, Amogelang Kalaemang for her motivation.

I would like to acknowledge my scholarship sponsors (Barclays Mogae) for allowing me to pursue my studies at the Botswana University of Agriculture and Natural Resources (BUAN). I could also not forget the Ministry of Agricultural Development and Food Security for providing digital soil data and the Department of Meteorological Services (DMS) for providing climatic data of the study area.

My thanks also go to Prof C. Patrick for his coordination of the MSc Program. I highly acknowledge Prof F. Meulenberg, Mr. G.Yuyi, Mr. I. Makoyi, Mr. B. Jibichibi and my colleague Mr. O. Maiketso for their technical and scientific help and support and other Department of Agricultural & Biosystems Engineering (ABE) staff with your advice. I would like to thank my family members and friends for supporting and encouraging me to complete this work.

Above all, I would like to thank the Almighty GOD for everything.

DEDICATION

This study is dedicated to my son, Kenzo.

ABSTRACT

This study was conducted in the Taung watershed of the Ramotswa Agricultural District in the south eastern part of Botswana. The main objective of this study was to assess the soil erosion risk using Revised Universal Soil Loss Equation (RUSLE) and Soil Loss Estimation Model for Southern Africa (SLEMSA) integrated with Remote Sensing (RS) and Geographical Information System (GIS). The rate of soil loss was determined using rainfall, topography, soil and land use/land cover (LULC) data within the RUSLE and SLEMSA framework. The estimated mean annual soil loss averaged 12.04 t/ha/year in 2000 and 12.74 t/ha/year in 2020 for the RUSLE model. The SLEMSA model estimated the mean annual soil loss of 11.77 t/ha/year in 2000 and 12.57 t/ha/year in 2020. It is evident that soil erosion increased over the years (2000-2020). The predicted soil loss using the two models for Taung watershed was slightly above the recommended limits of 11 ton/ha/year. The results indicate that up to 30.5% of the watershed experiences high soil loss above 12 tons/ha/year when using the RUSLE model and about 43.5% for SLEMSA. It is recommended that conservation efforts should focus on areas with high soil loss as indicated by both models as they form a reasonably large proportion of the study area (covering 23% in RUSLE and 33% in SLEMSA). Furthermore, the findings from this study may be useful to guide the development of a functional soil conservation planning and watershed management plan for the Taung watershed.

Key words: Taung watershed; Soil erosion; RUSLE; SLEMSA; RS; GIS

Table of Contents

LIST OF FIGURES

LIST OF TABLES

LIST OF ACRONYMS AND ABBREVATIONS

ARAP	Accelerated Rainfed Arable Programme
DEM	Digital Elevation Model
DMS	Department of Meteorological Services
IDW	Inverse Distance Weight
FAO	Food and Agricultural Organisation
GCP	Ground Control Points
GIS	Geographic Information System
LULC	Land Use and Land Cover
NADP	National Agricultural Development Policy
NDP	National Development Plan
OM	Organic Matter Content in (%)
RS	Remote Sensing
RUSLE	Revised Universal Soil Loss Equation
SLEMSA	Soil Loss Estimation Model for Southern Africa
SRTM	Shuttle Radar Topographic Mission
TLGP	Tribal Grazing Lands Policy
USGS	United States Geological Survey
USLE	Universal Soil Loss Equation
UTM	Universal Transverse Mercator
WGS 84	World Geodatic System 1984

1.0 INTRODUCTION

1.1 Background

Soil erosion is a serious environmental hazard throughout the world that threatens food production through its negative impact on soil fertility (Rahman et al., 2009). The existing body of research on land degradation indicates that land degradation particularly soil erosion negatively impacts affected communities leading to poverty, hunger, and migration of population (Sefe et al., 1996). Soil erosion is a slow process that takes place unnoticed or can occur at alarming rates. Soil erosion can be accelerated by anthropogenic activities such as excessive cutting of trees without replacing them, overgrazing (Snyman, 1999) and also tillage operations (Department of Primary Industries, 2014). According to Pimentel and Burgess (2013), about 10 million hectares of arable land in the world is lost due to soil erosion hence reducing the arable land that is available for world food production. About 16% of the land in Africa is degraded and soil erosion is of great concern in Sub- Saharan African countries (Bai et al., 2008). Moreover, soil erosion is going to be severe in Southern African due to the change in climate and increase in population figures (Feda, 2018; Phindzi, 2018)

To select suitable conservation actions, the identification and quantification of soil loss sources are necessary (Feda, 2018). However, Popp et al. (2000) reported that erosion modelling techniques can be used to predict and assess soil erosion. Modeling soil loss provides vital information to help select suitable soil conservation practices. Generally, soil erosion can be assessed using different soil erosion models and the models vary in their degree of complexity (Ganasri and Ramesh, 2016). Soil erosion models such as empirical models have proved to be the best cheaper way of assessing the distribution and magnitude of erosion in watershed areas in Southern Africa (Smith, 1999). The most widely applied empirical soil loss models are the Universal Soil Loss Equation (USLE), and Revised Universal Soil Loss Equation (RUSLE) and Soil Loss Estimation Model for Southern Africa (SLEMSA) (Mhangara et al., 2012; Feda, 2018; Bvindi, 2019; Kidane et al., 2019; Moisa et al., 2020).

Over the years, researchers have shown an increased interest in combining RS-GIS and soil loss models to determine the erosion potential in different cell sizes (Jain et al., 2005). It has several

advantages in terms of identifying areas that are highly susceptible to physical degradation, quantifying rates of soil loss, and mapping erosion prone areas (Chen et al., 2010). Moreover, the combination can be used as a guideline to come up with a plan on soil and water conservation (Feda, 2018). Extensive research has been done from using the empirical models together with RS-GIS (Mhangara et al., 2012; Feda, 2018; Bvindi, 2019). The combination of the model and RS-GIS consider rainfall, soil properties, cover and management, topography and conservation practice as factors that influence soil loss (Fenta et al., 2020).

There have been a few empirical investigations into soil erosion assessment. Akinyemi and Mashame (2017) carried out a research study using RUSLE to assess soil erosion in the Lotsane catchment in the North-Eastern part of Botswana using GIS software. Alemaw et al., (2013) also conducted a study on the sediment yield and their impact on small dams located at Lotsane catchment. The authors also integrated RUSLE with GIS and were able to estimate soil loss from 0.54 to 85.29 tonnes/ha/year in the area. Very little is currently known about the assessment and mapping of high erosion areas in the South-east of Botswana. The livelihood of the people in the Ramotswa Agricultural District of South East Botswana relies on crop and animal production (Darkoh, 1999). The most commonly planted crops in the study area are sorghum, beans, and maize. Soil erosion and decline in the fertility of the soil yearly are accelerated by anthropogenic activities. Soil erosion is an environmental problem that varies spatially on a landscape, thus reducing agricultural productivity, soil fertility, and aggravating poverty. It is vital to have information on the distribution patterns of soil loss as it can be used for soil conservation planning (Feda, 2018). The current study was aimed to assess the soil erosion risk in the Taung Watershed of Ramotswa Agricultural District.

1.2 Statement of the problem

Several attempts have been made to address the issue of land degradation by the use of national action programme/policies such as Tribal Grazing Lands Policy (TLGP) (Government of Botswana, 1975), National Agricultural Development Policy (NADP) (Government of Botswana, 1991), National Development Plan (NDP) 11 (National Development Plan 11, 2016) and also international frameworks such as UNCCD (United Nations Convention to Combat Desertification) (UN, 2007; MOA, 2018). However, neither of those attempts has not yet

determined soil loss estimates on a watershed scale and also spatially identify hotspots of areas that are more vulnerable to soil loss.

Foster (2006) reported that Kweneng, Kgatleng, and Southern District in Botswana are marked as highly degraded areas due to an increase in population, deforestation and overgrazing. The Ministry of Agricultural Development and Food Security (2019) also reported that there is currently no data available on degraded agricultural land and also on agricultural land under restoration. Moreover, the SWOT analysis for Ministry indicates that there is a lack of capacity in research and development for soil erosion and therefore this research will try to address that issue in a way.

Information on soil erosion assessment using models in South East Botswana is scanty. Abel and Stocking (1987) estimated soil loss (using SLEMSA) for two rangelands in South East Botswana to be 1 to 12 tonnes/ha/year. The proposed study area is known for its rugged topographic features, deforestation, and overgrazed land (Foster, 2006). There is evidence of soil erosion for some areas found in and around the Taung Watershed (Huesken et al., 1989). However, the spatial variability of the vulnerability of soils to erosion has not been assessed and mapped in the study area.

Therefore, the current study was aimed at assessing soil erosion severity using RUSLE and SLEMSA integrated with RS and GIS useful for soil conservation planning.

1.3 OBJECTIVES

1.3.1 General objective

The main objective of the proposed study was to assess the soil erosion risk of Taung Watershed in Ramotswa Agricultural District by using RUSLE and SLEMSA integrated with RS-GIS. The main objective was met by the following specific objectives:

1.3.2 Specific objectives

The specific objectives of this study were:

- To map spatial variability of erosion and identify high-risk areas for conservation planning using SLMESA and RUSLE models;
- To account for soil loss resulting from due to Land use/ Land cover change over a 20 year (2000-2020) period in the Taung watershed; and
- To validate the findings from the two models through field observations

1.4 Significance of study

Understanding the rates of soil loss and identifying the primary regulating elements that increase or retard these processes are both necessary for reducing the on- and off-site effects of soil erosion. This study seeks to identify areas that are more susceptible to erosion and provide useful information to land-use planners, policymakers, and decision-makers for soil conservation planning within the Taung watershed. One of the priority areas under Sustainable Development Goals in Botswana is Sustainable Land Management focusing on the degraded agricultural production land with the objective of arresting land degradation. According to MOA (2019), there is no data on the percentage of agricultural land degraded in Botswana. Therefore, the findings of this study could be used to provide information on agricultural degraded land, policy formulation and also be useful for projects related to the watershed's Soil Protection Strategy. Furthermore, this work could be useful in providing a baseline for further research by identifying topics that should be dealt with in much more detail in the study area

1.5 Scope of the study

The present study was limited to RUSLE and SLEMSA models integrated with Geographical Information Systems (GIS) and Remote Sensing (RS) in relation to soil erosion assessment. This study was based on quantifying soil loss occurring in the Taung Watershed. A field validation or ground truthing was done to assess the accuracy of the identified areas vulnerable to soil erosion.

2.0 LITERATURE REVIEW

2.1 Soil erosion, and its forms

According to Humberto and Rattan (2010), the soil is a fundamental resource that serves many functions such as producing fuel, fiber, and food for the world. Nevertheless, most topsoil is the one that is responsible for production because it contains valuable nutrients, plant humus, and microbial activity. Soil erosion affects the capacity of the water reservoirs and pollutes water bodies and diminish resulting in the reduction in the quality of the water (Toy et al., 2002).

Soil erosion harms the environment which ends up affecting the world (Pimentel, 2006). It involves the process of carrying soil particles from one place of origin to another and it is caused by water, wind, tillage, waves and glacier ice (Morgan, 2005; FAO, 2015). Erosion has three distinct phases namely detachment, transport and deposition that take place during the process as shown in Figure 1. The detachment process is a result of the breaking down of soil aggregates by kinetic energy from raindrop impact (Feda, 2018) and it is frequently escalated by human activities and animals (Mhangara et al., 2012). Transport is when the topsoil is relocated to another area by flowing water and wind (Morgan, 2005). Lastly, deposition occurs when the speed of water or wind is reduced by the effect of topography or vegetative cover on the as it is being exceeded by the sediment load (Lal, 2001).

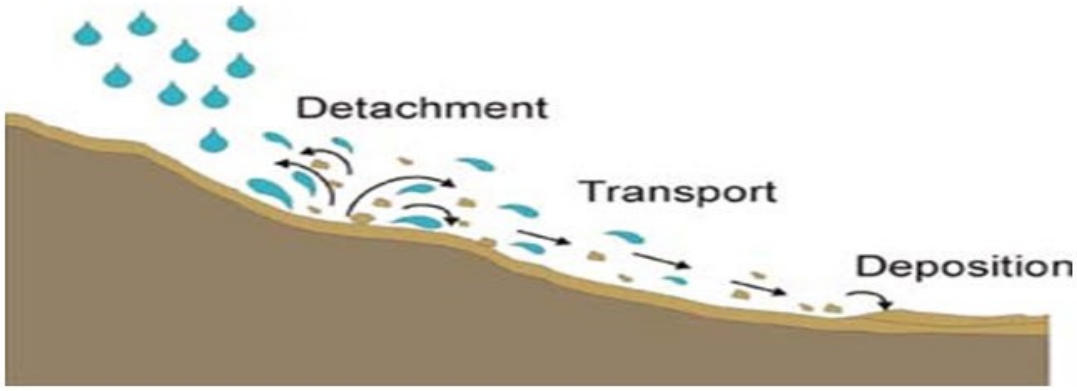

Figure 1: Water erosion process by the impact of raindrops *Source: (www.landfood.ubc.ca)* retrieved on 12/11/2020

2.2 Types of soil erosion

Only two major types of soil erosion (geological and accelerated), have been recognized by

several authors (Tesfamichael, 2004; Humberto and Rattan, 2010; Feda, 2018). Geological erosion is a normal process of weathering that occurs naturally at a tolerable rate because the process is very slow and is not influenced by any anthropogenic activities. According to Troeh et al. (1980), the average annual soil particles lost by geologic erosion is approximately less than 1 metric ton ha^{-1} year- ^{1}. However, high erosion rates may likely occur due to natural events such as veld fire, huge rainstorms, plant disease, or a flock of wildlife that affect both the soil and vegetative cover (Toy et al.,2002). On the other hand, when soil loss exceeds the soil formation rate (Thornes, 1985) and becomes fast, it is called accelerated erosion. This process is a result of human activities in search of desirable life or survival (Hudson, 1995), which end up exposing soils, disturbing vegetative cover, and also increasing slope steepness (Toy et al.,2002). Moreover, it is caused by tillage, deforestation, urbanization, intensive plowing and overgrazing and biomass burning (Humberto and Rattan, 2010).

Soil erosion risk varies from watershed to watershed depending on the configuration of the watershed topography, soil characteristics, local climate, and therefore land use and management practices implemented (Alkharabsheh et al.,2013; Le Roux and Sumner, 2013). Soil lost by water is considered a severe form of land degradation that negatively affects the environment and socio-economic (Phinzi and Ngetar, 2019). There are four forms in which removal of topsoil takes place in water erosion. These include rain splash, sheet, rill, and gully, (Le Roux and Sumner, 2013). Figure 2 shows various forms of soil erosion.

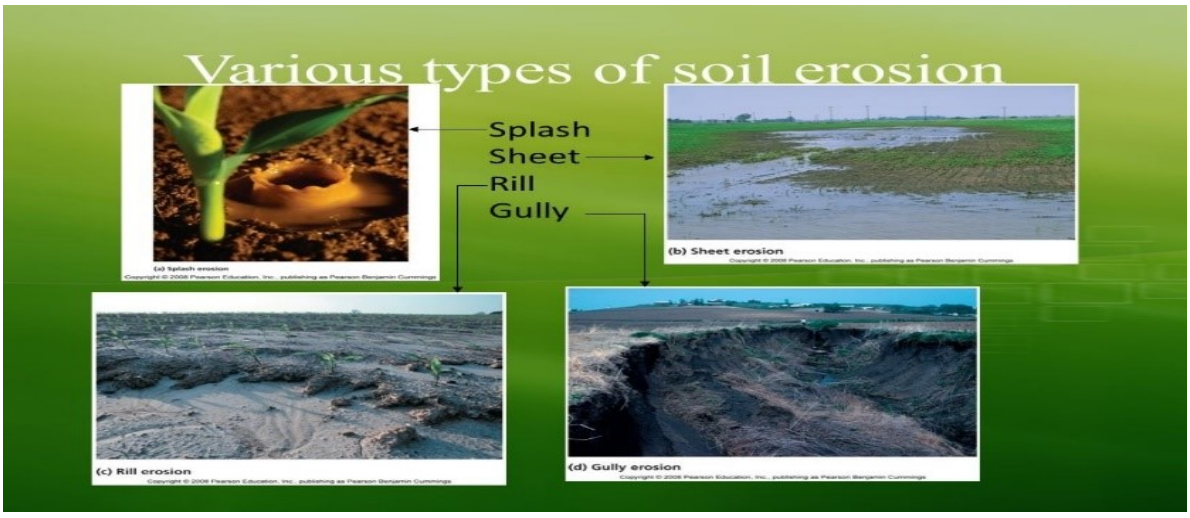

Figure 2: Various forms of soil erosion (Adopted from http://www.quora.com/What -are-various-types-of-soil-erosion) retrieved on 12/11/2020

2.3 Factors affecting soil erosion by water

Soil erosion is mainly influenced by the following main environmental factors such as Climate, topography, soils, vegetation characteristics and land cover (LULC) (Toy et al., 2002; Fangmeier et al., 2006). The following section examines the factors associated with soil erosion.

2.3.1 Climatic factors

They are several factors that affect soil erosion and these include rainfall, temperature, wind, humidity, and solar radiation (Feda, 2018). Soil erosion by water results from falling raindrops and runoff. The main purpose of the falling raindrops is to break down soil particles and spread them, whereas surface runoff transport soil from the source (Telkar, 2018). Normally, the surface flow occurs when the infiltration rate is exceeded by the precipitation hence runoff is generated (Toy et al., 2002). The ability of rain to cause erosion is known as erosivity (R) (Wischmeir and Smith, 1978; Renard et al., 1994). As noted by Angulo-Martínez and Beguería (2009), the R factor is a function of rainfall amount and intensity, and therefore it should be used to estimate soil erosion. The amount, intensity, and frequency of rainfall are the most predominant climatic factors that influence soil loss by water (Lal, 2001). The higher the rainfall intensity, frequency and period of a rainstorm, the more the erosion potential (Foster et al., 2003). This view is supported by Goldman et al. (1986), who assert that extreme rainfall over a short duration is more erosive as compared to high rainfall amounts over a long time with low intensity.

2.3.2 Soil Properties

The chemical properties (Fangmeier et al., 2006) and physical properties of soil affect the runoff, infiltration capacity, and extent to which soil particles are separated and carried from the source area (Thomas et al., 2018). The intrinsic vulnerability of soils to erosion by raindrops and runoff is referred to as soil erodibility (K) (Thomas et al., 2018). It is derived from the particle size distribution, organic matter, soil structure, and permeability (Wischmeier and Smith, 1978; Phinzi, 2018).

Generally, coarse-textured soils such as sands have lower K values and are resistant to erosion because of the force required to displace them, although they are easily detachable (Pimmentel, 2006). Fewer sediments are usually produced from these soils because of reduced runoff from

higher infiltration (Toy et al., 2002). Fine-textured soils such as clays are also erosion-resistant due to their difficulty to break them down. Clays soils are more easily transported when detached (Lal and Elliot, 1994). These soils have also low K values (Wordofa, 2011). Medium textured soils, which are high in silts, are easily detached and transported thus making them the most erodible soils with a high K value because of lower infiltration rate capacity (Fangmeier et al., 2006; Saavedra, 2005).

Soil aggregate stability and infiltration rates may be influenced by different soil parameters: aggregate size and bulk density, soil texture, and soil structure (Mainam, 1999). The soils with high quality of aggregate stability of soils increase the resistance to mechanical, physical, or chemical destructive forces. Organic matter is one of the soil properties that have a very positive impact on the soil quality and structure because of the ability to bind soil particles and creating forces between particles (Brady and Weil, 2008). Previous research has established that soils vary in soil erodibility. Soil erodibility tends to intensify during the late winter and early spring months than in the late summer months (Toy et al., 2002). Moreover, more erosion in the summer months is caused by raised soil moisture that accelerates the runoff and peak rate per unit of rainfall in addition to low temperatures.

2.3.3 Topography

Topography means the geometry of the land surface (Toy et al., 2002). The components of topography important for soil erosion to occur include the slope length (L) and slope steepness (S), which have a huge impact on the susceptibility of soil loss on a given site (Agele et al., 2013; Naqvi et al., 2013) and are normally denoted as LS factor in the RUSLE and SLEMSA models (Telkar, 2018: Bvindi, 2019). These two factors combine to represent the rill and interill erosion of a location. There are three types of slope shapes, namely uniform, convex, and concave (Toy et al., 2002) as illustrated in Figure 3. Convex shapes cause more erosion than the concave ones, due to the accelerated runoff in the convex shape than in the concave one (Toy et al., 2002).

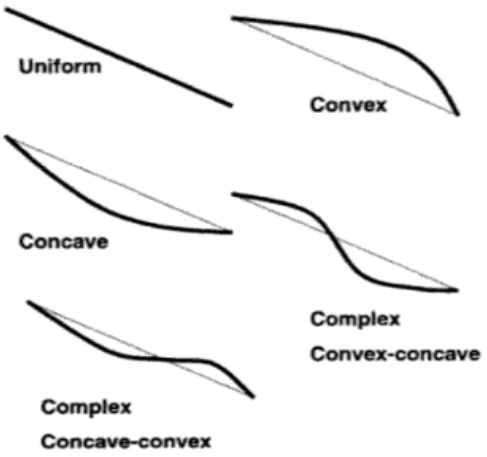

Figure 3: Common slope shapes (Adopted from Toy et al., 2002)

Naturally, areas with steep slopes experience more soil loss as compared to flat or gently sloping areas. Besides, soil erosion rise with increasing slope length due to significant accumulation of runoff at high velocities and vice versa **(**Doere, 2005). Slope steepness has a great effect than slope length on soil loss (Mhangara et al., 2012). According to Renard et al. (2011), slope steepness is very sensitive to soil loss and a minor error could result in the wrong estimation of the overall soil loss.

The Digital Elevation Model (DEM) is usually used as an input parameter and incorporated into a GIS so that the LS factor can be determined accurately across the landscape in the RUSLE and SLEMSA models (Mhangara et al., 2012; Bvindi, 2018). The precision with which LS factors can be estimated depends on the resolution of the DEM. The DEM with high resolution tends to have much better results as compared to the one with lower resolution. A large and growing body of literature has compared Shuttle Radar Topography Mission (SRTM) and Advanced Spaceborne Thermal Emission and Reflection (ASTER) DEM'S with the same resolution of 30m. De vente et al., (2009) reported that results obtained from the SRTM DEM surpassed those of the ASTER DEM. Renard et al. (2011), however, reported that both SRTM DEM and ASTER DEM datasets lack the spatial resolution capable of picking up the little concentrated flow channels usually found at the base of RUSLE hillslope on which a significant deposition may occur. There are other different satellites such as SPOT, GeoEye, QuickBird, IKONOS, and IRS where good quality DEMs with much higher spatial resolution can be obtained (Lillesand et al., 2004). Nevertheless,

due to the high costs associated with acquiring these DEM's, the use of SRTM and ASTER DEM's has been explored by many researchers (Alkharabsheh et al., 2013; Bakkelund et al., 2018; Feda, 2018; Pham et al., 2018;).

2.3.4 Ground cover/Crop cover

Vegetation cover protects the soil from raindrops impact and reduces surface runoff (Toy et al., 2002). It does that by raising the level of infiltration of water into the soil and lowering the speed of the surface runoff (De Asis and Omasa, 2007). According to Knijff et al. (2000), vegetation cover is an important factor that controls soil erosion risks. Crop residues have a significant effect on reducing soil loss (Stocking, 1994; Fangmeier et al., 2006). Crop cover improves the yield, which in turn is likely to benefit economically (Stocking, 1994). The C- factor refers to the ratio of soil loss from land cropped under specified conditions to the corresponding clean-tilled continuous fallow (Wischmeier and Smith, 1978). Also, the C value ranges from 0 to 1 and a value of 1 represents the absence of cover whereas 0 indicates a strong cover on the ground (Arhem and Freden, 2014; Pham et al., 2018;).

A considerable amount of resources and time was needed some years ago to derive this C factor. Initially, this parameter was derived from a combination of several variables such as canopy cover, the ground cover, the soil surface roughness, the ridge height, the daily biomass, the soil consolidation, and the antecedent soil moisture (Jones et al., 1996). With time, researchers developed new scientific ways of deriving the factor with ease. Satellite images have proved to be the best cheaper way of obtaining the C factor. The Land use/Land cover (LULC) map has been used by a wide range of scientists to derive the C factor (Feda, 2018; Tesfaye, 2018). The C factor estimation can be done by using satellite imagery (Mhangara et al., 2012). Thus far, several studies have indicated that some remote sensing techniques are used to derive the C factor. Examples are found in the LULC classification (Reusing et al., 2000). Normally, the C values are given by different researchers for different land use classes (Ganasri and Ramesh, 2016; Tesfaye et al., 2018). Under LULC, there are two main methods of image classification: supervised and unsupervised classification (Lillesand and Keifer, 1994). Tesfate et al. (2018) performed a supervised classification on the Landsat image and generated a LULC map for Somodo watershed in the south west of Ethiopia to which corresponding C factor values were assigned. Tesfamichael

(2004) also mapped the C-factor values of Weenen Game Reserve, South Africa from the Landsat ETM+ using the same classification. So, it is imperative to accurately classify the remotely sensed image and also select the satisfactory ground cover factor values for each cover class (Panagos et al., 2015).

The other alternative of deriving the C factor through the image is by using the vegetation indices such as the Normalized Difference Vegetation Index (NDVI) (Arhem and Freden, 2014; Ngetar,2017). The application of NDVI has been explored several times by different researchers. It has proved to be useful and successful in providing an estimate of C, thus making it reliable for soil erosion risk assessment (Mhangara et al., 2012; Alkharabsheh et al.,2013). It is calculated from the red (R) and infrared (NIR) wavelengths only (Seboka, 2016) and it is expressed as $NDVI = (NIR - RED)/(NIR + RED)$ Arhem and Freden, 2014). In contrast, some researchers have reported a low correlation between NDVI and C factors in some regions (Smith et al., 2007). This may be due to the reason that the technique does not take into account the climatic conditions when computing C factor. Under tropical conditions Dutta (2016), the techniques used in Knijff et al. (2000) tend to give lower C values for the same vegetation.

2.3.5 Conservation Practices

Support practice factor (P) is the ratio between soil loss with support practice such as contouring, strip cropping, or terracing and the corresponding loss with upslope and downslope tillage (Renard et al., 1997; Alkharabsheh et al.,2013). Renard et al. (1994) and Schulze (1995) explained that support practice affects soil erosion by altering the flow pattern, gradients, direction of surface runoff, and by reducing the amount and rate of runoff. These practices have a remarkable effect on soil erosion as they reduce soil losses (Renard et al., 1997). Historically, research investigating the P-factors associated with soil erosion assessment has focused on field observation and visual image interpretation. The use of aerial photographs (Lord and McLean, 1969; Morgan et al., 2010) was common as they provided high spatial details of a given site for assessing agricultural management practices. According to Wener (1981), P-factor can be derived straight from the slope map percentage. To obtain the accurate P factor usually depends on the quality of the spatial resolution of the DEM used to derive the slope map. However, good quality and high-resolution images come with more costs. In South Africa, Phinzi (2018) used the percentage slope

information to derive the P factor in the RUSLE model to estimate soil erosion. Another alternative is to use the LULC maps just like the C factor (Naqvi et al., 2013; Feda, 2018; Tesfaye et al., 2018). Satellite images that are freely available such as Landsat are commonly used (Mashame and Akinyemi, 2016). It is possible to combine some of the methods to derive the P-factor information. For example, field observations monitored using a Global Positioning System (GPS) in combination with protected areas maps were used in South Africa (Mhangara et al., 2012).

2.4 Causes of soil erosion

Anthropogenic activities disturbs the natural stability as they accelerate soil erosion. The activities include overgrazing, deforestation, intensive cultivation, construction of roads (Tesfamichael, 2004), soil management, cultivation of steep slopes, and urbanization (Humberto and Rattan, 2010). Those activities are normally influenced by social, economic, and political factors (Lal, 2001). The extent of poverty is associated with soil erosion in developing countries. Farmers with small size farms (0.5-2ha), who are involved in subsistence farming produce food yearly using practices that may degrade the area, and end up impeding the adoption of conservation practices that lowers soil erosion hazards (Lal, 2007). Nevertheless, Humberto and Rattan (2010), reported that there are 3 main causes of accelerated soil erosion. These are overgrazing, deforestation, and the mismanagement of cultivated fields.

2.4.1 Overgrazing

Overgrazing is caused by overstocking livestock on the farm for a long period (Humberto and Rattan, 2010) and also a congregation of wildlife in a small area through trampling and crushing. Uncontrolled grazing usually leads to the removal of plant cover, thus exposing the bare soil to wind and water erosion more especially in steep areas (Bari et al., 1995). The soils in an overgrazed land are often compacted because of the trampling of overcrowded animals. Edridge (1998) researched the trampling effects of overstocked sheep and found out that the trampling of sheep's hooves led to 33% of the total soil loss in the area. In the Kgalagadi district, South West of Botswana, Reed et al. (2015), observed that the areas around the boreholes were degraded due to overcrowded livestock. Similarly, the Ministry of Agricultural Development and Food Security started an experimental fencing project that excluded livestock to stabilize sand dunes. However, due to financial constraints, the fence could not be maintained thus allowing livestock to graze at

rates high enough to remobilize dunes (Reed et al.,2015). Foster (2006) carried out a land degradation assessment in Botswana and reported that Kweneng, Kgatleng, and Southern District were highly degraded areas due to increased population, deforestation and over-grazing.

2.4.2 Deforestation

Previous research has established that Forest plays a vital role in the ecosystem such as soil erosion control and climate change. Due to rapid population growth, there is an increased pressure on natural resources such as the forest thus can increase the seriousness of soil erosion risk (Troel et al., 2003). According to the Central Statistics Office (2008), deforestation in Botswana is done mainly to harvest construction and fencing materials, clearing of the land for arable farming, and collecting fuelwood. About 74000ha of wood resources were cleared during the Accelerated Rainfed Arable Programme (ARAP) in Botswana and farmers were paid to destump their fields without certainty that they would plough and plant (Department of Crop Production and Forestry, 2003, cited in Central Statistics Office,2008).

2.4.3 Excessive Cultivation

Intensive cultivation implies the use of more pesticides, fertilizers, heavy tillage implements, and bringing more land under production. It speeds up the runoff which carries nutrients and pesticides off-sites, thereby reducing the quality of the soil and water and worsening soil erosion loss (Humberto and Rattan, 2010). Generally, excessive cultivation creates conditions that promote changes in soil physical characteristics (Yimer et al., 2008), such as soil structure disturbance and soil organic matter (OM) loss (Liiri et al., 2012). It is now well established from a variety of studies that OM is higher in no-tillage soils compared to minimum tillage (Celik, 2005). Seasonal crops are normally cleared after the harvest thereby leaving the farm without crop cover hence making it susceptible to erosion (Tesfamichael, 2004). Laker (2000) found out that cultivation on erodible soils in South Africa significantly contributed to erosion. Intensive agriculture in Botswana is often practiced in Pandamatenga and Mosesedi farms.

2.5 Effects of soil erosion

Soil erosion is not only an agricultural crisis. Generally, accelerated erosion is the one that is reported to cause extreme ecologic, agronomic, environmental, and economic effects both on-site

and off-site (Humberto and Rattan, 2010; Lal, 1998) with its associated intensification in different farming activities.

2.5.1 On-site effects

The on-site effects of soil erosion primarily involve the loss of soil from the field, thus leading to soil structural degradation. The most important on-site effects include loss of organic matter, and water holding capacity, nutrient depletion (Tesfamichael, 2004; Pimentel, 2006), poor seeding emergence (Lal, 2001), and reduction in soil depth to support roots (Pimentel et al.,1995). According to Mullan (2013), all the above-mentioned effects merge to reduce the agricultural productivity of soils. Low soil fertility is one of the major constraints of arable dryland crop production in Botswana (Kashe et al., 2019). A study was carried out by Larney et al. (2000) in Alberta, Canada, on the effects of topsoil removal. They found out that topsoil removal by 20cm led to a 53% decrease in grain productivity. Similar results were also reported by (Pradhan et al., 1997; Littleboy et al., 1996). Moreover, it becomes expensive to maintain productivity as the costs of other items such as fertilizers rise (Morgan, 2005). Nonetheless, productivity losses can be used to compute monetary loss using a physical modelling technique called Erosion Productivity Impact Calculator (EPIC).This model was used in United States of America (USA) to estimate annual soil loss amounting to $252 million (Crosson, 1998). The costs that are calculated for on sites effects are based within the productive units (cultivable land).

2.5.2 Off-site effects

Unlike on-site effects, the off-site ramifications are concerned with what happens when soil leaves the agricultural property. Moreover, the sediments, chemicals, and fertilizers are transported from the source area by streams, thus causing pollution, sedimentation, and silting of water reservoirs (Tesfamichael, 2004). Some studies have reported that sedimentation and siltation are major issues for agricultural dams in Botswana due to their impacts that include reducing the storage capacity and life span of the reservoirs, culminating in high maintenance costs (Alemaw et al., 2013). Goldman et al. (1986), reported that Cull Canyon Reservoir in California cost around $1 million to remove the sediments from it after 10 years since construction. Alemaw et al. (2013), stated that the average annual sedimentation loss was from 0.54 to 85.29 ton/ha/yr. The life expectancy of dams in the USA, especially in semi-arid areas, is reduced to 30 years or less due to accelerated

erosion (Goudie, 1981). Humberto and Rattan (2010) reported, that the off-sites effects also include loss of habitat for wildlife due to the sediments transported, livestock production through a decrease in weight and forage production, and an increase in tree mortality.

During erosion, more carbon is quickly oxidized and therefore encourages the release of carbon dioxide and methane to the atmosphere (Lal, 2003). Flooding usually occurs in alluvial plains due to the accumulation of eroded materials. Normally, the flow has more devastating power in steep areas, such that it can destroy crops easily (Troeh et aI, 1980). In Botswana, Magole and Thapelo (2005) carried a research on the impact of extreme flooding at Tubu village, Ngamiland district, and reported that there was damage to property, lives of people around the flood plains were threatened, and destructive floods could occur at 10-20 years interval.

2.6 Soil erosion models

The natural resources and landscapes experience pressure due to different factors such as deforestation, increased population, and cultivation (Humberto and Rattan, 2010), thus triggering the need to predict the ramification of any changes to the environment (Shougang et al, 2014). These changes include soil degradation and soil erosion, amongst others (Foster, 2006; Arhem and Freden, 2014). However, the estimation of some of the changes such as soil loss is often considered hard because of the complex interaction of many factors. Soil erosion models can be used to describe the basics of the water erosion process which include detachment, transport, and deposition (Jetten et al., 2003). In concept, a model is a simple representation of complex systems (Feda, 2018). Modeling soil erosion can be defined by the process of mathematically describing detachment, transport, and deposition on land surfaces. Shougang et al. (2014) reported that soil erosion modeling is vital as it assists us in comprehending the environment and forecasting possible effects.

Moreover, erosion models play important roles because of their ability to estimate soil loss and runoff rates from agricultural land, to provide relative soil loss indices, to plan land-use strategies, and to guide the government policy on soil and water conservation (Smith, 1999). Wordofa (2011), reported that in most cases, the land managers and policymakers are usually focused on the spatial distribution of soil erosion risk than absolute values of soil erosion loss. Data from several sources

have identified that several erosion models exist and "these models differ in terms of complexity, processes considered, and the data required for the model, calibration, and model use" (Merritt et al.,2003). It has been reported that validating soil erosion models is the main issue because of a lack of available data for comparing the estimates of the models with the actual losses (Lazzari et al., 2015; Ganasri and Ramesh, 2016).

2.6.1 Erosion models selected for this study:

2.6.1.2 Revised Universal Soil Loss Equation (RUSLE)

The USLE model was originally developed by the United States Department of Agriculture (USDA) around the 1970s, for soil erosion estimation in croplands (Wischmeier and Smith, 1978). It was updated to the RUSLE model to broaden its uses to dissimilar situations such as forest, rangeland and other disturbed areas (Renard et al.,1997; Kayet et al., 2018). The model is specifically used as a decision support tool in soil conservation and land use planning. It uses a set of simple mathematical equations to predict the long-term average annual rate of soil erosion on a given landscape due to the incorporation of the following parameters: rainfall, soils, topography, vegetative cover and management practices (Renard et al., 1997). Moreover, these factors allow easy analysis of the role of each factor in contributing to the estimated soil erosion rate. RUSLE requires less data input and it has been reported to be reliable when it comes to soil loss estimates thus making it more beneficial in terms of applicability (Smith, 1999). It has been noted that rainfall erosivity and soil erodibility are more significant to soil erosion prediction when using the RUSLE model (Igwe et al.,2017).

Although the RUSLE still uses the same formula as that of the USLE model, the main difference is that there has been an improvement in the RUSLE parameters (Renard et al., 1997). The model is specifically designed for rill and inter-rill soil erosion (Wischmeier and Smith, 1978). In contrast, RUSLE does not give proper estimates when predicting gully erosion or deposition of material and thus is not suitable for approximations to the contribution of hillslope erosion to basin sediment yield (Morgan, 2005). RUSLE model has poor performance in sandy soil (Vargas and Ronald, 2016).

Calculation of Soil Loss using RUSLE

The RUSLE formula is expressed mathematically (Renard et al., 1997) as:

$$A = \mathrm{R} * \mathrm{K} * \mathrm{LS} * \mathrm{C} * \mathrm{P} \qquad \text{Equation 1}$$

where A is the mean annual soil loss rate (t ha/year); R is rainfall erosivity factor (MJ mm/ha/yr); K is the soil erodibility factor (tons^{-1} ha^{-1} MJ-$^{-1}$ mm); LS is slope length and slope steepness factor (dimensionless); C = cover and management factor (dimensionless); and P is support practice factor (dimensionless).

Explanation of the above RUSLE parameters can be found from the factors affecting soil erosion by water sub-section.

2.6.1.3 Soil Loss Estimation Model for southern Africa (SLEMSA)

The Soil Loss Estimation Model for southern Africa (SLEMSA) model was developed in Zimbabwe for estimating long-term annual soil loss from sheet erosion on arable land (Smith, 1999). Despite being developed in Zimbabwean Highveld, SLEMSA is also quite widely used in African conditions (Elwell and Stocking, 1982). The application of the model has been investigated in Southern Africa including Schulze (1979) in Richards Bay in South Africa, Abel and Stocking (1987) in Botswana, Paris (1990) in Malawi, and Vargas and Ronald (2016) in Malawi. Around the 1970s, the model performed well during the prediction tests on the Zimbabwe Highveld, where mean annual soil erosion predicted from field plots had 50%, 70% and 90% confidence (Elwell, 1979). It has since been used to develop soil loss hazard maps, predict soil erosion rates, and also determine sediment sources (Vargas and Ronald, 2016). SLEMSA is effectively used to differentiate areas of high and low erosion potential (Smith, 1999). SLEMSA also requires less data inputs (Tesfamichael, 2004 cited in Elwell, 1978).

SLEMSA relates measured erosion losses from plots of standard dimensions to actual field conditions by a series of empirically derived parameters. According to Smith (1999), reported that the soil erosion loss values acquired from SLEMSA should be looked at as relative values and more calibration and verification of parameter estimate is a prerequisite before the model could be used in soil conservation planning. The model has 4 physical systems namely; crop, climate, soil

and topography. Nevertheless, the model had shown some limitations in estimating sediment yield, as well as soil deposition in depressions and gully erosion (Schulze, 1979) hence, work is still needed to refine it for ubiquitous utilization. SLEMSA model has poor performance in sandy soil (Vargas and Ronald, 2016). Only five parameters in the SLEMSA model are considered (Elwell, 1978); i is the amount of rainfall energy intercepted by the crop, E is rainfall energy, F is soil erodibility, L is slope length and S is slope percentage (Figure 4).

Calculation of Soil Loss using SLEMSA (Figure 4)

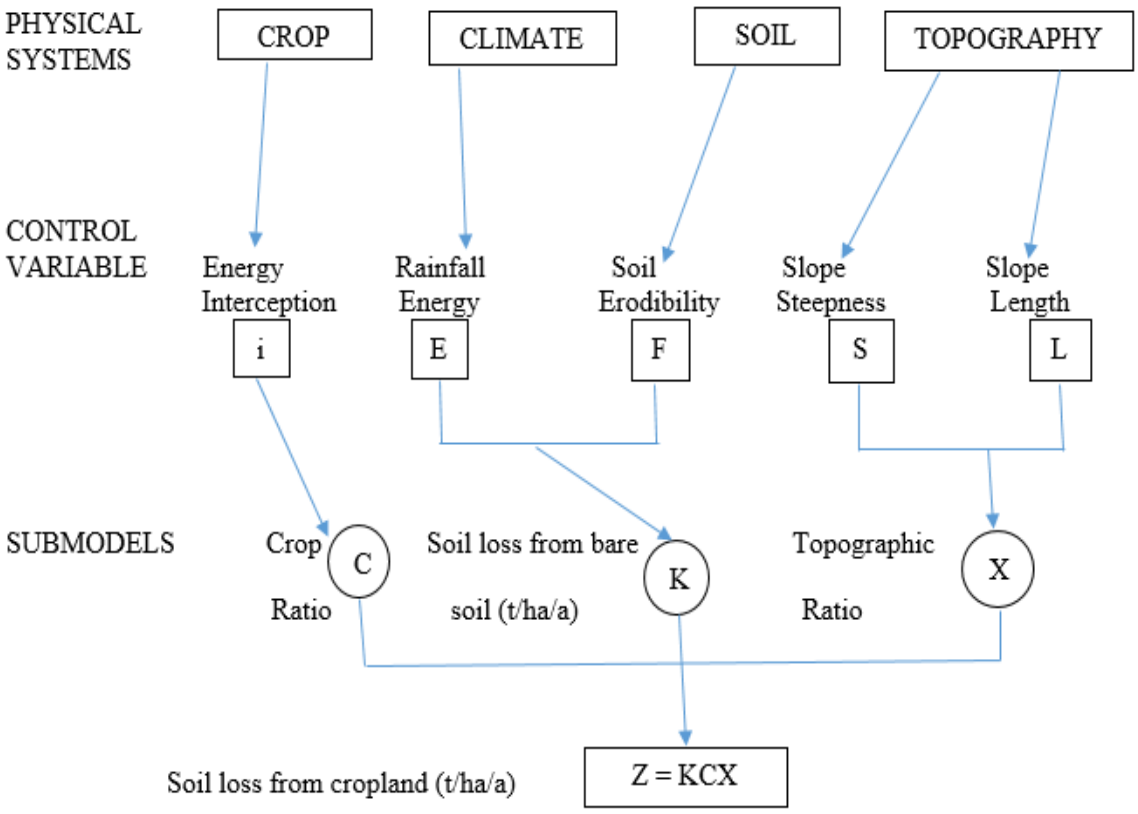

Figure 4: The SLEMSA model (Adapted from Elwell, 1978)

These control variables are subsequently combined into three sub-models; the crop sub-model, bare soil sub-model and topographical sub-model to finally form the overall model.

$$Z = K * C * X \qquad \text{Equation 2}$$

Where Z is the mean annual soil loss from the land (tons.ha-^{1}.yr^{-1}); K is Principal factor (tons.ha^{-1}.yr^{-1}); X is Topographic Factor; and C is Crop factor.

Crop Factor (C) is the ratio of the soil lost from a cropped plot to that from a bare fallow (Stocking, 1980). SLEMSA can be used to estimate the soil loss from rangeland using a slightly different sub-model to relate C to i.

Topographic Factor (X) is a ratio to account for different slope steepness (%) and length (m) (Stocking, 1980).

Principal Factor (K) combines the influences of mean seasonal rainfall energy and soil erodibility to give the estimated mean annual (seasonal) soil loss from conventionally tilled bare soil on 4.5% slopes and 30 m long by 10m (Stocking,1980). The K factor is obtained from the rainfall energy and soil erodibility control variable.

The main discrepancy between SLEMSA and RUSLE is that the P factor of RUSLE in SLEMSA is left out as the effect conservation practices can be allowed for in topographic factors (L/S) or soil erodibility factor (F) (Mutowa and Chkodzi,2013).

2.7 The use of Remote Sensing and GIS in soil erosion modeling

It is a widely held view that soil erosion is a spatial phenomenon (Yazidhi, 2003). The prediction of soil erosion is applicable at a wide range of spatial scales and that is from the plot scale up to the global scale (Saavedra, 2005). The author went on to state that, at small scales, timing and volume of overland flow hydrograph are vital components whereas, at a larger scale, topography, soil, and vegetation patterns are the ones considered to be more crucial. Moreover, in those situations, GIS and Remote sensing become a very handy tool because of their ability to be integrated with soil erosion models (Saavedra, 2005).

Beck (1987), reported that data produced from RS with their spatial locations can be linked. Previous research has established that GIS and RS have the potential for quantitatively assessing and mapping soil erosion loss (Feda, 2018). Moreover, a combination of RS, GIS with empirical models has been implemented across the world (Chadli, 2016; Tesfaye et al., 2018). Satellite imagery can be used to derive land cover/land use (LULC) maps and also estimate soil erosion parameters (Bvindi, 2019). Moreover, the C factor from both models can be derived from

vegetation indices called Normalized Difference Vegetation Index (NDVI) (Wordofa, 2011). Besides, the Digital Elevation Model (DEM) can, however, be used to derive topographical parameters such as slope length and slope degrees which are very useful in soil erosion modeling through the use of GIS techniques (Chadli, 2016).

2.7.1 Remote sensing (RS)

2.7.1.1 Land-Use/Land-Cover Change

Land cover is a material that is found above the earth's surface such as vegetation, water, etc while Land use is what that material is being used for, examples include agriculture, settlement, etc (Lillesand and Keifer, 1994). LULC information is very crucial for modeling and understanding the earth's feature system. According to Chuenchum et al. (2020), vegetation cover such as forest, grassland and agricultural area has a massive effect on the soil loss process. The soil erosion rate is influenced by land use and cover practices such as deforestation, overstocking, overgrazing, and agricultural intensification on arable lands (Arhen and Freden, 2014). Moreover, the characteristics of LULC are also very helpful in deciding and estimating the crop management factor (C) (Ganasri and Ramesh, 2016).

2.7.1.2 Image classification

Image classification is the process of categorizing all pixels in an image or raw remotely sensed satellite data into land cover/land use classes (Lillesand and Keifer, 1994). It is the process of using training samples to classify image pixels without a known identity (Campbell, 1996). Image classification consists of two broad classifications namely supervised and unsupervised classification. Supervised classification is a method in which the analyst does the classification alone without the help of the software while in unsupervised classification, the software does the classification alone (Feda, 2018). Both classifications are based on spectral groupings. However, in supervised classification, preceding knowledge of the area is required to provide the software with unique training classes, there is also more extensive user interaction. (Lillesand and Keifer, 1994). In, unsupervised classification, there is minimal user interaction, considers only spectral distance measures, and also requires interpretation after classification. Most researches on image

classification have been carried out using the supervised classification method (Arhem and Freden, 2014; Ganasri and Gamesh, 2016; Choudhary, 2018; Worku, 2018; Sourlamantas, 2019).

2.7.1.3 Accuracy assessment of the classification

Accuracy assessment is a general term used to determine the correctness of the classified image based on pixel groupings. The image is said to be accurate if the image classification corresponds closely with the standard that is assumed to be correct. Classification accuracy is usually represented in the form of an error matrix (Congalton and Green, 1999). The error matrix is made up of the ground control data and classified data (reference data) listed in the rows and columns to represent the number of correctly classified samples. Generally, four measures of accuracy are calculated, namely overall Accuracy, Kappa Statistic, Producer's Accuracy and User's accuracy.

Overall Accuracy shows the accuracy of the whole classification and it is calculated by dividing the total number of the correctly classified pixels (summation of the diagonal) by the total number of pixels (grand total). Kappa statistics give information about the quality of a map. It allows us to detect if two datasets have statistically different accuracy. The kappa statistic value normally ranges from -1 to 1. A value of 1 represents a perfect agreement between the ground points and the map whereas -1 represents no agreement. The producer's accuracy (omission error) is the probability of a correctly classified reference point and that is the probability that a land cover, in reality, has been classified correctly (Congalton, 1991). It is determined by dividing the number of the classified pixel by the total number of pixels of the category in the reference data. The user's accuracy (commission error) refers to the probability that a point in the classified map/image is represented by the same land cover class on the ground (Congalton, 1991). It simply tells us the likelihood that a point classified as a certain class represents that class.

According to Geomatics (2016), there are different ways of doing the accuracy assessments of image classification. The first method Geomatics (2016) identified is comparing the classified image to a reference image. For this method, a random set of points are created and the classification results are compared with the true information classes in the reference image. Another method includes fieldwork through the use of a GPS. Similarly, just like in the first method, a random set of points is created over the classified image. Ground truthing is normally

done to find accurate location point data for each LULC class. It is vital to make sure that the reference image or GPS points collected should be obtained around the same time of the year as the imagery to make a fair comparison. A couple of researchers have utilized the GPS method and google earth pro software for collecting ground truth data to support classification for accuracy (Worku, 2018; Feda, 2018; Matlhodi et al., 2019). The study conducted by Phinzi (2018) also showed that ground truth data and high spatial resolution Google Earth images, merged with Remote sensing and GIS make it possible to derive the C Factor and also conduct accuracy assessment.

2.7.2 Geographical Information Systems (GIS)

Geographical Information Systems application is an important tool used to carry out environmental research as opposed to field surveys which need large manpower, cost and money (Marble, 1987). Nevertheless, the GIS application is growing more in predicting soil erosion of the watershed (Kim, 2006). GIS softwares can roughly calculate soil loss from the following datasets; rainfall data, topography data, soil data and LULC maps (Kim, 2006) through a raster calculator or overlay toolsets in GIS software. The relationship between GIS and the soil loss models is based on the GIS and the erosion model itself. GIS can analyze raster data and therefore, the grid cell-based models can be integrated with it easily (Shahram et al., 2007). Historically, researchers assessing soil erosion associated with models have focused on spatial models, but nowadays has the functionality of GIS being merged with soil erosion models to generate reality spatially (Breetzke, 2004). Bvindi (2019) reported that empirical models such as RUSLE and SLEMSA can be interfaced with GIS because of the simple equation they possess to get the spatial distribution of soil erosion that is essential for decision making. They are a lot of GIS operations involved, just from starting to delineate the watershed, deriving soil erosion parameters up to combining them to produce the final soil loss output.

2.8 Chapter Summary

Many studies have been carried out by different researchers on soil erosion risk modelling. However, the implementation of the RUSLE and SLEMSA models has received little attention in Botswana. Less is known about the spatial extent and distribution within anthropogenically disturbed areas at a watershed scale. This gap can be addressed by the use of SLEMSA and RUSLE

models integrated with GIS and Remote Sensing to model soil loss taking place in the watershed and also quantify the spatial area of soil erosion. The combination of the models with RS and GIS provides an effective tool for predicting soil erosion risk. In addition, the information gathered can be used by policymakers, decision-makers, and land users.

2.9 Case studies

Several studies on the assessment of soil erosion using SLEMSA and RUSLE have been conducted throughout Africa, as shown in Table 1.

Table 1: A summary of some of the Studies that described Soil Erosion Models and their Applications

Author	Title	Model Developed/Applied	Result(s)	Recommendation(s)	Conclusion
Tesfaye et.al., (2018)	Soil Erosion Risk Assessment Using GIS Based USLE Model for Soil and Water Conservation Planning in Somodo Watershed, South West Ethiopia	RUSLE	Results from the study showed that, mean annual soil loss of the watershed was 18.69 ton ha^{-} $year^{-}$ ranging from 0 to 131 ton ha^{-} $year^{-}$.	The results obtained from this study should be used for effective watershed management and soil conservation planning	Soil erosion models are useful to estimate soil loss and runoff rates at watershed and basin level, to plan land management strategies, to provide relative soil loss indices and guide government policy and strategy on soil and water conservation practices
Chadli, (2016)	Estimation of soil loss using RUSLE model for Sebou watershed (Morocco)..	RUSLE	The results show that 78.83 % of the study area has a low risk of erosion, 17.36 % medium risk, 3.04	Concerning management strategies to reduce soil loss, the intervention will focus only on the LS, C, and P factors, as the K and	The present study allowed the author to quantify and map potential erosion throughout the Sebou watershed.

Author	Title	Model Developed/Applied	Result(s)	Recommendation(s)	Conclusion
			% high risk and 0.77 % a very high risk.	R factors cannot be changed (Stone and Hilborn 2012) -For the LS factor, the management of terraces will reduce the length of the slope and consequently the soil loss, – For the C factor, the choice of the types of cultivation and tillage methods will lead to reduction of erosion. – For the P factor, conservation practices, such as culture against the slope, should be used to ensure that sediments are deposited close to their source	
Alemaw et.al., (2013)	Assessment of Sedimentation Impacts on Small Dams—A Case of Small Reservoirs in the Lotsane Catchment	RUSLE	The average annual sedimentation rate ranges between 0.54 and 85.29 ton/ha/yr.	The approach and results can be used as a maintenance planning system by estimating recurrence interval of siltation filling up of active storage of small reservoirs.	High sedimentation rates were observed where there are steep slopes and high rainfalls, this indicates that sedimentation rate is highly dependent on the slope factor and the rainfall intensity

Author	Title	Model Developed/Applied	Result(s)	Recommendation(s)	Conclusion
Bvindi, (2019)	Assessment of soil erosion hazard around the abandoned Nyala mine in formerly Mutale Municipality, Limpopo Province, South Africa.	SLEMSA	Results from the study indicated that 74.3 % of the watershed experiences low to moderate erosion hazard, with an estimated annual soil loss of 2.76 tons/ha/yr. The low rates of soil erosion in most parts of the watershed are associated with the low topographic ratio and low rainfall erosivity	The parameters of the model should be validated within the area in which they are being applied. Further studies with limited spatial scale using high resolution and multi-temporal data is recommended to closely monitor and mitigate erosion hazard appropriately.	This research demonstrates how GIS and remote sensing enhances our capacity to assess and model soil erosion hazard in an affordable and time effective way.
Abel and Stocking(1987)	A Rapid Method for Assessing Rates of Soil Erosion from Rangeland: an Example from Botswana	SLEMSA	Two contrasting areas of rangeland in Botswana we assessed. On the granite soils erosion rates varied from about 1 to 12 tonnes/ ha/ year, while on the dolomite soils	Under ungrazed rangeland, the soil erosion was less than 1 tonne, and intermediate values occurred for other treatments. We feel therefore that the use of vegetation cover survey, kriging, and a simple soil loss model gives figures for	This modelling appoach gives gross soil loss and allows the estimation of sediment yield. It is easy and cheap to apply and gave results in line with field experience.

Author	Title	Model Developed/Applied	Result(s)	Recommendation(s)	Conclusion
			they were considerably less.	rangeland erosion that are both explicable and of approximately the right magnitude.	

3.0 MATERIALS AND METHODS

3.1 Description of the study area

The study was conducted in Taung watershed south of the capital city Gaborone, about 35km from the city. The watershed is located within Ramotswa Agricultural District and covers about 43958.07 ha (Figure 5). It extends from 24° 50’0’’-25 50’0’S latitude and 25° 35’0’’- 25 50’0’’ E longitude.

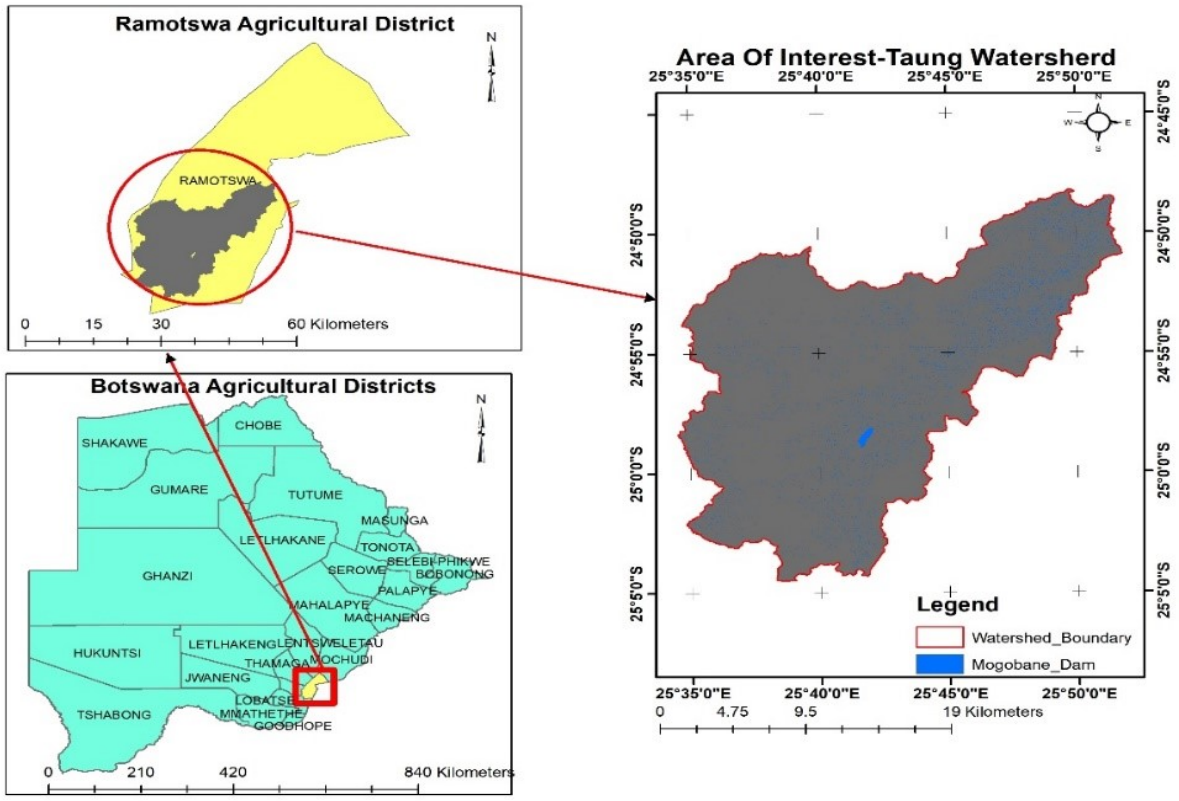

Figure 5: Map of Study area

3.1.1 Climate

The watershed area is generally considered semi-arid. The rainfall is seasonal, with the wet season normally occurring between October and March while dry and cold winter months range from May to July which accounts for less than 10% of the annual rainfall (Arntzen et al., 2000). The total mean annual rainfall ranges from 400 to 550mm. High temperatures are experienced during the wet season, recording between 30 to 32°C on average during the day (Maximum high

temperature up to 41°C) and between 16 to 20°C on average at night. During the dry and cold months, night temperatures near zero have been recorded over time.

3.1.2 Topography and Soils

In general, the study area is fairly hilly which is typical for South East Botswana. The watershed has a highly uneven elevation ranging from 1012 to 1489m above sea level (Figure 6a). The study area is covered by 5 different soil texture ranges, starting from fine sands - loamy Fine sand to Sandy Loams - Sandy Clay (Figure 6b).

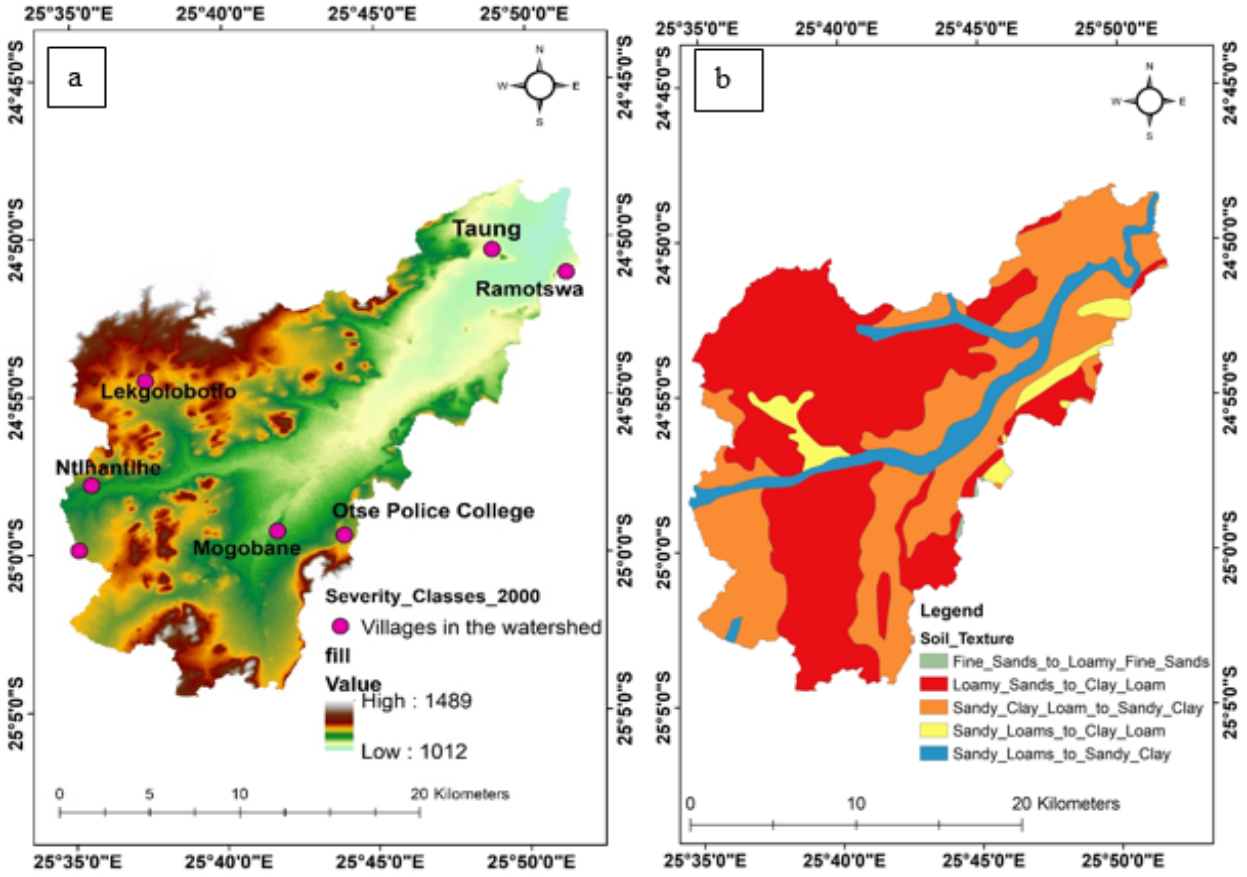

Figure 6: Elevation of study area (a) and Soils of the study area (b)

3.1.3 Land use land cover (LULC)

Taung watershed has the following major land covers; cropland, bareland, shrubland, built-up areas, tree savanna and waterbody (Matlhodi et al., 2019). The main crops grown in the study area include maize, sorghum and legume crops. The vegetation cover within the watershed is predominantly mixed shrub savannah and tree savannah (Huesken et al, 1989). There is a dam

called Mogobane in the watershed from which residents of Mogobane village and surrounding areas source water. The dam is exposed to the risk of sedimentation which erodes from upper catchments.

3.1.4 Socio-Economic Characteristics

The majority of the residents in the watershed practice subsistence agriculture which **i**s the main income source for the community**.** The most common crops produced are field crops especially sorghum, maize, and beans. The majority of the inhabitants in the watershed rely more on rainfed agriculture except for those who are closer to Mogobane dam who practices irrigation. The dam is exposed to the risk of sedimentation which erodes from upper catchments. According to Integrated Water Resource Management (IWMI) and International Ground Resources Assessment Centre (IGRAC) (2017), the maximum area under irrigation is about 3.9 hectares and the crops grown include maize, cabbage, green pepper, tomatoes, and lettuce, amongst others. The crop residues left in the fields after harvesting are normally used as livestock feed. Moreover, animals are allowed to graze on the cultivated land after harvest. Pastoral farming is also practiced within the watershed. Mostly, the livestock in the watershed are grazers, with cattle being in large numbers, as well as sheep, goats, and donkeys. Cutting down trees for construction purposes or firewood is also common in the study area. Shrubs are also cut down for fencing of fields or plots, causing local denudation. The most common source of fuel used for household heating in the study area is wood (Statistics Botswana, 2011). A combination of overgrazing, the cutting down of trees and bushes, with very intense rainfall events results in soil erosion.

3.1.5 Population

The study area includes six villages namely Ramotswa, Taung, Mogobane, Magotlhwane, Lekgolobotlo, and Ntlhantlhe; the first three villages are part of South East administrative District which have an estimated population of 94 252 and the other three are found in the Southern Administrative District with 133753 (Statistics Botswana, 2020). The major part of the Taung watershed is found in the South East administrative district. Based on 2020 Cities/Town and Village projections of Botswana, the total estimated population of the six villages was 48345, of whom 22489 were male and 25551 female (Statistics Botswana, 2020).

3.2 Data Sources and Softwares

RUSLE and SLEMSA models used the same data types and the same Softwares as shown in Table 2 and Table 3.

Table 2: Data sources and their description for RUSLE model

RUSLE parameters	Data Type	Description	Source
Rainfall Erosivity factor (R)	Rainfall Data	Long-time annual Rainfall point data for a period of 26 years from 7 stations in and around Taung watershed	Department Of Meteorological Services (DMS)
Soil Erodibility factor (K)	Soil	Digital soil map	Ministry of Agricultural Development and Food Security
Topographic features factor (LS)	DEM	Shuttle Radar Topographic Mission (SRTM) 90m	United States Geological Service (USGS)
Crop Management factor (C)	Satellite Images	➢ Landsat 7, 30m resolution (2000) ➢ Landsat 8, 30m resolution (2020)	USGS
Practice Mananagent factor (P)		➢ Landsat 7, 30m resolution (2000) ➢ Landsat 8, 30m resolution (2020)	USGS

Table 3: Data sources and their description for the SLEMSA model

SLEMSA control variables	Data type	Description	SLEMSA sub-models	Source
Energy Interception	Satellite Images	➢ Landsat 7, 30m resolution (2000) ➢ Landsat 8, 30m resolution (2020)	Crop ratio (C)	USGS
Rainfall Energy	Rainfall	Long-time annual Rainfall point data for a period of 26 years from 7 stations in and around Taung watershed	Principal Factor (K)	DMS
Soil Erodibility	Soils	Digital Soil map		Ministry of Agricultural Development and Food Security
Slope Steepness	DEM	Shuttle Radar Topographic Mission (SRTM) 90m	Topographic ratio (X)	USGS
Slope Length	DEM	Shuttle Radar Topographic Mission (SRTM) 90m		USGS

3.2.1 Software packages and Data Analysis

Geomatica 2018 software was used to carry out image processing and image classification. After the supervised classification process was done in Geomatica, the land cover raster was exported to ArcMap for accuracy assessment with the aid of Google Earth Pro software (Table 4). The GIS analysis was conducted using ArcMap 10.7. The GIS layers; Taung watershed boundary map, soils, rainfall, land cover, and DEM were spatially organized with the same resolution and coordinate system using ArcMap 10.7. Microsoft Office 2013 was used for presentation and documentation.

Table 4: Software used and their specific application

Software	Application
Geomatica 2018	Image pre-processing, LULC classification
ArcMap 10.7	Database creation, dataset preparation, and raster calculation and Accuracy Assessment
MS Office	Documentation and presentation
Google earth pro	Accuracy assessment of the LULC

3.3 Watershed Delineation

A 90m resolution SRTM DEM was used for Watershed delineation using spatial analyst tools in ArcMap 10.7. This dataset is readily available at the Department of Agricultural & Biosystems. The DEM was resampled to 30m using Geomatica Software so that it is the same resolution as other datasets, the resampling algorithm in Geomatica produces very accurate resampled DEMs. Delineating watershed requires using the following spatial analyst tools respectively;

- Fill sinks
- Flow direction
- Flow accumulation
- Basin
- Conversion
- Clip

The DEM was transformed into the projected coordinate system WGS84/UTM Zone 35S. It was also used to create slopes that were used to determine the topographic factors for RUSLE and SLEMSA.

3.4 Soil Loss Analysis

3.4.1 Revised Universal Soil Loss Estimation (RUSLE)

The RUSLE and SLEMSA have been applied widely across Southern Africa, however, the RUSLE model has proved to perform better than the SLEMSA model (Smith, 1999). The following five parameters were used to estimate soil loss in the RUSLE model; Rainfall Erosivity, Soil Erodibility, Slope Length and Steepness factor, Cover Management factor. The formula of RUSLE is expressed as

$$A = R \times LS \times K \times C \times P \qquad \text{Equation 3}$$

Where A is the mean annual soil loss rate (t ha/year); R is rainfall erosivity factor (MJ mm/ha/yr); K is the soil erodibility factor ($tons^{-1}$ ha^{-1} $MJ\text{-}^{-1}$ mm); LS is slope length and slope steepness factor (dimensionless); C = cover and management factor (dimensionless); and P is support practice factor (dimensionless). ArcMap software was used to implement those factors. A simplified flow chart of the data analysis is shown in Figure 7. The following section describes how the RUSLE factors were derived:

Figure 7: The overall flow chart of the RUSLE methodology

3.4.1.1 Rainfall erosivity factor (R)

Rainfall erosivity refers to the ability of rain to cause soil erosion. It is the result of kinetic energy (E) of a rainstorm and its maximum 30-min intensity (EI30) (Brown and Foster, 1987). However, nowadays they are a lack of rainfall intensity and storm energy data at the national meteorological stations, including the Taung watershed. Therefore the mean annual rainfall is usually used to estimate the R factor (Arnoldus, 1977). Renard et al. (1997), however, suggested that input rainfall data should be for a period of at least 20 years. In this study, the R factor was computed from rainfall amounts recorded at 7 different rainfall stations within and near the watershed. These

stations are Seepapitso Secondary School, Moshupa Police Station, Mogobane, Lobatse Police Station, Moeding College, Ramotswa Station and Gaborone Met. H.Q as shown in Table 5.

Table 5: Mean annual rainfall

Weather Stations No	Rainfall Weather Stations	Years of Observation	Mean Annual Rainfall (MAR) in mm	Northings	Eastings
1	Seapapitso-Kanye	1990-2015	453	-24.93333	25.36667
2	Moshupa Police Station	1990-2015	510	-24.76667	25.43333
3	Mogobane	1991,1992,1993,1997,2001 and 2005	480	-24.95000	25.70000
4	Ramotswa Station	1971-2014	483	-24.88333	25.86667
5	Gaborone MET H.Q	1989-2015	498	-24.66667	25.91667
6	Moeding College	1995-2019	505	-25.01667	25.73333
7	Lobatse Police Station	1999-2015	488	-25.25000	25.65000

Source; Department of Meteorological Services

The Inverse Distance Weight (IDW) spatial interpolation technique was applied to estimate the spatial variability of rainfall in the study area (Figure 8a). Jacobs et al. (2010) reported that IDW estimates values at unsampled points using a linear combination of values at sampled points. This means that the less the distance between the sampled points, the more influence the input sample point value has on the output cell value and vice versa. After interpolation, the R factor was computed from the mean annual rainfall map using the Raster Calculator tool using the following empirical equation derived by Roose (1977).

$$R = 0.5 * P \qquad \text{Equation 4}$$

Where R is rainfall erosivity and P is the mean annual precipitation

The R factor results varies from 240 MJmm/ha/h/yr to 252.5 MJmm/ha/h/yr. The rainfall erosivity was high at the south and low towards the centre of the study area (Figure 8b).

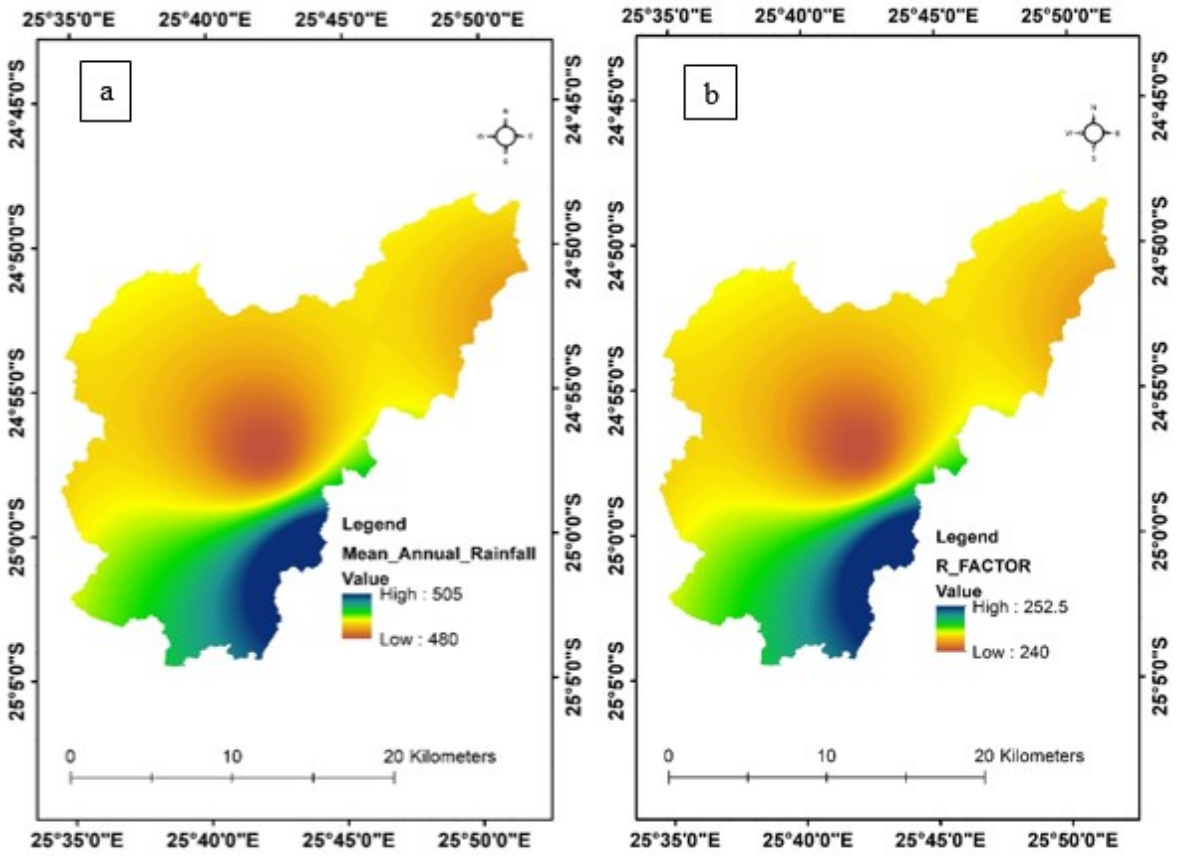

Figure 8: Interpolated mean annual rainfall (a) and rainfall erosivity factor (b) map

3.4.1.2 Soil erodibility factor (K)

The soil erodibility shows the vulnerability of soil to erosion by raindrops and runoff. Soil erodibility of a particular soil is determined by soil texture, organic matter, structure and permeability (Wischmeier and Smith, 1978). The K factor is considered one of the most challenging soil erosion factors that require substantial time, cost and resources to carry out field surveys and analyses (Manyiwa and Dikinya, 2013). For this study, the erodibility factor was obtained from the digital soil map looking at the budget and time. This method is normally used when there is little data such as a soil type map but without organic matter content information present for the area of interest. It is one of the most well-known methods for deriving the K factor (Kim, 2006; Alkharabsheh et al., 2013; Sourlamtas, 2019).

The K factors for this study were derived from the table by Roose (1977). The table provides information on different soil textures and their organic matter content. From the soil map, each

soil texture was identified and assigned the K values corresponding to their organic matter content as shown in Table 7. When a soil texture is near the borderline of the two texture classes, have to use the average of the two K values (Roose, 1977). The soil erodibility values extracted from the table are given in unspecified metric units and range from 0.02 to 0.6 which suggests that they are not in $tons^{-1}$ ha^{-1} $MJ\text{-}^{-1}$ mm. To convert the metric values of Roose (1977) they were multiplied by the conversion factor (0.1317) (Wischmeier and Smith, 1978). The organic matter (OM) in the Taung Watershed was assumed to be less than 2% (Huesken et al., 1989).

From the soil map data acquired from the MoA, Fine sands to loamy fine sands, Loam sands to clay loam, sandy clay loam to sandy clay, sandy loams to clay loam and sandy loam to sandy clay were recognized in the Taung watershed Table 6. The values indicate that Fine sands to loamy fine sands and Loam sands to clay loam have lower erodibility, whereas sandy loams to clay loam and sandy loam to sandy clay had relatively medium erodibility and Sandy clay loam to sandy clay higher erodibility (Figure 9a). The results showed that the K factor value in the watershed varies from 0.026340 $tons^{-1}$ ha^{-1} $MJ\text{-}^{-1}$ mm to 0.063875 $tons^{-1}$ ha^{-1} $MJ\text{-}^{-1}$ mm (Figure 9b). The highest erodibility values were located in the central, northern and southwestern parts of the watershed area.

Table 6: Soil Erodibility in the study area

No#	Soil Textures	Area Coverage (ha)	Soil Erodibility K factor
1	Fine sands to loamy fine sands	53.73	0.026340
2	Loam sands to clay loam	21701.01	0.026820
3	Sandy clay loam to sandy clay	16726.18	0.063875
4	Sandy loams to clay loam	1696.11	0.035559
5	Sandy loam to sandy clay	3781.04	0.042144

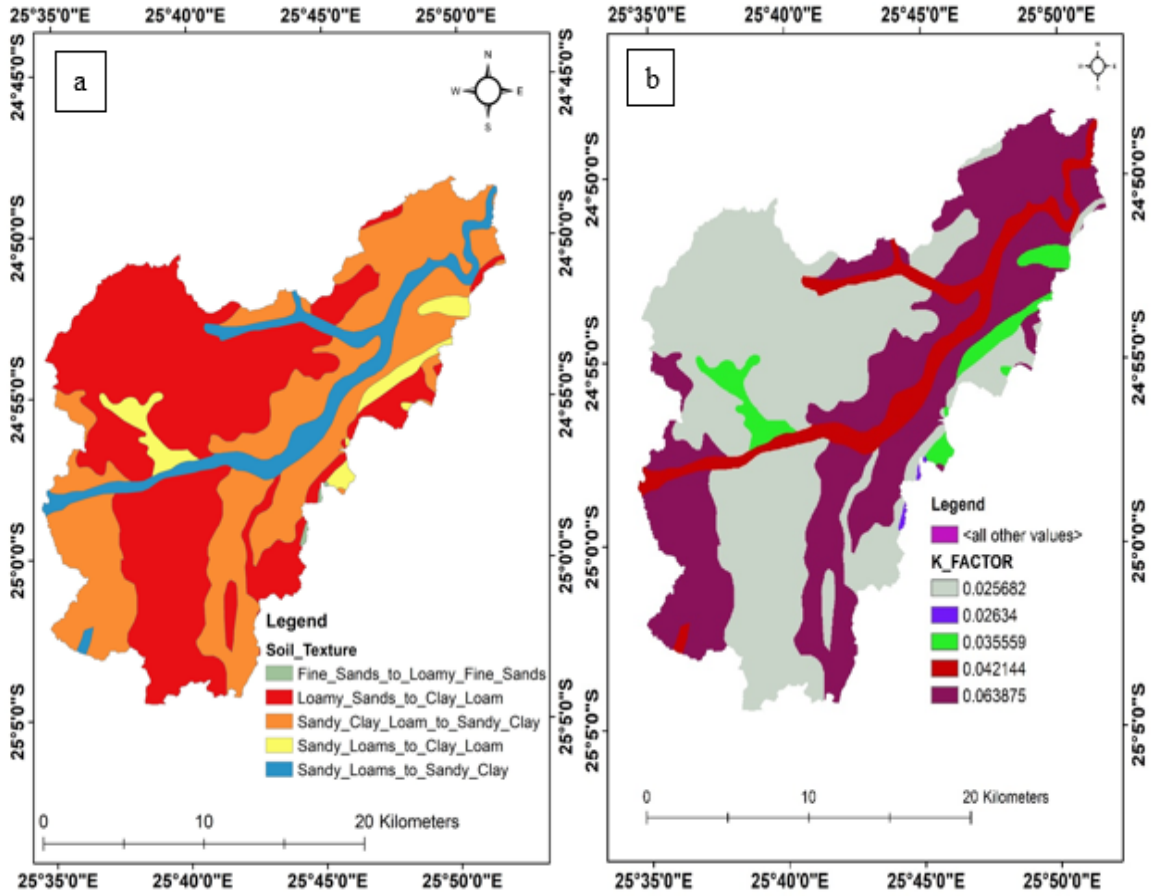

Figure 9: Spatial distribution of Soil texture map (a) and K factor map (b)

Table 7: Soil Erodibility Factor (K) for each soil type

Textural Class	Organic Matter Content		
	<0.5%	**2%**	**4%**
Sand	0.05	0.03	0.02
Fine sand	0.16	0.14	0.10
Very fine sand	0.42	0.36	0.28
Loamy sand	0.12	0.10	0.08
Loam fine sand	0.24	0.20	0.16
Loam very fine sand	0.44	0.38	0.30
Sandy loam	0.27	0.24	0.19
Fine sandy loam	0.35	0.30	0.24
Loam	0.47	0.41	0.33
Silt loam	0.38	0.34	0.29
Silt	0.48	0.42	0.33
Sandy clay loam	0.60	0.52	0.42
Clay loam	0.27	0.25	0.21
Silty clay loam	0.28	0.25	0.21
Sandy clay	0.37	0.32	0.26
Silty clay	0.14	0.13	0.12
Clay	0.25	0.23	0.19

Source: (Roose, 1977)

3.4.1.3 Slope length and steepness (LS)

The LS factor shows the effect of topography on soil erosion. According to Wordofa (2011) and Renard et al. (1997), the slope length factor L is the distance from the source of runoff to the point where deposition begins and slope steepness (S) reflects the influence of slope gradient on erosion (Agele et al., 2013). For this study, a resampled DEM of 30m was used for generating the LS factor. The DEM was filled to generate a depression-free DEM using the fill sink tool. Then the

flow directions were computed from the flow direction toolset. From the flow direction, flow accumulation was derived. The slope in degrees (Figure 10a) and flow accumulation were used to calculate the LS factor using the Raster Calculator in ArcMap 10.7 from the following equation derived by Bizuwerk et al. (2008) and its values ranged from 0 to 14.1895 (Figure 10b). The map was resampled to a 30m cell size.

$$LS = \sqrt{\frac{X}{22.1}} m\,(0.065 + 0.045s + 0.0065s^2)$$ Equation 5

Where X=Flow accumulation*cell size and cell size is the resolution of the grid (i.e., 90 m), s=Slope gradient (%), and m is a slope contingent variable.

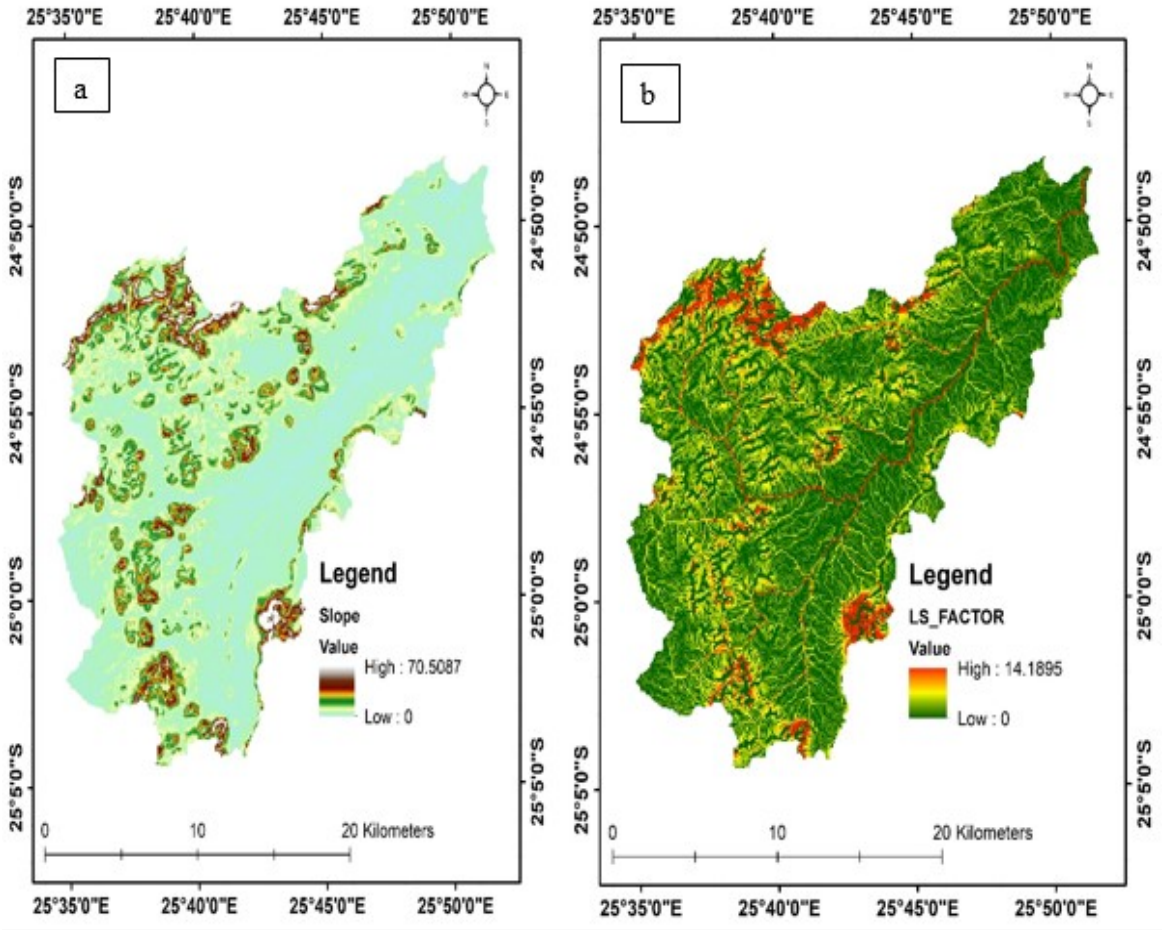

Figure 10: Spatial distribution of (a) Slope and (b) LS factor in Taung Watershed

3.4.1.4 Cover Management factor (C)

3.4.1.4.1 Land Use/Land cover (LULC) mapping

Landsat images downloaded from the United States Geological Service (USGS) Earth Explorer (http://earthexplorer.usgs.gov) were used for the LULC classification of the Taung Watershed. These were dry season Landsat 7 and Landsat 8 Imager for the years 2000 and 2020 (Table 8). The selection of those Landsat images was started with the elimination of all images that had high cloud cover. The mapping steps were as follows: pre-processing, training sample collection, supervised image classification and accuracy assessment respectively.

Table 8: Landsat images used for the study

Year	Sensor	Spatial Resolution	Number of Bands	Date of Acquisition	Sources	Row-Path
2000	ETM+	30 m	7	11 August	USGS	172-077
2020	OLI	30 m	11	10 August	USGS	172-077

3.4.1.4.2 Image pre-processing

According to Lillesand et al. (2004), image pre-processing is done to correct flaws in the data. In this study, Landsat image data available for download was processed by the data provider to Level-1C which includes radiometric and geometric corrections along with ortho-rectification and spatial registration (Worku, 2018). After downloading the Landsat images, the researcher performed the following pre-processing operations such as image stacking, image enhancement and sub-setting (clipping).

All the composite images were created using band combinations that included near-infrared, red and green bands for image enhancement to determine changes in LULC. Linear enhancement operation was applied to both satellite images. Following the linear enhancement, both false composite images were used for collecting training sites and also applied for the LULC classification. Both satellite images were then clipped/subset based on Area of Interest (AOI).

3.4.1.4.3 Image Classification

Supervised image classification was applied in the study. The classes included cultivated land, shrubland, built-up areas, woodland (tree savanna), and waterbody as shown in Table 9. After identifying the classes, the following procedures were followed.

- Collection of training samples. Training samples for supervised classification were created using polygons.
- Analysing training samples. This was done before a classification could be run and it involved checking the signature separability and also a review of the classification.
- Lastly, the maximum likelihood classifier (MLC) algorithm was applied to the supervised image classification in Geomatica 2018 software to determine the watershed LULC categories. It is also considered to be one of the most accurate classifiers (Choudhary et al., 2018).

Table 9: The LULC classification scheme used in the study (Source: FAO, 1997*)*

No	Class	Description	Pictures
1	Cultivated land	Cropland, horticultural land, forage, orchards, fallow land, intensively, moderately, sparsely cultivated lands, bare cultivated lands. **NB**: The Bareland class was combined with the cultivated land because they had a similar spectral signature and also because it occupied extremely less area compared to all cover classes.	
2	Shrubland	Woody plant, less than 5 m in height, no defined crown, have a mixture of trees with grasses.	

No	Class	Description	Pictures
3	Built-up	Land areas are covered by buildings such as residential, commercial, and industrial surface features.	
4	Tree savanna (Woodland)	Woody plant more than 5 m in height with a somehow definite crown.	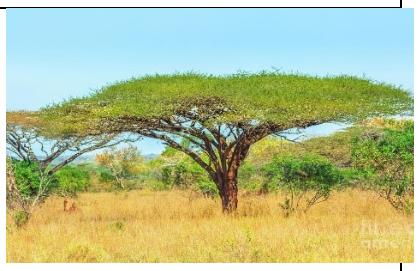
5	Waterbody	Areas with water coverage on the earth surface that forms naturally such as streams and rivers, etc. or made by people such as ponds, dams, etc.	

3.4.1.4.4 Accuracy Assessment Landsat images classification

After the classification process, an accuracy assessment was performed to verify to what extent the produced classification is compatible with what exists on the ground. In this study, the LULC classification accuracy of remotely sensed data was done using the error matrix. The results of the classification were then compared with ground truth data observations in an error matrix. Before starting the accuracy assessment process, the classified images from Geomatica software were exported to ArcMap in GeoTiff format. ArcMap and Microsoft Excel were used to achieve that, whereby reference data (validation points) were generated then compared with the classification output. Stratified Random sampling was used to generate 150 validation points by using the Create Accuracy Assessment Points tool in each classified map and saved them in shapefile format. Afterward, loaded the shapefile into google earth pro to compare generated validation points with

what is on the ground using high-resolution images from google earth pro. Where there was uncertainty, the point was visited on the ground to resolve the LULC, for example, an area that has been debushed after the image was taken or built-up area (expansion of settlements) or newly cultivated lands. Google earth has been exploited in a wide range of land cover studies (Arhem and Freden, 2014; Feda, 2018, Worku, 2018; Sourlamantas, 2019).

3.4.1.4.5 Deriving the C factor

Cover Management factor (C) is defined as the ratio of soil loss from a particular cropped area under specified conditions to the corresponding loss from continuous tilled fallow (Wischmeier and Smith, 1978). The C factor is one of the most vital factors that control soil erosion Wang et al., 2013). For this study, the LULC map for 2000 and 2020 with a 30m resolution was created with a maximum likelihood supervised classification of five different LULC classes (Cultivated land, Shrubland, Built-up areas, Woodland (tree savanna), and Waterbody) using Geomatica 2018 (Figure 11a and Figure 12a). After the classification, the raster layer was converted into a vector layer and the C-factor values were assigned for each land-use/land-cover class according to the following researchers (Wishmeir and smith, 1978; Hurni, 1985; Ganasri and Ramesh, 2015; Feda, 2018; Kidane et al., 2019; Moisa et al., 2020) based on Table 10 using ArcMap 10.7. Then the C values were converted to raster by conversion tool method from polygon to raster (Figure 11b and Figure 12b). Normally, a better cover on the ground has the ability to reduce energy from the raindrop and also reduce runoff and therefore have a low C value because it can protect the soils from wind and water erosion. The C factors ranged from 0 to 0.2 (Table 10).

Table 10: RUSLE C factor of the study area

No	LULC	C-value	Source
1	Built-up	0.01	Hurni (1985) and Kidane et al.,(2019)
2	Cultivated land	0.2	Hurni (1985) and Kidane et al.,(2019)
3	Shrubland	0.1	Wishmeir and smith (1978)
4	Woodland (Tree Savanna)	0.001	Hurni (1985) and Moisa et al.,(2020)
5	Waterbody	0	Ramesh and Ganasri (2016) and Feda (2018)

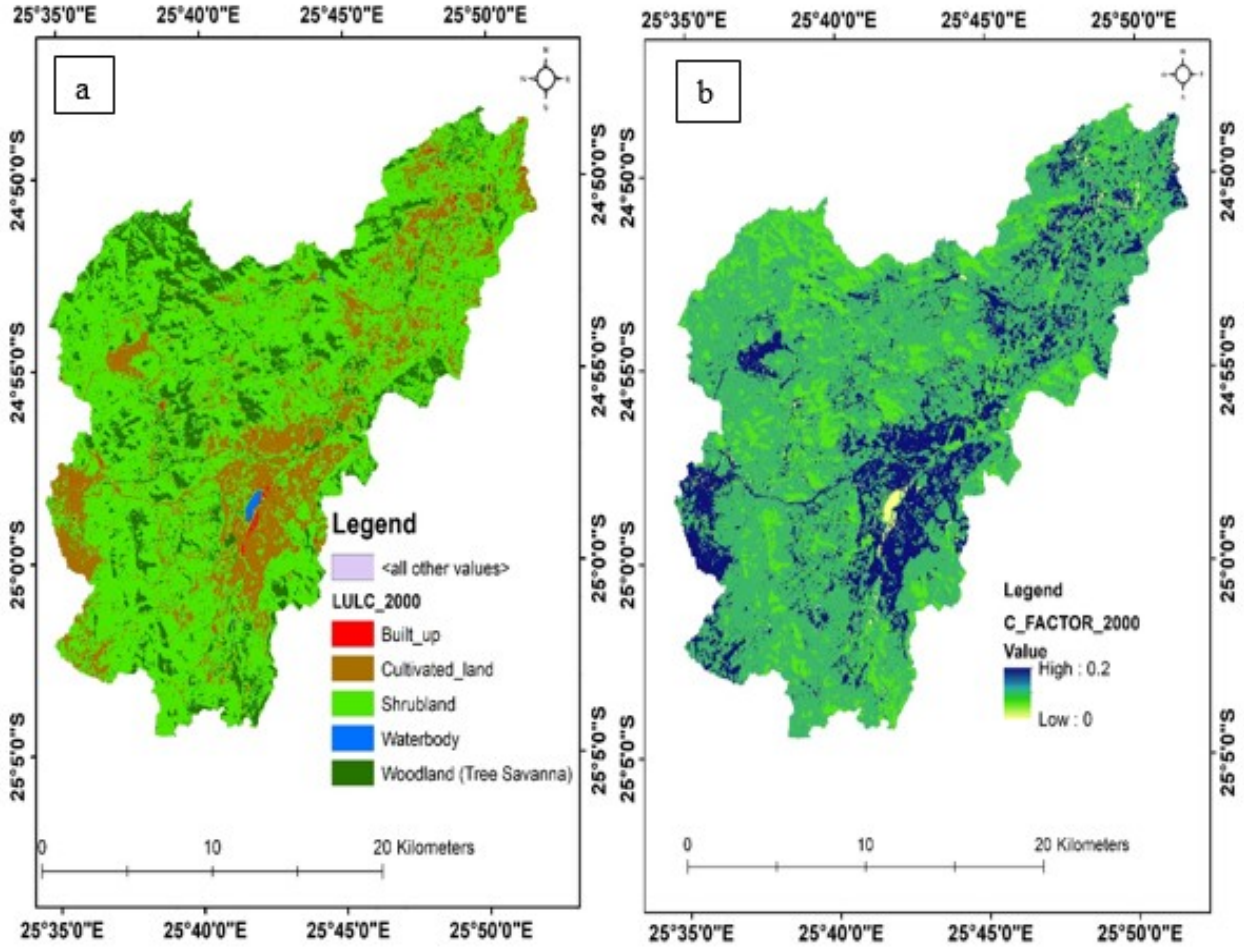

Figure 11: Spatial distribution of (a) Land-use and land-cover for 2000 and (b) RUSLE Cover management (C) factor in the Taung Watershed

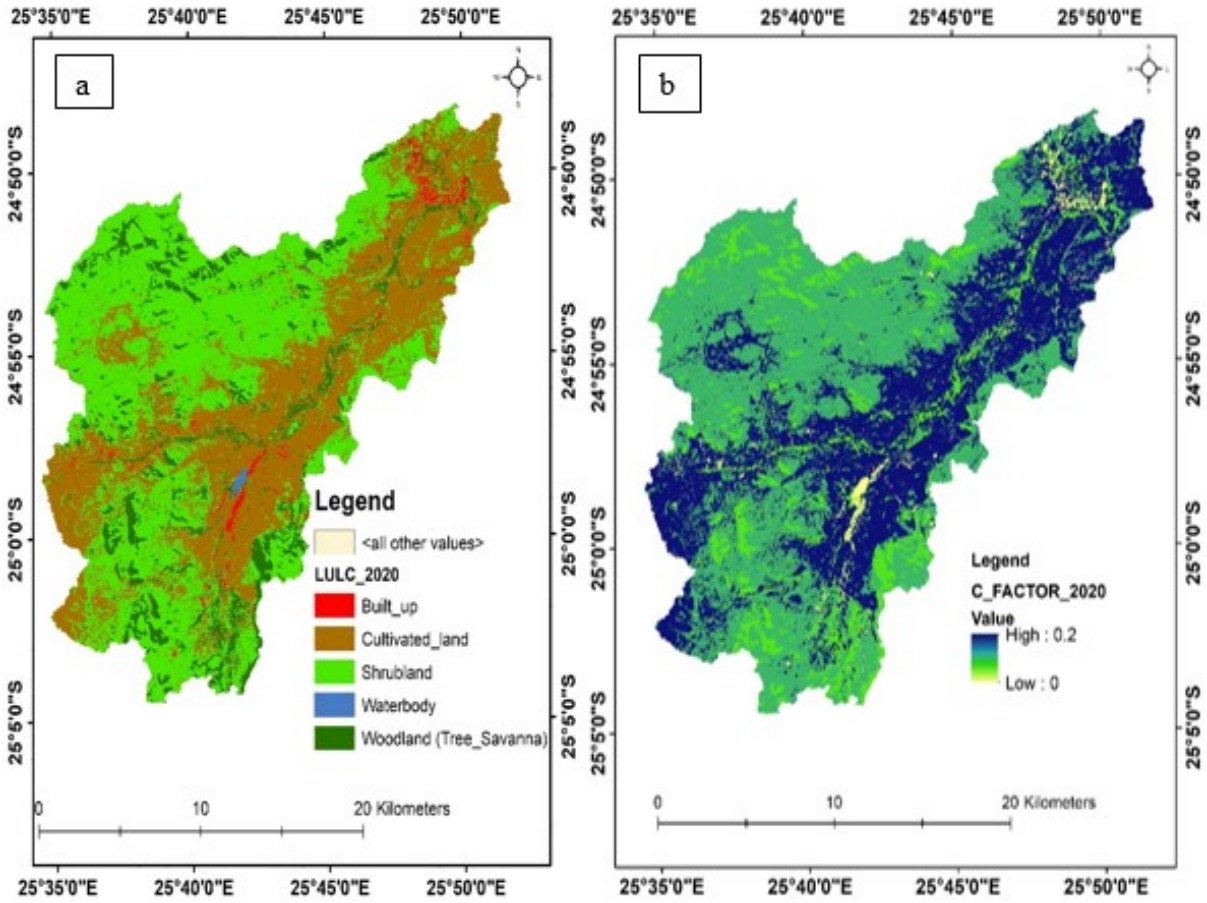

Figure 12: Land-use and land-cover for 2020 (a) and RUSLE Cover management(C) factor map for 2020 (b)

3.4.1.5 Management Practice Factor (P)

The management practice factor (P) represents the ratio of soil loss after a specific conservation practice to the corresponding soil loss after upward and downward cultivation" (Renard et al., 1997). The P factor ranges from 0 to 1 (Kaltenrieder, 2007). Areas with poor support practice are assigned 1 (Simms, 2003) while 0 indicates good conservation practice (Gansari and Ramesh, 2016). In some parts of the Taung watershed, agronomic control practices such as ploughing across the slope and deep ploughing are not commonly practiced within the individual farm field. There is also minimal usage of mechanical control practices where contour bunds, gabion structures exist however, there is poor maintenance from the farming community side and it is no longer serving the purpose due to its high cost and technical know-how. Considering these aforementioned circumstances along with the lack of satisfactory conservation practices-related data in the Taung

watershed, the P factor was derived from the LULC maps. The P-values were derived from the literature varying from 0 to 0.9 across different LULC classes (Table 11). The map output for the P factor in 2000 and 2020 are shown in Figure 13a and Figure 13b.

Table 11: P factor of the study area

No	LULC	P-Value	Source
1	Built-up	0.63	Moisa et al.,(2020)
2	Cultivated land	0.90	Hurni (1985) and Moisa et al.,(2020)
3	Shrubland	0.63	Hurni (1985) and Feda (2018)
4	Woodland (Tree Savanna)	0.53	Hurni (1985) and Feda (2018)
5	Waterbody	0	Hurni (1985) and Feda (2018)

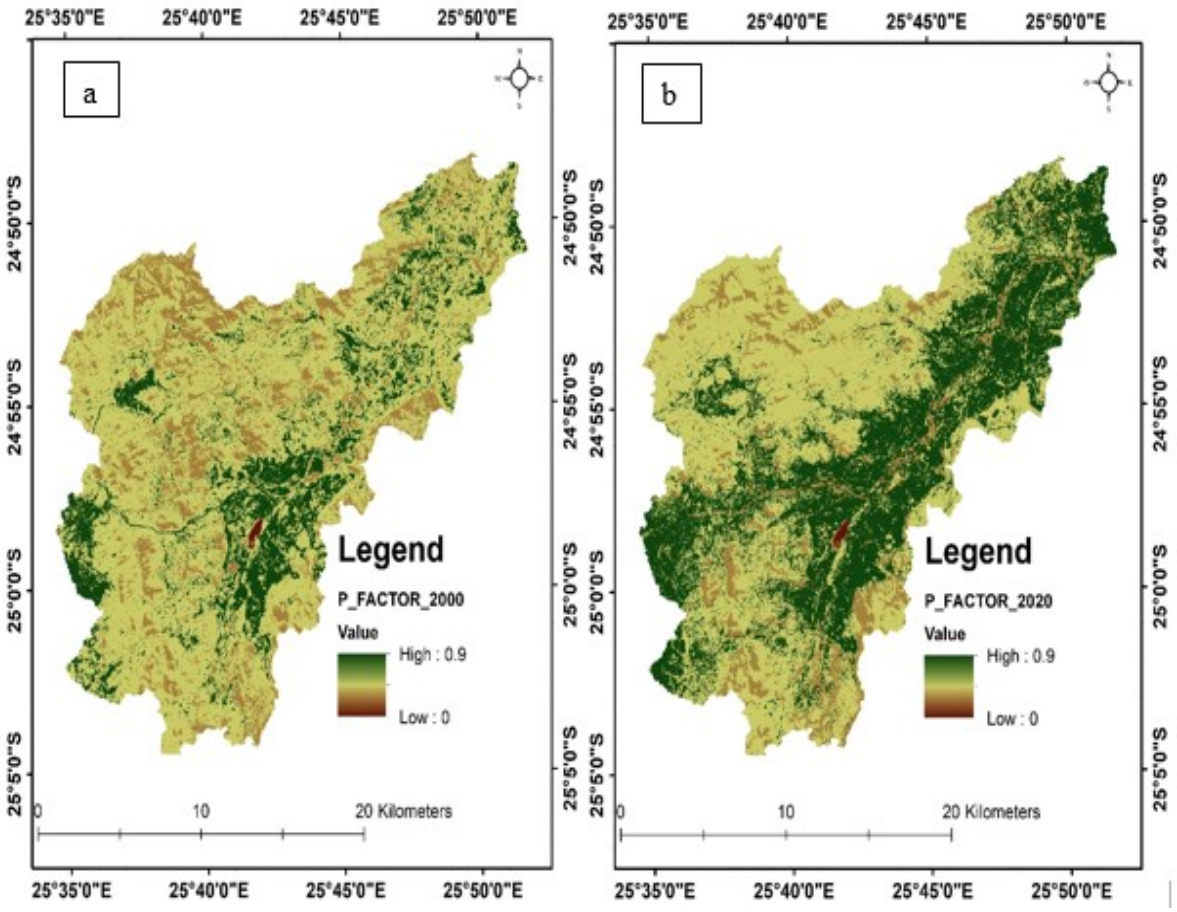

Figure 13: Management practices (P) factor map for 2000 (a) and 2000 (b)

3.4.1.6 Estimation of soil erosion rate of the study area

All the six RUSLE factors (R, K, LS, C and P) that were identified were all converted into a raster format and each layer was then changed to the same cell size of 30m. Lastly, layers were overlaid/multiplied through the use of the Raster Calculator toolset in ArcMap 10.7. The results of those factors were recorded as the soil loss of the study area in tons/ha/year for the years 2000 and 2020.

It should be noted that the R, C and P factors varied over the years while K and LS were assumed to be the same for both 2000 and 2020 because twenty years is not long enough for the soil to change, hence there is so significant variation of the soil in the study time frame.

3.4.1.7 Mapping the spatial variability of erosion and identify high-risk areas

After the computation of the soil loss in the study area, the erosion rates were classified into six categories using ArcMap 10.7 software. Erosion rates from 0-5 tons/ha/year, 5-12 tons/ha/year, 12-25 tons/ha/year, 25-60 tons/ha/year, 60-150 tons/ha/year and >150 tons/ha/year were categorized as very low,low,moderate,high,very high and extremely high risk areas respectively (Phinzi, 2018). Moreover, each severity class was given a priority class number ranging from 1 to 6.

3.4.2 Soil Loss Estimation Model for southern Africa (SLEMSA)

The following sub-models were utilized in SLEMSA to estimate soil erosion. Crop ratio (C), Principal Factor (K), and Topographic ratio (X). The formula of SLEMSA is expressed as;

$$Z = K * C * X \qquad \text{Equation 6}$$

Where Z is the mean annual soil loss rate (ton/ha/year); K is the principal factor (tons/ha/yr)**;** C is the Crop factor (dimensionless) and X is the topographic factor (dimensionless). ArcMap was used to implement those factors. A simplified flow chart of the data analysis is shown in Figure 14.

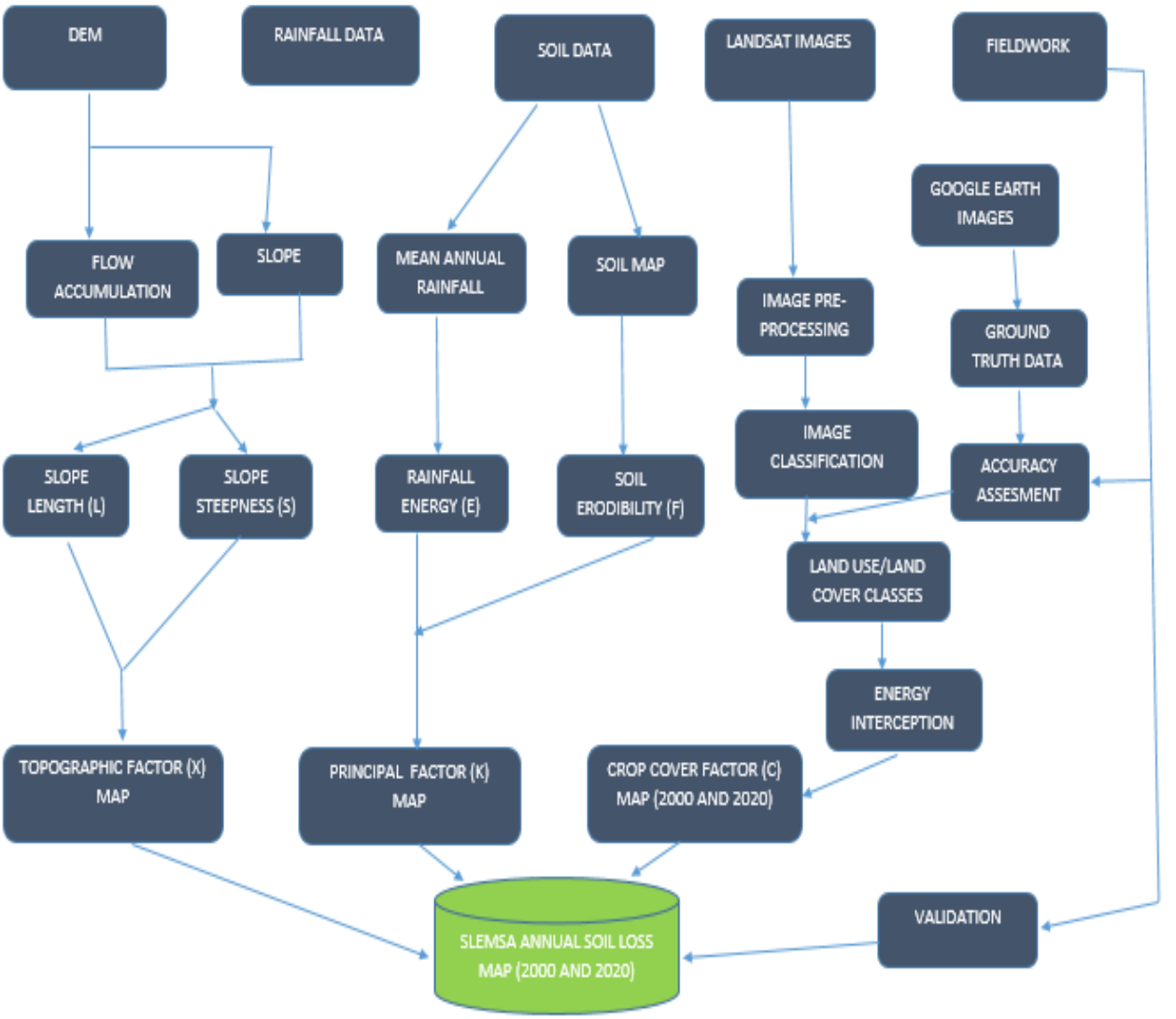

Figure 14: The overall flow chart of the SLEMSA methodology

3.4.2.1 Principal Factor (K)

It combines the influence of the rainfall energy and soil erodibility to give the estimated mean annual soil loss from conventionally tilled bare soil on 4.5% slopes and 30 m by 10m (Stocking, 1980). The K factor in this study was derived from soil erodibility (F) and soil erosivity (E) using the following equation by Morgan (1995).

$$K = \exp[(0.468 + 0766F)InE + 2.88 - 8.121F] \qquad \text{Equation 7}$$

The K factor values varied from 0.306871 tons/ha/yr to 28.5627 tons/ha/yr (Figure 15). It was also recognized that the highest K factor values occurred in the south east and western areas of the Taung watershed.

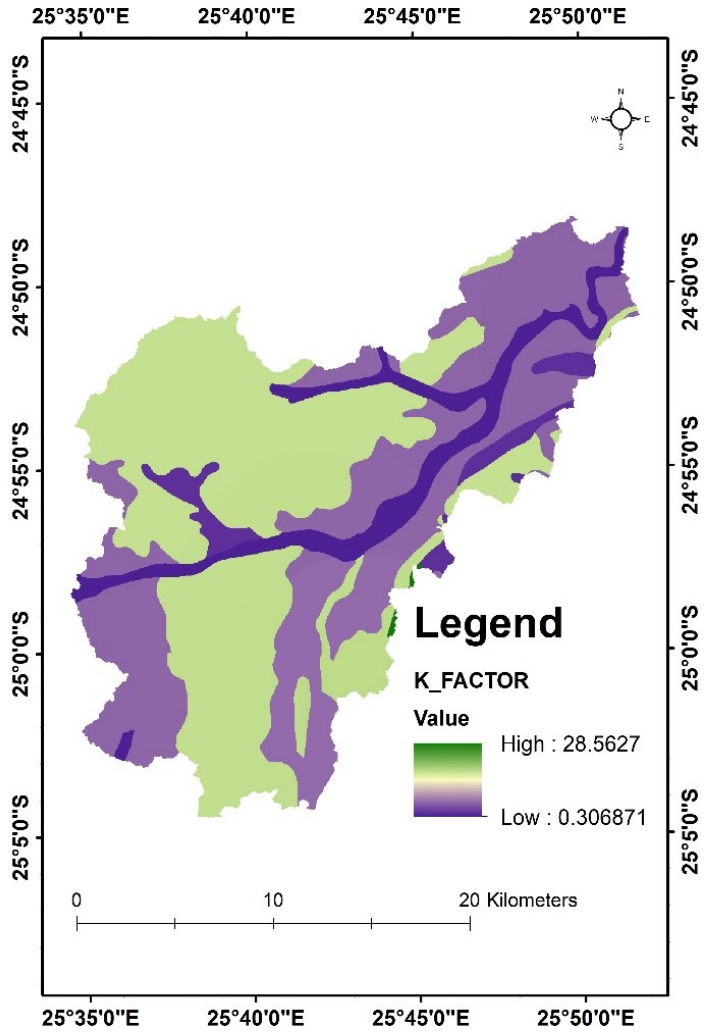

Figure 15: Principal K factor map

Soil erodibility factor (F)

Soil erodibility is the ability of soil particles to resist detachment and transportation by rainfall. It is derived from the inherent physical properties of soil such as soil texture. However, it has been noted that the F value ranges from a scale of 1 to 10. The most erodible soils are set to be 1 while 10 indicates the least erodible soils. There is no direct way of measuring F, However, the basic index is normally derived from soil textural classes and then modified by adding or subtracting the

adjustment value, which represents management practices (Elwell, 1978). In this study, Table 12 proposed by Morgan (1986) was used to obtain the F-value.

Table 12: Calculation of the F value for soil erodibility in SLEMSA

The first calculation of the F value				**Adjustments to the 1st calculation of the F Value Add**	
Soil texture	Class	F value		Add	Soil and manage characteristics
Sands	Light	4		-1	Light textured soil consisting mainly of sand and silts
Sandy loams				-1	Restricted vertical permeability within 1m from the surface or severe crusting
Loamy sand				-1	Ridging up and down the slope
				-1	Deterioration in soil structure due to more than 20ton/ha/yr. in the previous year
Sandy clay loam	Medium	5		-1	Poor management
Clay loam				-0.5	Slight to moderate surface crusting
Sandy clay				-0.5	Soil loss 10-20 t/ha/yr. in the previous year
				2	Deep well-drained light-textured soil
Clay	Heavy	6		1	Tillage operations encouraging high water retention (contour ridging
Heavy clay				1	First season on no-tillage
					Subsequent season on no-tillage

(Source: Morgan, 1986)

Rainfall energy (E)

According to Schultze (1979), the E factor is the kinetic energy of raindrops as they strike the soil or vegetation**.** Initially, the E factor equation was derived by Hudson (1965) as shown below:

$$E = 0.298(1 - \frac{4.29}{Imax}) \quad \text{Equation 8}$$

Where E is the rainfall energy in ($Mjmm^{-2}$)and I is the rainfall intensity in (mm).

Due to lack of rainfall intensity data, a relationship between resultant total rainfall energy (E) and annual rainfall amount was developed by Elwell (1978) for the SLEMSA model and it is expressed by

$$E = 18.846 * P \text{ for normally aggressive climates} \quad \text{Equation 9}$$

$$E = 17.368 * P \text{ for areas prone to drizzle} \quad \text{Equation 10}$$

Where P is the Annual rainfall amount in (mm).

There is a lack of available continuous rainfall intensity data in the Taung watershed. Therefore, for this study, mean annual rainfall data was used to estimate the E factor. The rainfall energy (E) was calculated from rainfall amounts recorded at 7 different rainfall stations in and around the watershed shown in Table 5. It was calculated the same way as in the RUSLE model except that in the SLEMSA model, a different equation by Elwell (1978) was used.

$$E=18.846*P \quad \text{Equation 11}$$

Where E is the rainfall energy in ($Mjmm^{-2}$) and P is the mean annual rainfall amount in (mm).

3.4.2.2 Topographic Factor (X)

The topographic factor represents the ratio of soil erosion from slope length L in (m) and slope steepness S in (%). It has been reported that a steeper and longer slope corresponds to greater erosion rates (Doere, 2005). The Topographic factor was derived the same way as in the RUSLE model except that a slightly different equation was implemented. From the map output, the X factor values range between 0 to 417.689 (Figure 16). The X factor was computed using an equation below derived by Bizuwerk (2008).

$$X = L^{0.5}(0.76 + 054S + 0.0765S^2)/25.65 \qquad \text{Equation 12}$$

where X is the topographic factor, S is the slope steepness in (%), L is the slope length in (m) and is calculated from Flow accumulation * cell size.

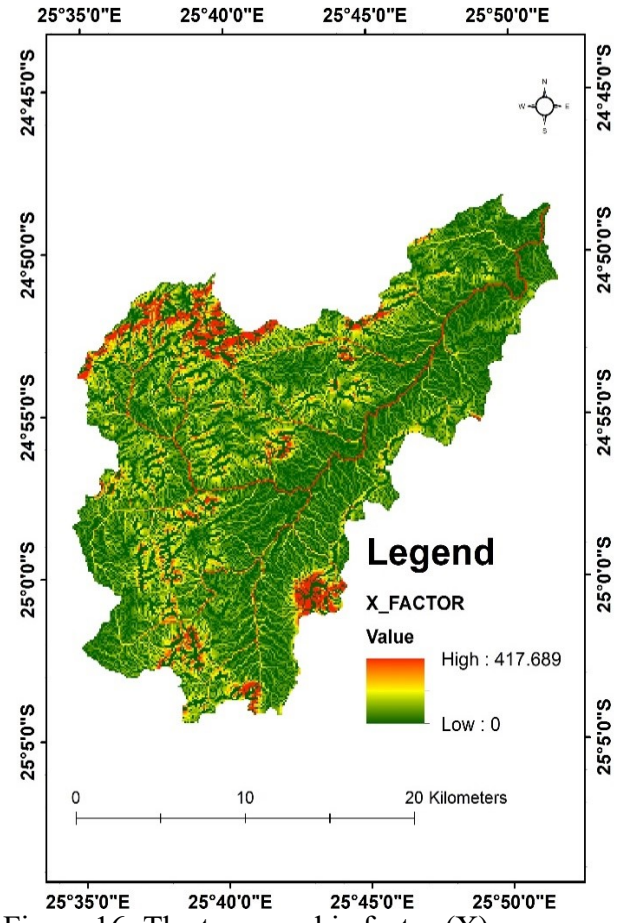

Figure 16: The topographic factor (X) map

3.4.2.3 Crop cover Factor (C)

According to Alphan et al. (2009), the C factor is the ratio of soil loss from a vegetated land compared to soil loss from the bare fallow. The C factor is derived from the control variable i which indicates the rainfall energy that is intercepted by vegetation cover. The cover factor is based on a Zimbabwean model (SLEMSA) originally developed for grassland by Elwell and Stocking (1976) and Figure 17 shows how the C factor is derived. In this study, the crop factor was obtained from two classified Landsat images for the years 2000 and 2020. The prepared LULC maps of the watershed were used to find the C values corresponding to each land cover class. The corresponding C values for each land cover class were sourced from other studies (Wishmeir and smith, 1978; Eweg & Van Lammeren 1996; Ganasri and Ramesh, 2016; Feda, 2018) (Table 13). The i value was obtained from the corresponding C value using the graph in Figure 17 and C values ranged from 0 to 0.63 as shown in Figure 18a and Figure 18b. After the i values were obtained, the Cover Model C1 formula was used to compute C in this study.

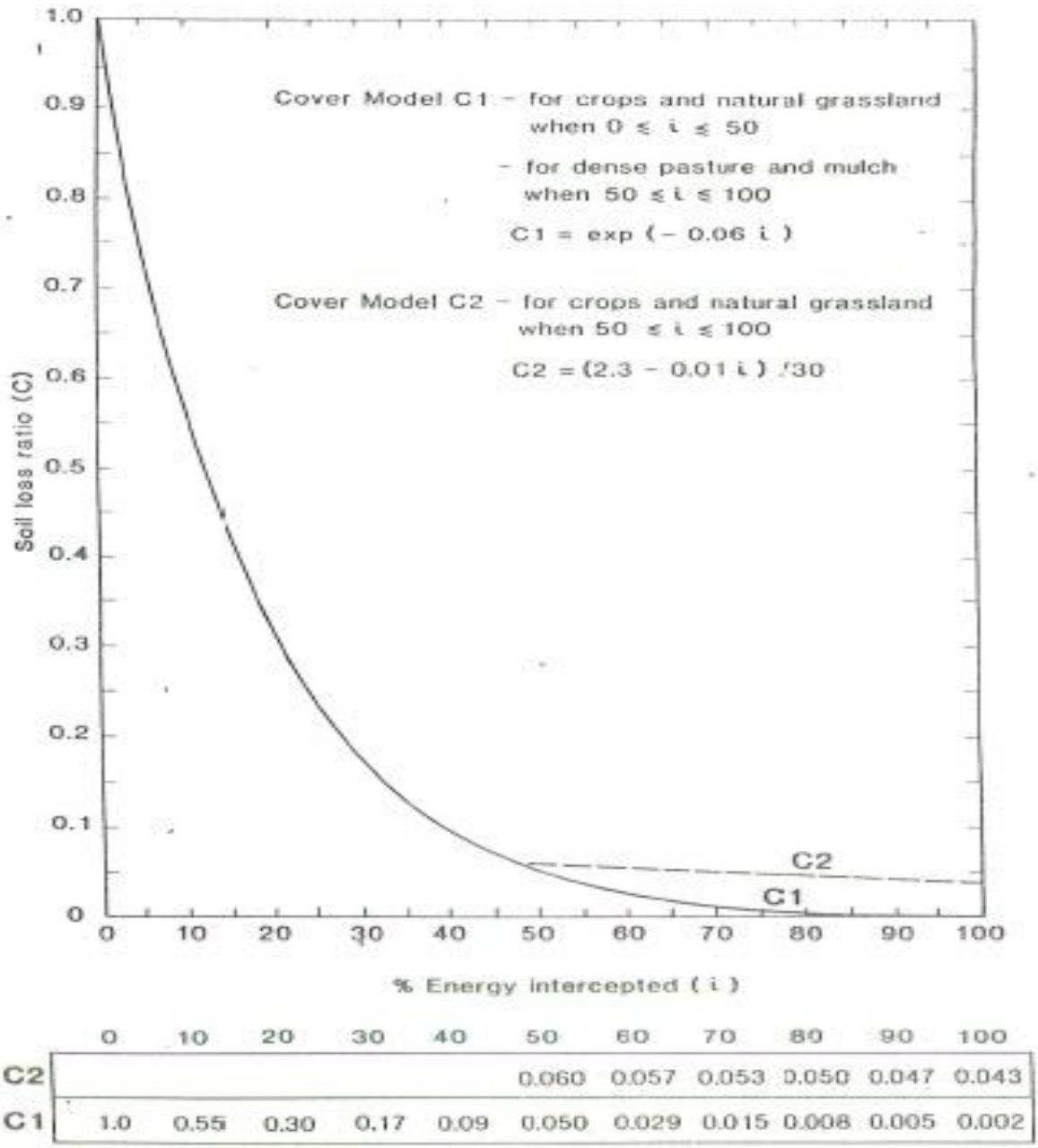

	0	10	20	30	40	50	60	70	80	90	100
C2						0.060	0.057	0.053	0.050	0.047	0.043
C1	1.0	0.55	0.30	0.17	0.09	0.050	0.029	0.015	0.008	0.005	0.002

Figure 17: Relationship between vegetation cover factor (C) and energy interception (i) showing i value greater than or less than 50 (Elwell, 1978) for SLEMSA model

Table 13: SLEMSA C factor of the study area

No	LULC	C-value	Source
1	Built-up	0.09	Ramesh and Ganasri (2016)
2	Cultivated land	0.63	Ramesh and Ganasri (2016)
3	Shrubland	0.1	Wishmeir and smith (1978)
4	Woodland (Tree Savanna)	0.06	Eweg & Van Lammeren (1996)
5	Waterbody	0	Ramesh and Ganasri (2016) and Feda (2018)

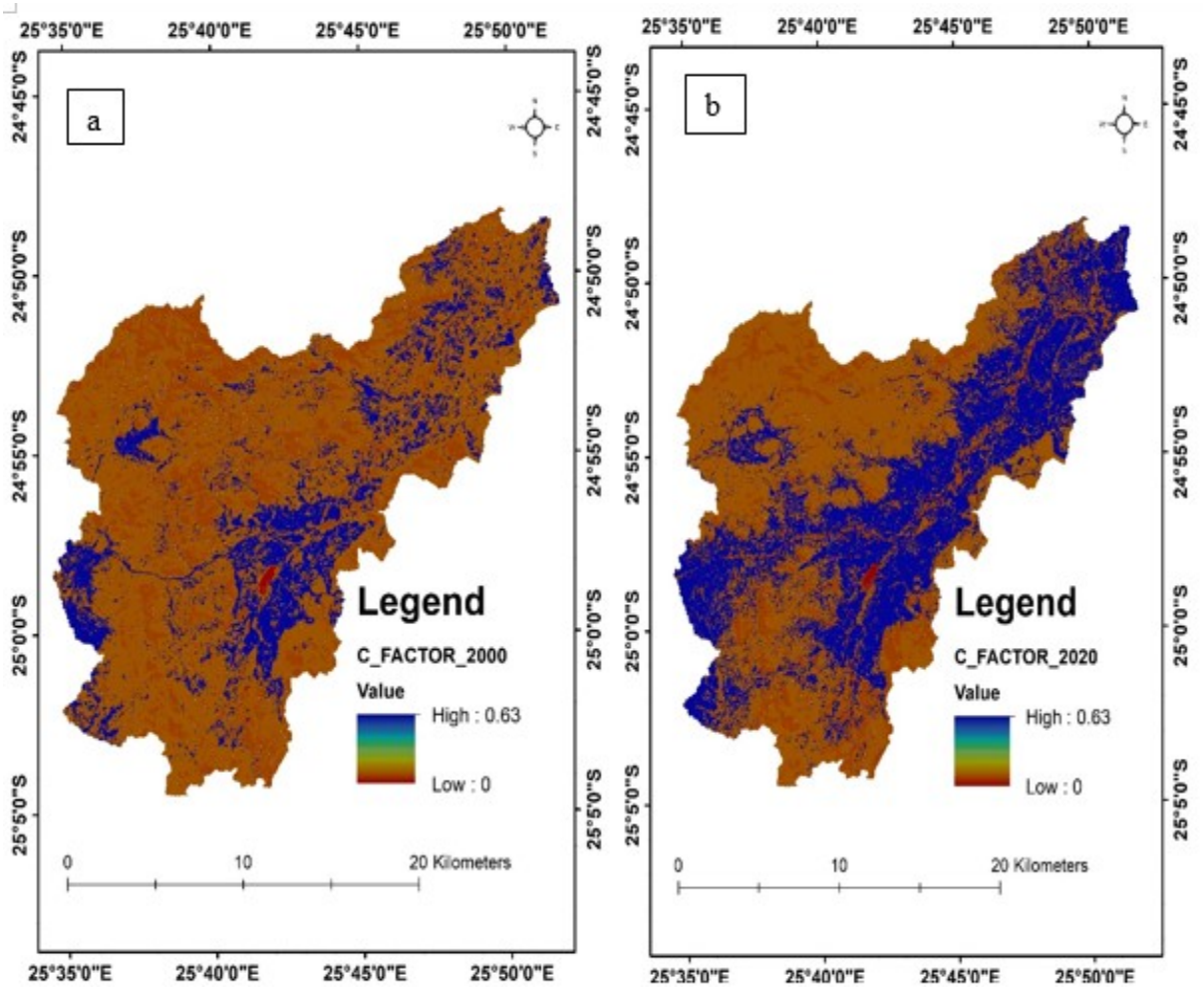

Figure 18: SLEMSA Crop management (C) factor map for 2000 (a) and 2020 (b)

3.4.2.4 Estimation of soil erosion rate of the study area

All three factors (K, X, and C) that were identified, were converted into a raster format then each layer was changed to the same cell size of 30m. Lastly, they were overlaid/multiplied through the use of the Raster Calculator toolset in ArcMap 10.7. Then the results of those factors were recorded as the soil loss of the study area in tons/ha/year for the years 2000 and 2020. It should be noted that the K and X were assumed to be the same for both 2000 and 2020 while the C factor varied.

3.4.2.5 Mapping the spatial variability of erosion and identify high-risk areas

The same classification of identifying high-risk areas used in the RUSLE model was also implemented in the SLEMSA model.

3.4.3 Validation of soil erosion models

Validation of the empirical erosion models is not easy because of the lack of available soil loss data in the Taung watershed area for comparing the estimates of SLEMSA and RUSLE with the actual losses. However, a similar method of soil erosion accuracy assessment done by Phinzi (2018) was adopted in this study to ascertain the quality and reliability of the model's results. Kappa was used to validate the model's result in terms of eroded and non-eroded areas. The soil loss was reclassified into high and low soil loss classes from the different soil loss severity classes, for example, low soil loss was composed of very low and low severity classes while high soil loss included moderate to extremely high soil loss severity classes. After the reclassification of the soil loss maps, 10 random points were generated and loaded into a handheld GPS. The GPS was then used to locate and verify these points on the ground. Afterward, a confusion matrix tool in ArcGIS was used to compute the Kappa Coefficient of agreement.

Only 2020 soil loss maps for SLEMSA and RUSLE were used for validation since 2000 is the historical hence could not be assessed.

4.0 RESULTS

4.1 Erosion Risk in the Watershed as Determined from RUSLE and SLEMSA

Table 14 shows the soil loss statistics of the study by using RUSLE and SLEMSA models. The estimated soil erosion risk maps were produced for 2000 and 2020. The estimated mean soil loss averaged 12.04 t/ha/year in 2000 and 12.74 t/ha/year in 2020 for the RUSLE model. The spatial patterns of the estimated soil erosion risk indicate areas with high soil erosion loss mostly on the cultivated areas and along the streams at steep slopes (Figure 19). For the RUSLE model, more soil loss is observed in the northeast, central, eastern and southwestern parts of the Taung watershed. SLEMSA model estimated the mean annual soil loss of 11.77 t/ha/year in 2000 and 12.57 t/ha/year in 2020. SLEMSA results show the highest mean annual soil loss within the watershed, particularly on cultivated land on the highlands, woodland and some parts of shrubland which are mainly located in the steeper slopes of the study area. From Figure 20, the soil loss is more dominant in the northwestern, central, and also southern zones of the study area. The results from Table 14 show that soil loss increased over the years (2000-2020) for both the models, although the SLEMSA recorded the highest soil loss as compared to RUSLE in this study. Comparing the two models' results, it can be seen that a value of 0 was recorded in both models, specifically in the waterbodies.

Table 14: Soil loss statistics for the Taung watershed using RUSLE and SLEMSA models

	RUSLE		SLEMSA	
	2000	2020	2000	2020
Average soil loss (t/ ha/ year)	12.04	12.74	11.77	12.57
Maximum soil loss (t/ha/year)	918.08	970.14	1641.24	1943.20
Minimum soil loss (t/ha/year)	0	0	0	0

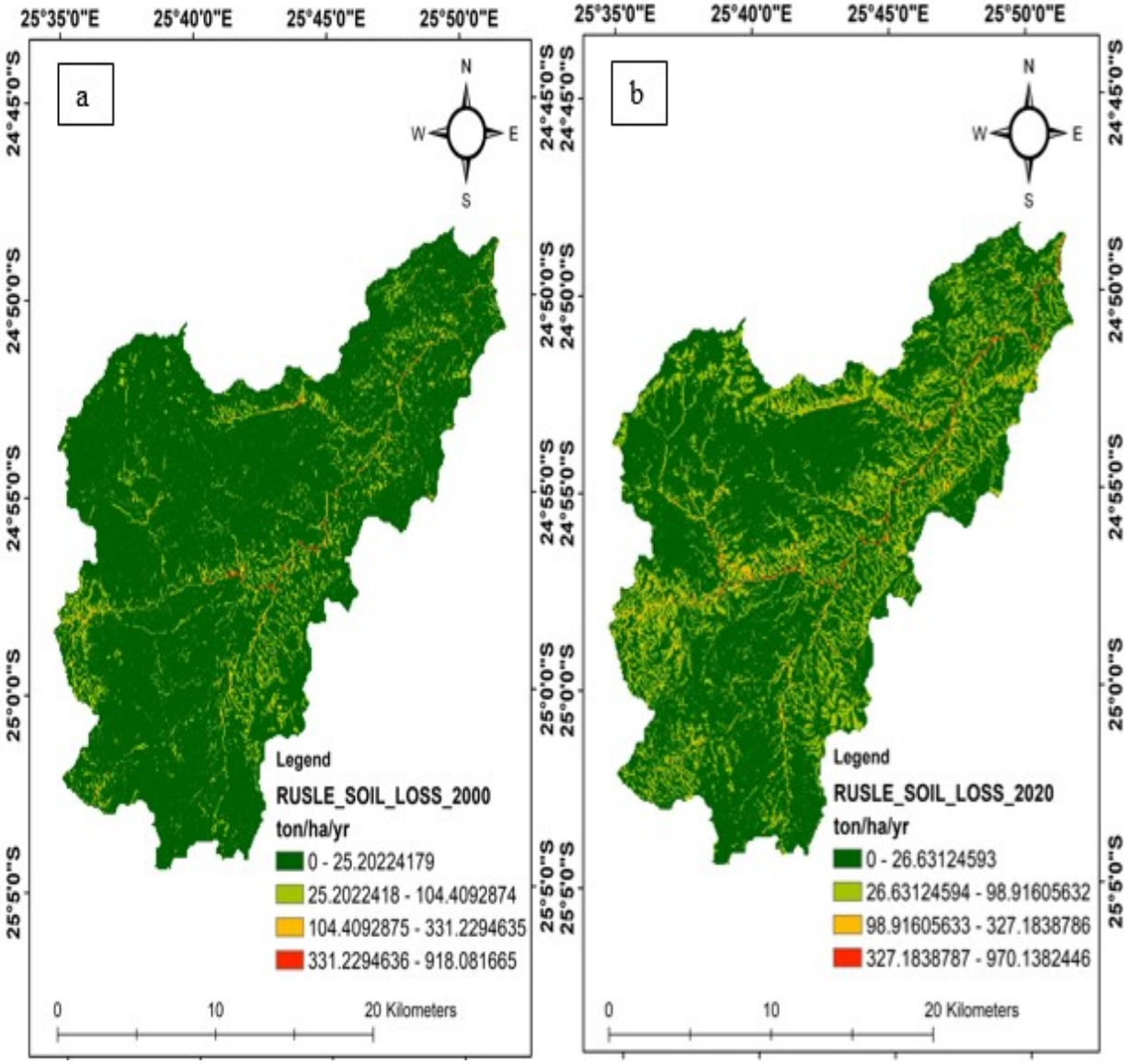

Figure 19: RUSLE soil loss (ton/ha/year) map of the study area for 2000 (a) and 2020 (b)

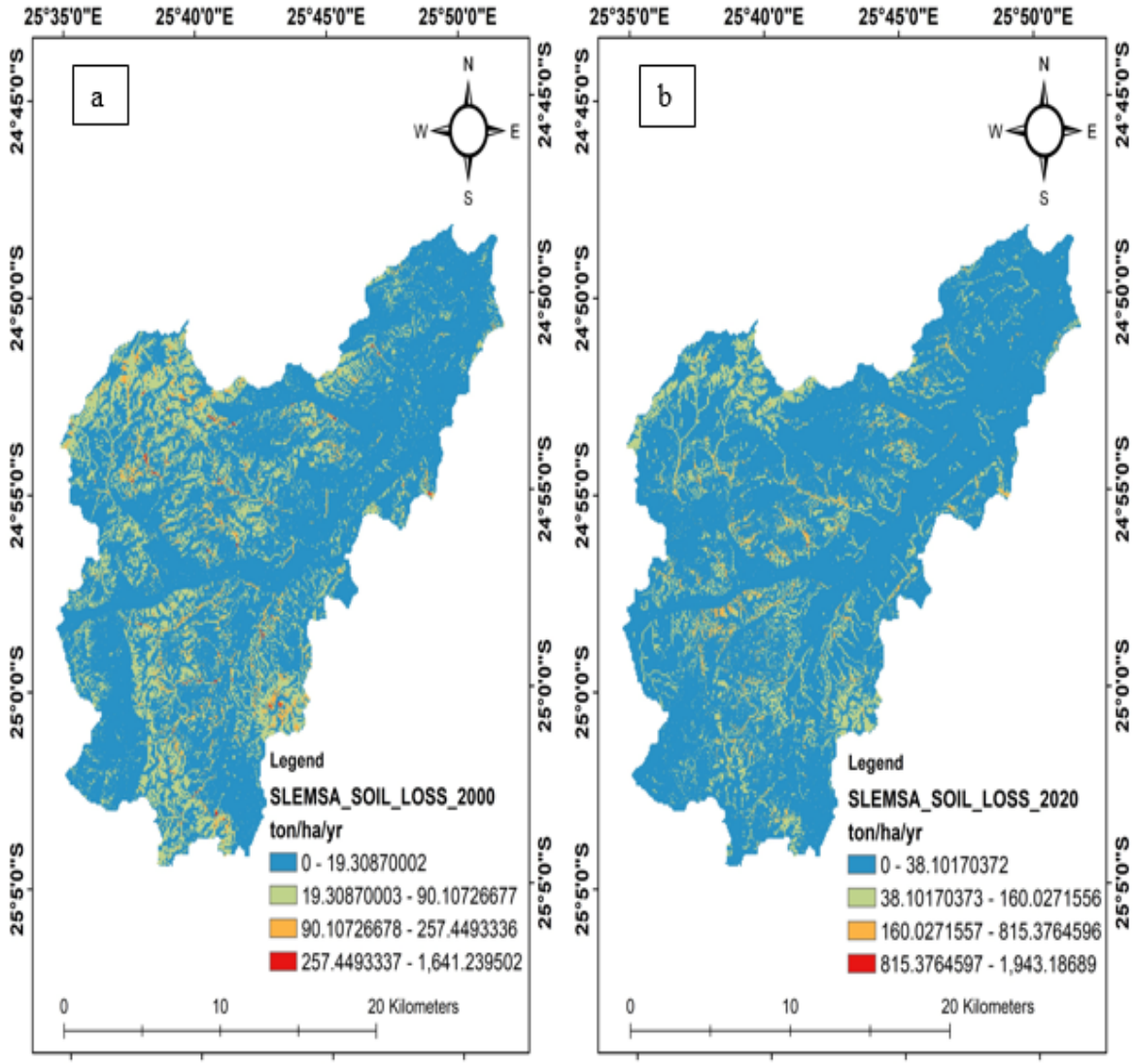

Figure 20: SLEMSA soil loss (ton/ha/year) map of the study area for 2000 (a) and 2020 (b)

The soil loss data for the study area was further classified into soil erosion severity classes, namely, very low, low, moderate, high, and very high (Figure 21 and Figure 22) adapted from Phindzi (2018). It can be seen from Table 15 and Table 16 that the largest proportion of the watershed experienced very low erosion in the two periods for both models. Very low, and low severity classes decreased with time while areas with moderate, high, very high, and extremely high classes increased. The acceptable soil loss tolerance for tropical climates is about 11 tons/ha/year (Morgan, 2009). The results indicate that up to 30.5% of the watershed area experience high soil loss above 12 tons/ha/year and close to 23% occurs on the moderate and high severity classes when using the RUSLE model and about 43.5% for SLEMSA and about 33% is also found in similar classes as

RUSLE (Table 17). These results may be due to the rise in population which leads to severe deforestation, overgrazing and also, animal pathways that contribute to the development of rill erosion through the removal of vegetative cover over time (Figure 23). Some of the soil loss was also observed along the roadside on steep areas of the Taung watershed during ground truthing as depicted in Figure 24. A possible explanation for this might be that construction activities negatively impact the stability of soil structure and therefore give rise to soil erodibility. In this study, the priority class has been assigned based on the mean annual soil loss rates and the severity, ranging from 1 which shows that the area needs immediate attention up to 5 which means the area needs less attention (Table 15 and Table 16). Moreover, only recent soil loss estimates of 2020 for both SLEMSA and RUSLE are considered for prioritized soil conservation measures and land use planning.

Table 15: RUSLE soil loss for 2000 and 2020

Annual Soil Loss (tons/ha/year)		**Priority Class**	**2000**		**2020**	
	Severity Classes		**Area (ha)**	**Area (%)**	**Area (ha)**	**Area (%)**
0-5	Very low	5	25502.12	58.01	22939.04	52.18
5-12	Low	4	8509.56	19.36	7616.4	17.33
12-25	Moderate	1	4691.83	10.67	4897.72	11.14
25-60	High	1	3000.79	6.83	5314.97	12.09
60-150	Very high	2	1755.66	3.99	2519.87	5.73
>150	Extremely high	3	498.11	1.13	670.07	1.52

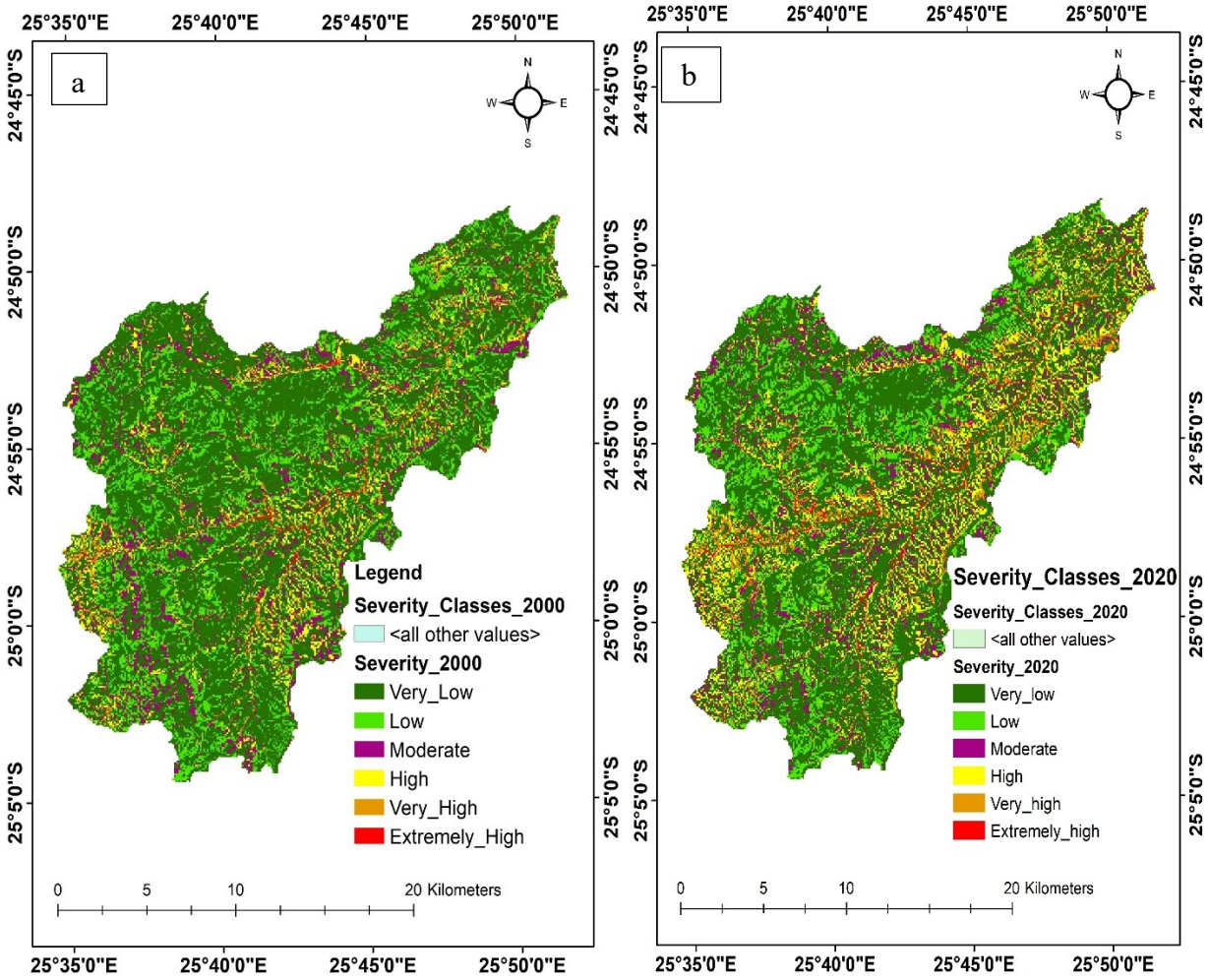

Figure 21: RUSLE Severity classes map of the study area for 2000 (a) and 2020 (b)

Table 16: SLEMSA soil loss for 2000 and 2020

Annual Soil Loss (tons/ha/year)	**Severity Classes**	**Priority Class**	**2000**	**2020**		
			Area (ha)	Area (%)	Area (ha)	Area (%)
0-5	Very low	5	22730.85	51.71	20236.61	46.04
5-12	Low	4	5197.71	11.82	4592.98	10.45
12-25	Moderate	1	6970.24	15.86	7575.21	17.23
25-60	High	1	5772.11	13.13	6980.97	15.88
60-150	Very high	2	2639.06	6.00	3318.92	7.55
>150	Extremely high	3	648.10	1.47	1253.38	2.85

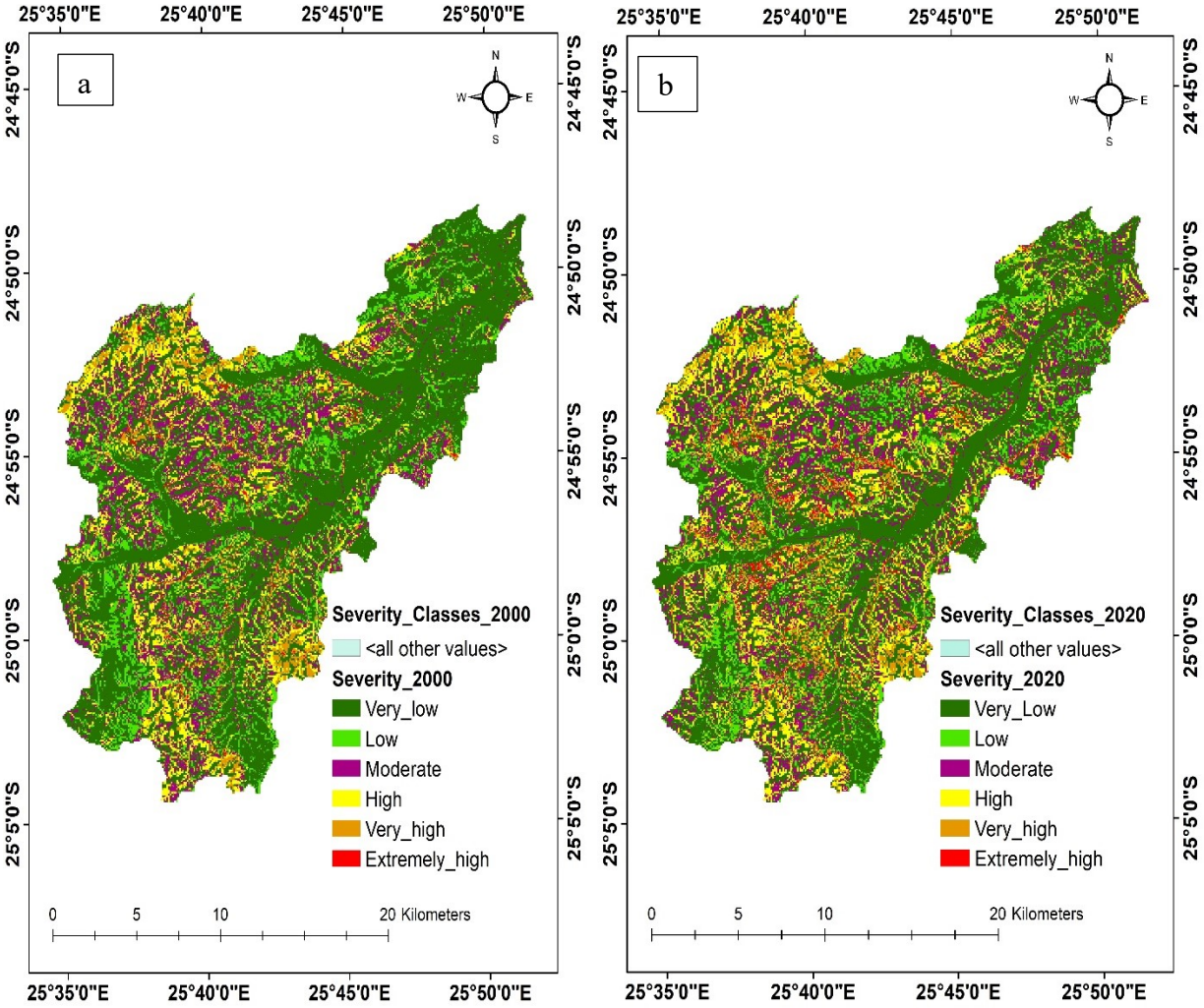

Figure 22: SLEMSA Severity classes map of the study area for 2000 (a) and 2020 (b)

Table 17: Erosion status and area coverage used for validation

Severity Classes	Erosion status	RUSLE	SLEMSA
		Area %	Area %
Very low	No Erosion (less than or equals 12 tons/ha/year)	69.5	56.5
Low			
Moderate	Erosion (more than 12 tons/ha/year)	30.5	43.5
High			
Very high			
Extremely high			

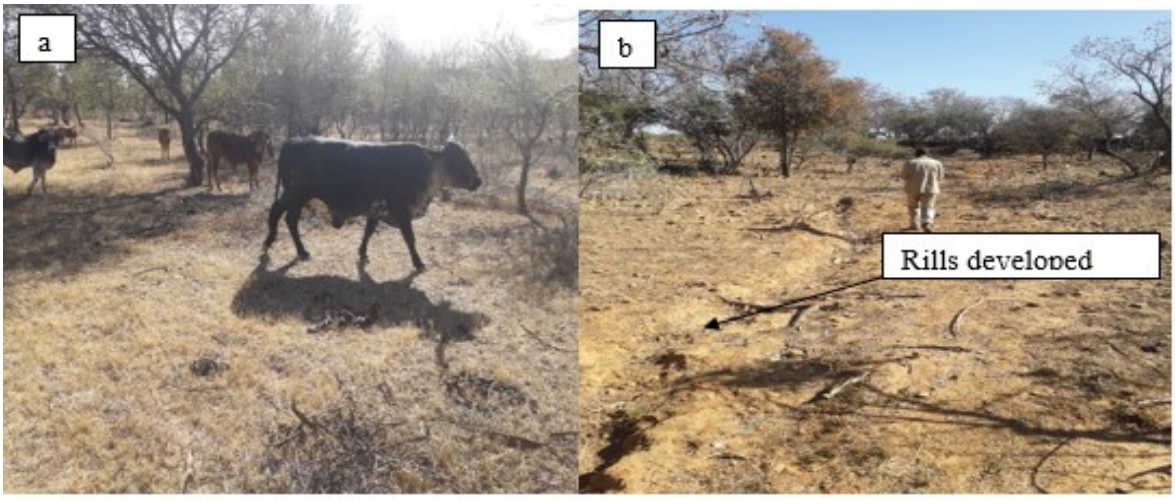

Figure 23: Overgrazed area in the watershed (a) and Rills developed on steeper slopes (b)

Figure 24: The magnitude of erosion observed along a tarred road going towards Magotlhwane village

4.2.1 Validation of RUSLE and SLEMSA

The ground truth data was obtained through a handheld GPS to validate RUSLE and SLEMSA's results. Table 17 contains information that was used to help validate the models. A Kappa coefficient of 0.78 and 0.40 for RUSLE and SLEMSA was attained, respectively (Appendix 3). The overall accuracy for RUSLE was 90% while SLEMSA had 70%.

4.2 Land Use/Land Cover between 2000 and 2020

Cultivated land increased while shrubland and woodland decreased between 2000 and 2020 as shown in Figure 25. The cultivated land increased by 8846 ha between 2000 and 2020 (Table 18). The total change for built up area increased during the study period from 619 ha in 2000 to 878 ha in 2020 due to an increase in population over the years. The major part of the Taung watershed is found in the South East administrative district which had an estimated human population of 60623 in 2001 (Statistics Botswana, 2011) and 94252 in 2020 (Statistics Botswana, 2020), thus indicating a 35% increase in human population over the period. Shrubland decreased from 67% of the watershed in 2000 to 48% in 2020 (Figure 26). Woodland similarly dropped from 14% to 11%. However, there was a sharp rise in cultivated land from 18% to 38% in 2020. For the full extent of LULC see Appendix 1.

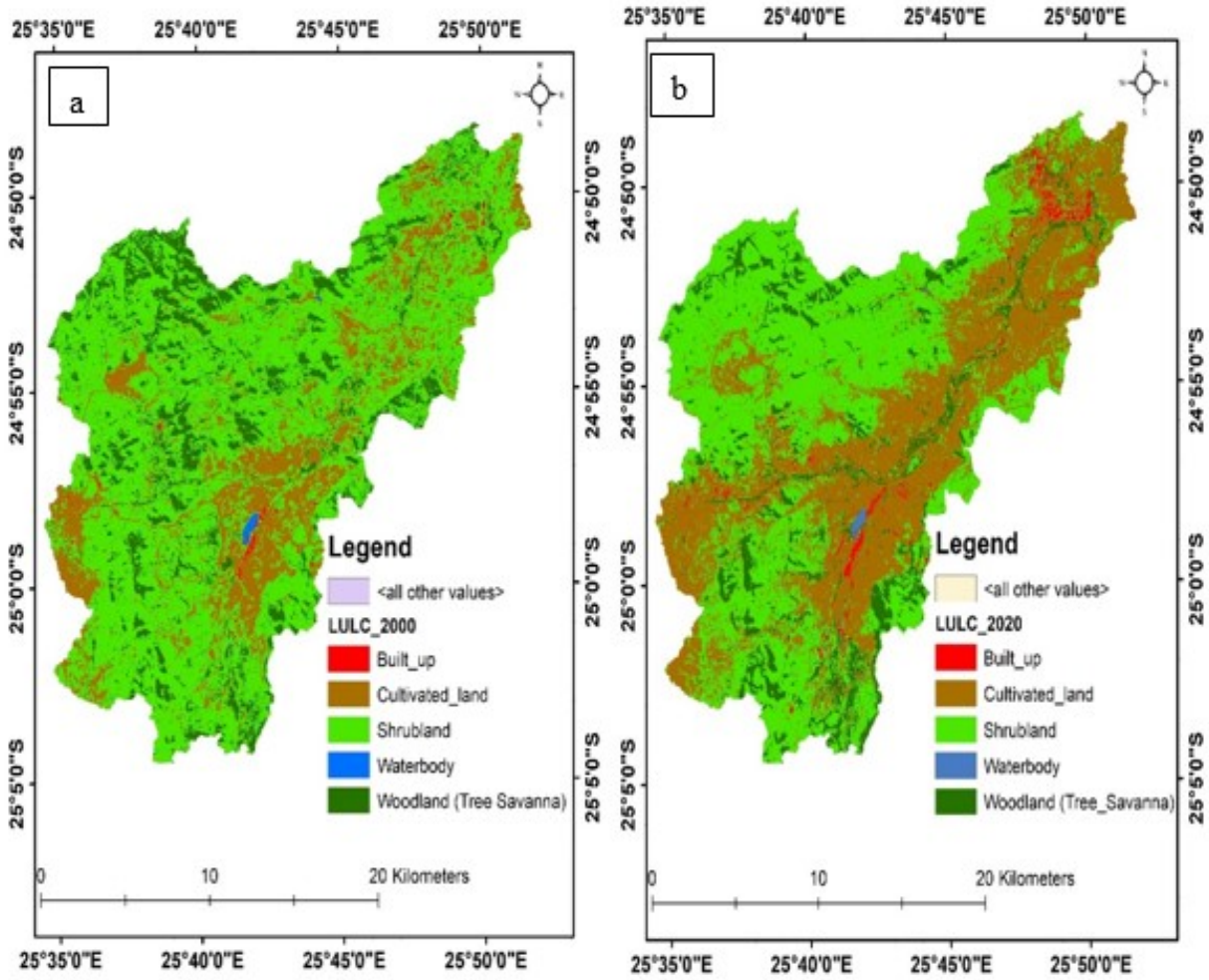

Figure 25: LULC for 2000 (a) and 2020 (b)

Table 18: LULC for 2000 and 2020

LULC	Area (ha) 2000	Area (ha) 2020
Built-up	619.20	878.40
Cultivated land	7872.30	16718.67
Shrubland	29457.45	21314.97
Woodland (Tree Savanna)	5935.05	4963.32
Waterbody	74.07	82.71
Total area	**43958.07**	**43958.07**

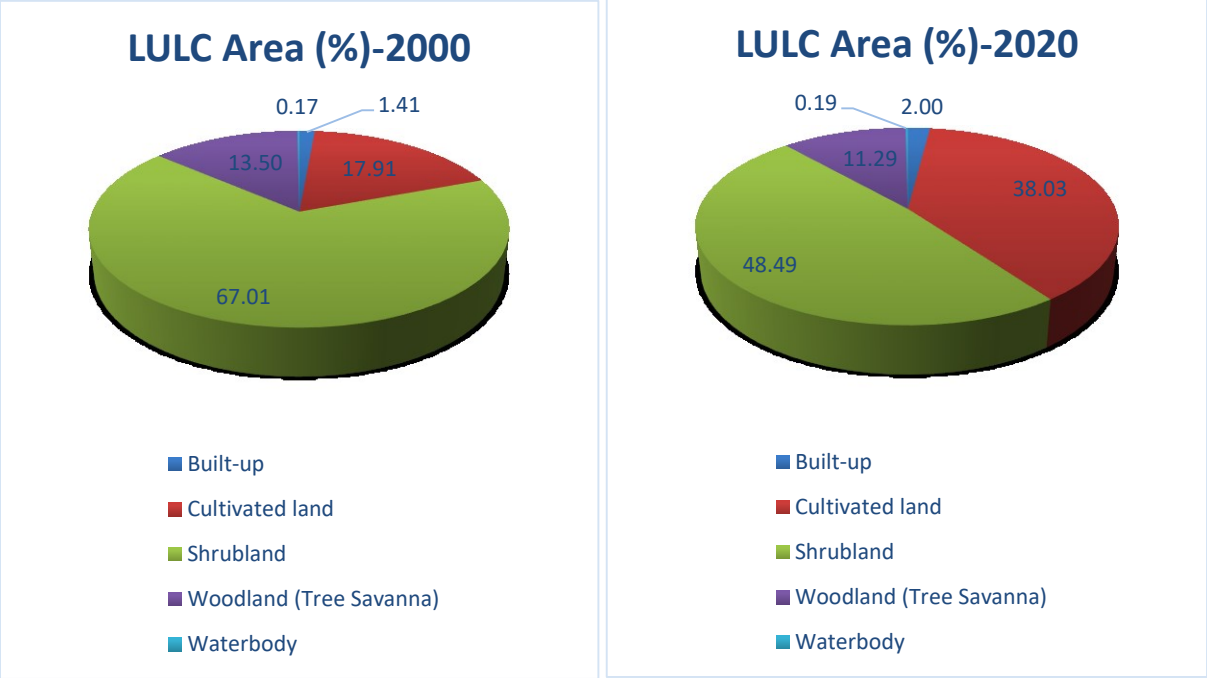

Figure 26: LULC change (%) in the study area

4.2.1 Accuracy Assessment of the Land Use/Land Cover

The ground truth data obtained from a high-resolution image was used to compare the accuracy of the image classification with what was in the field. An overall accuracy of 81.0%, and 87.0% was attained, with a Kappa coefficient of 0.71, and 0.81 for the two images (Landsat ETM+ 2000, and Landsat OLI 2020), respectively (Appendix 2).

5.0 DISCUSSION

5.1 Erosion Risk in the Watershed as Determined by RUSLE

Noticeable changes in LULC took place across the Taung watershed. The mean average soil losses increased from 12.04 in 2000 to 12.74 tons/ha/year in 2020. Due to the lack of data on soil formation rates for the soils of Botswana, estimation of tolerable soil loss needs further investigation in the country. However, an acceptable soil tolerable level of 11 tons/ha/year due to erosion for tropical ecosystems (Morgan, 2009) was used in this study. Since there was no actual soil loss measurement in the study area, other studies with similar conditions were consulted for comparison. Several studies have modelled and measured soil loss in Southern Africa. Marondedze and Schütt (2020) obtained a potential erosion risk of 13.2 ton/ha/year between 1984 and 2018 in Epworth District in Zimbabwe**.** In Botswana, Alemaw et al. (2013) obtained higher average soil loss values that were twice as high as those obtained in this study. These results are likely to be related to the fact that naturally, the erosion modelling technique output depends on the physical environment.

The C factor for cultivated lands was given high values because of its high susceptibility to erosion as compared to other LULC classes. Therefore, the estimated soil loss rose when the LULC class changed to cultivated land as other model factors were assumed to be constant. Similar findings were also reported by Abebe (2015). The northeast, central, eastern and southwestern parts of Taung watershed have high erosion rates. This result may be explained by the fact that the large part of the area experienced the highest conversion into cultivated land as compared to other parts of the watershed and consequently a noticeable decrease in shrubland (in terms of area coverage). In addition, the soil types of the area (sandy clay loam to sandy clay and sandy loams to sandy clay) have a high K factor value of 0.042144 to 0.063875 compared to other soil types. Therefore, the LULC and soil type comprise the key determinants of high soil erosion risk. This finding was also reported by Feda (2018). Furthermore, more potential soil loss was shown along streams and rivers at steep slopes. It seems possible that these results are also due to the high LS factor which was found in hills and also along river banks as earlier reported by Ester (2009). It would seem that these results could also be due to the high LS factor which was in hills and also along river banks. This observation is supported by previous evidence (Ester, 2009). Similar results have been

reported by Abebe (2015). However, RUSLE can become less accurate at extreme slopes and climatic conditions (Manrique, 1993). Arhen and Freden (2014) reported that extremely high values of soil loss were not realistic as compared to the average soil loss rates and argued that the accuracy of the values required actual field measurements.

5.2 Erosion Risk in the Watershed as Determined by SLEMSA

This study also estimated soil erosion by using the SLEMSA model. The spatial patterns of soil erosion were then analyzed and visualized through the use of ArcMap. In reviewing the literature, no historic data was found for the Taung watershed and thus estimation of soil loss with SLEMSA was completed to provide information for this study area. However, Abel and Stocking (1987) estimated the soil loss adjacent to the study area in the south east of Botswana. The researchers reported total soil erosion of 1-12 ton/ha/year. However, the mean annual soil loss estimated in this study ranged from 11.77 to 12.57 ton/ha/year which is noticeably higher than the one found by Abel and Stocking (1987) and also above the acceptable soil loss tolerance of 11 ton/ha/year (Morgan, 2009). The very low rates by Abel and Stocking (1987) could be attributed to the gentle slope and the existing LULC rangelands in the study area.

Other SLEMSA studies by Vargas and Omuto (2016), Breetkze et al. (2016) and Bvindi (2019) reported mean annual soil losses of 29 (Malawi), 13.88 (South Africa) and 2.76 ton/ha/year (South Africa), respectively. These differences can be attributed to the varying physical environment of the reported areas. The greatest changes in erosion were found in the highland areas of the watershed. A possible explanation for these results could be that the highest conversion into cultivated land was accompanied by intensive cultivation on steep areas compared to RUSLE where high soil values were found in low and high cultivated land areas. Therefore, topography and LULC markedly contributed to a high soil erosion risk in this study. These results are in line with those reported by Arhem and Freden (2014). Hudson (1987), however, reported that SLEMSA becomes less accurate under extreme conditions of steep slopes and climatic conditions.

5.3 Comparison of Erosion Risk in the Watershed as Determined by RUSLE and SLEMSA

The difference between the estimated losses of the two erosion modelling techniques is comparable. As mentioned before, Table 14 provides soil loss statistics for the entire watershed. The mean estimated values were higher using RUSLE than SLEMSA. The revealed soil loss by

both SLEMSA and RUSLE due to soil erosion risk for Taung watershed was slightly above the recommended limits of 11 ton/ha/year (Morgan, 2009). The model results show that topographic characteristics (LS and X) influenced potential erosion and soil erosion risk in the Taung watershed, which are in line with the findings by Ester (2009) and Marondedze and Schutt (2020). From the erosion map outputs, soil loss by RUSLE was severe in the cultivated land areas at low and high altitudes while that by SLEMSA was severe in cultivated areas of steeper slopes. This could be explained by the fact that SLEMSA was developed in the Zimbabwean Highveld areas. This severe soil loss on the fields might have been influenced by little or no crop residues left on the cultivated lands, hence exposing the bare soils to precipitation at the onset of the rainy season (Morgan, 2005; Ferreira, 2015). In addition, animals in the study area are normally allowed to graze on the cultivated land after harvest. Furthermore, the pre-season land preparation also exposes the finely tilled soil to more rainfall energy due to reduced ground cover which generally dissipates and scatters the raindrop energy (Renard et al., 1997).

In line with these findings, it has been reported that high erosion is primarily driven by steep slopes (Bewket and Teferi, 2009). This implies that any future research emphasis should be placed on cover management and topographic factors. Surprisingly, rainfall erosivity from SLESMA and RUSLE was found to have less significance to the soil loss results.

The Kappa coefficients of agreement for RUSLE and SLEMSA were 0.78 and 0.40, respectively (Appendix 3). This indicates a very good agreement for RUSLE and a good agreement for SLEMSA (Sourlamtas, 2019). Furthermore, the RUSLE model results seem to indicate a higher degree of agreement with the state of soil erosion in the Taung watershed. Smith (1999) reported that the theoretical and sensitivity analysis that was performed on USLE, RUSLE and SLEMSA, clearly showed the advantages of the more flexible and dynamic structure of RUSLE against those other two empirical models. Jaramilo (2007) reported that the RUSLE model was specifically designed for deriving soil erosion on clear land where overland runoff occurs significantly

Although RUSLE is a better estimator of soil loss than SLEMSA, Smith (1999) highlighted that SLEMSA is useful in differentiating areas of high and low erosion potential, which was evident in

this study. It is important to bear in mind that this study's calculated soil loss rates are mere estimates as opposed to absolute values of soil loss (Le Roux et al., 2008), and therefore must be treated with caution. Overall, the technique employed in this study was sufficient for identifying the spatial patterns and distribution of the high soil erosion risk areas in the Taung watershed. Wordofa (2011) reported that land managers and policymakers are usually interested in the spatial distribution of soil erosion risk than absolute values of soil erosion loss. According to the RUSLE results in Table 16, it is recommended to concentrate conservation efforts on moderate to high severity classes with a combined area of 23% because they form a reasonably large proportion of the study area and also confined within the cultivated areas. The pattern of priority conservation under SLEMSA (covering 33% of moderate to high severity classes) is similar to RUSLE save the inclusion of shrubs and forested areas in the former due to their degradation for firewood, polls for fencing and overgrazing. Further research is still required to effectively evaluate the accuracy of SLEMSA and RUSLE by assessing the confidence limits of erosion estimates produced from these two models.

5.1 Land Use/Land Cover (2000-2020)

The study found that there was a major increase in cultivated land and built-up area coverage while other LULC categories such as shrubland and woodland decreased during that period (Figure *26*). These results confirm the findings of Matlhodi et al. (2019) in the Gaborone Dam Catchment area, which covers the Taung watershed. This increase and decrease in LULC coverage may be attributed to human and animal population growth, agricultural expansion and non agricultural activities (firewood collection, harvesting construction and fencing materials) (Feda, 2018). The majority of the Taung watershed is located in Botswana's South East administrative region, which had a human population of 60623 (Statistics Botswana, 2011) and 94252 (Statistics Botswana, 2020) in 2001 and 2020, respectively.

As a typical example, about 74000 ha of wood resources were cleared during the Accelerated Rainfed Arable Programme (ARAP) in Botswana (Department of Crop Production and Forestry, 2003, cited in Central Statistics Office, 2008). Increased anthropogenic activities have altered the LULC (Sebego et al., 2019; Matlhodi et al., 2020). The final accuracy of LULC achieved for the Taung watershed ranged between 81.0% and 87.0% which is comparable to Akinyime and Mashame (2018), who achieved an overall accuracy of 82% to 88%. In addition, prior studies

noted that an overall accuracy between 60.0 and 90.0% was acceptable (Mango, 2010) and therefore it means that the accuracy of LULC classes in this study is within the acceptable limit. In this study, Kappa coefficients of 0.71 and 0.81 for Landsat TM 2000 and OLI 2020 images were, respectively, attained (Appendix 2). The limitation of the LULC classification in this study was the misclassification of the classes with similar spectral signatures as it was not easy to distinguish them.

6.0 CONCLUSION

The main goal of this study was to spatially assess soil erosion risk in the Taung watershed of Ramotswa Agricultural District using RUSLE and SLEMSA models integrated with RS and GIS. This study estimated the soil erosion risk and its spatial distribution within the study area in 2000 and 2020. The results from the two models do not differ with the spatial distribution of soil erosion hazards in the Taung watershed. The estimated annual soil erosion averaged 12.04 t/ha/year in 2000 and 12.74 t/ha/year in 2020 for the RUSLE model. The SLEMSA model estimated the mean annual soil loss of 11.77 and 12.57 t/ha/year in 2000 and 2020, respectively. Thus, the results show that the estimated soil erosion risk escalated over the study period (2000-2020). The LULC and soil type are key determinants of high soil erosion risk when using the RUSLE model. In SLEMSA, however, topography and LULC markedly contributed to a high soil erosion risk. About 20.12% of the area in the watershed was converted into croplands from 2000 to 2020, and that accelerated the susceptibility of soil to erosion. The results indicate that a high soil loss of over 12 tons/ha/year covers 30.5% and 43.5% of the study area using RUSLE and SLEMSA, respectively. The model validation revealed that the RUSLE model had a high Kappa Coefficient of agreement of 0.78 indicating very good agreement (whereas SLEMSA recorded a low Kappa Coefficient of agreement 0.40 indicating a good agreement). This study provides valuable information that may help land-use planners, policymakers, and decision-makers on soil conservation planning and land reclamation for the study area.

6.1 LIMITATIONS

This study was limited by the absence of studies on soil erosion by water within the study area which reduced alternatives for comparison and validation. The study area had few sparse rain gauge stations to spatially represent the rainfall pattern. Rainfall erosivity from SLESMA and RUSLE was found to have less significance to the soil loss results. The reason for this could be due to interpolation of rainfall stations which were somehow distant from each other, prompting the need for a denser rainfall stations network for future studies. Since the study was limited to assessing soil erosion on rugged terrain, its findings may only be applied to areas with similar environmental characteristics in Botswana.

6.2 RECOMMENDATIONS

1. The findings gathered from this study could be applied for functional soil conservation planning and watershed management.
2. Measuring the actual soil loss using field plots is ideal for validating the SLEMSA and RUSLE models and therefore further research could be useful.
3. It would be wise to concentrate conservation efforts on moderate to high severity classes in both models because they form a reasonably large proportion of the study area (covering 23% and 33% under RUSLE and SLEMSA, respectively).
4. The use of empirical soil erosion models such as RUSLE and SLEMSA intergrated with RS and GIS should be applied in estimating the soil erosion rates and mapping of erosion hazard areas.
5. Further research should focus on the assessment of gully erosion and sedimentation in the Taung watershed.

REFERENCES

Abel, N., & Stocking, M. (1987). A Rapid Method for Assessing Rates of Soil Erosion from Rangeland: An Example from Botswana. Journal of Range Management, 40(5), 460. Retrieved from https://doi.org/10.2307/3899612.

Agele, D., Lihan, T., Sabihin, A. R. ., & Rahman, Z. A. (2013). Application of the RUSLE model in forecasting Soil Erosion at downstream of the Pahang. Journal of Applied Sciences Research, 9(1), 413–424.

Akinyemi, F. O., & Mashame, G. (2017). Mapping and Modelling Land Susceptibility to Water Erosion in Eastern Botswana, 19, EGU2017-909, 2017.

Alemaw, B. F., Majauale, M., & Simalenga, T. (2013). Assessment of Sedimentation Impacts on Small Dams—A Case of Small Reservoirs in the Lotsane Catchment. Journal of Water Resource and Protection, 05(12), 1127–1131. Retrieved from https://doi.org/10.4236/jwarp.2013.512118

Alkharabsheh, M. M., Alexandridis, T. K., Bilas, G., Misopolinos, N., & Silleos, N. (2013). Impact of land cover change on soil erosion hazard in northern Jordan using remote sensing and GIS. Procedia Environmental Sciences, 19, 912–921. Retrieved from https://doi.org/10.1016/j.proenv.2013.06.101 .

Alphan, H., Doygun, H., & Unlukaplan, Y. (2009). Post classification of land cover using multitemporal Landsat and ASTER imagery: the case of Kahramanmaras, Turkey. Environmental Monitoring and Assessment, 151(1-4), 327-336.

Angulo-Martínez, M., & Beguería, S. (2009). Estimating rainfall erosivity from daily precipitation records: A comparison among methods using data from the Ebro Basin (NE Spain). Journal of Hydrology, 379(1-2), 111-121.

Arhem, K., & Freden, F. (2014). Land cover change and its influence on soil erosion in the Mara region, Tanzania (MSc Thesis). Department of Physical Geography and Ecosystems Science, Lund University, Tanzania.

Arnoldous, H.M.J.(1980). An approximation of the rainfall factor in the USLE in assessment of Erosion. England: Wiley Chichester.

Arnoldus, H. M. J. (1977). The methodology used to determine the maximum potential average annual soil loss due to sheet and rill erosion in Morocco. Assessing soil degradation, 34. Rome; FAO Soil Bulletins

Bai, Z.G., Dent, D.L., Olsson, L.,& Schaepman, M.E. (2008). Proxy global assessment of land degradation. Soil Use & Management, 24: 223–234

Balasubramanian, A. (2017). Soil Erosion- Causes and Effects Soil Erosion; Centre for Advanced Studies in Earth Science, University of Mysore, Mysore. March, 7. Retrieved from https://doi.org/10.13140/RG.2.2.26247.39841

Bari, F., Wood, M. K., & Murray, L. (1995). Livestock Grazing Impacts on Interrill Erosion in Pakistan. Journal of Range Management. 48(3): 251-257

Beck, M.B.(1987). Water quality modelling: a review of uncertainty.Water Resources Research 23 (8), 1393–1442.

Bhattarai, R., & Dutta, D. (2007). Estimation of soil erosion and sediment yield using GIS at catchment scale'. Water Resources Management, 21(10), 1635-1647.

Bizuwerk, A., Taddesse, G., and Getahun, Y. (2008). Application of GIS for modelling soil loss rate in Awash Basin, Ethiopia. Addis Ababa: International Livestock Research Institute (ILRI).

Bobe. B (2004). Evaluation of Soil Erosion in the Harerge Region of Ethiopia, Using Soil Loss Models, Rainfall Simulation and Field Trials. Unpublished PhD thesis, University of Pretoria, South Africa, 205 pp.

Breetzke, G. D. (2004). A critique of soil erosion modelling at a catchment scale using GIS (Master's thesis). Faculteit der Aard-en Levenswetenschappen, Vrije Universiteit Amsterdam, Netherland.

Breiby, T. (2006). Assessment of Soil Erosion Risk within a Subwatershed using GIS and RUSLE with a Comparative Analysis of the use of STATSGO and SSURGO Soil Databases Todd Breiby. Analysis, 8, 1–22.

Brady C.N., & Weil, R. R (2008). The Nature and Properties of Soils. 14th Edition, Prentice Hall: New Jersey.

Brown, L. C., & Foster, G. R.(1987): Storm erosivity using idealized intensity distributions, Transactions of the Asae, 30, 379–386.

Campbell, J.B. 1996. Introduction to Remote Sensing. Second Edition. Taylor & Francis Ltd. ISBN: 0- 7484-0663-8.

Central Statistics Office. (2008). Botswana environment statistics. Gaborone, Botswana.

Central Statistics Office. (2011). Population & Housing Census. Preliminary Result Brief. Gaborone, Botswana.

Chadli, K. (2016). Estimation of soil loss using RUSLE model for Sebou watershed (Morocco). Modeling Earth Systems and Environment, 2(2), 1–10. Retrieved from https://doi.org/10.1007/s40808-016-0105-y.

Chen, Y., Yu, J., & Khan S. (2010). Spatial sensitivity analysis of multi-criteria weights in GIS-based land suitability evaluation. Environmental Modelling & Software, 25(12): 1582-1591.

Choudhary, K., Boori, M. S., & Kupriyanov, A. (2018). Spatial modelling for natural and environmental vulnerability through remote sensing and GIS in Astrakhan, Russia. Egyptian Journal of Remote Sensing and Space Science, 21(2), 139–147. Retrieved from https://doi.org/10.1016/j.ejrs.2017.05.003

Chuenchum, P., Xu, M., & Tang, W. (2020). Predicted trends of soil erosion and sediment yield from future land use and climate change scenarios in the Lancang–Mekong River by using the modified RUSLE model. International Soil and Water Conservation Research, 8(3), 213–227. Retrieved from https://doi.org/10.1016/j.iswcr.2020.06.006.

Congalton, R.G., & K. Green. (1999). Assessing the Accuracy of Remotely Sensed Data: Principles and Practices. Boca Raton, Florida: Lewis Publishers. 137 pp.

Crosson, P. (1998). The On-Farm Economic Costs of Soil Erosion. In: Lal, R., Blum, W. H., Valentine, c., and Stewart, B. A. (Editors). Methods for Assessment of Soil Degradation. New York: CRC Press. pp. 495-511.

Darkoh, M. B. K. (1999). Desertification in Botswana. Rala Report, 267, 61–74. Retrieved from http://www.rala.is/rade/ralareport/darkoh.pdf.

De Jong, S. M. (1994) .Derivation of Vegetative variables from a Landsat TM image for modelling soil erosion. Earth Surface Processes and Landform,19(2):165-78.

Deore, S.J. (2005). Prioritization of Micro-watersheds of Upper Bhama Basin on the Basis of Soil Erosion Risk Using Remote Sensing and GIS Technology (PhD thesis). University of Pune, Pune.

Department of Primary Industries, N. (2014). Fact sheet 1: Types of erosion. 2. Retrieved from http://www.dpi.nsw.gov.au/agriculture/resources/s.

De Vente, J., Poesen, J., Govers, G., & Boix, F. C. (2009). The implications of data selection for regional erosion and sediment yield modelling. Earth Surface Processes and Landforms, 34, 1994-2007.

Durigon, V. L., Carvalho, D. F., Antunes, M. A. H., Oliveira, P. T. S., & Fernandes, M. M. (2014). NDVI time series for monitoring RUSLE cover management factor in a tropical watershed. International Journal of Remote Sensing, 35, 441-453.

Dutta, S. (2016). Soil erosion, sediment yield and sedimentation of reservoir: a review. Modelling Earth Systems and Environment, 2(123), 1-18.

Eldridge, D. J. (1998). Trampling of Microphytic Crusts on Calcareous Soils, and Its Impact on Erosion Under Rain Impacted Flow. Catena, 33(3-4): 221-239.

Elwell, H.A.(1979). Modelling soil losses in Zimbabwe Rhode- sia. Paper presented at the Summer Meeting of ASAE and CSAE, University of Manitoba, Winnipeg, Canada.

Elwell, H. A. (1978). Modeling Soil Losses in Southern Africa. Journal of Agricultural Engineering Research, 23: 117-127.

Elwell, H.A. & Stocking, M.A.(1982). Developing a simple yet practical method of soil-loss estimation. Trap. Agric. 59, 43—48.

Emeribeole, A. C., & Iheaturu, C. J. (2015). Mapping of Potential Soil Erosion Risk Areas in IMO State Using the Revised Universal Soil Loss Equation (RUSLE), Remote Sensing (RS) and Geospatial Information System (GIS) Techniques, (10), 36–44.

Ester, W.M. (2009). Using GIS techniques to determine RUSLE's R and LS factors for Kapingazi River Catchment (MSc Thesis). Jomo Kenyatta University of Agriculture and Technology. Kenya.

Fangmeier, D.D., Elliot, W.J., Workman, S.R., Huffman, R.L. & Schwab, G.O. (2006). Soil and Water Conservation Engineering, 5th Edition. Thomson Delmar Learning; Printed in USA.

FAO. (1997). Africover Land Cover Classification. In Environment and Natural Resources Service; Sustainable Development Department S.D., Ed.; Food and Agriculture Organisation: Rome, Italy.

FAO. (2020). Sustainable agricultural solutions to meet food demands. Retrieved from http://www.fao.org/global-soil-partnership/resources/highlights/.

Farhan, Y., & Nawaiseh, S. (2015). Spatial assessment of soil erosion risk using RUSLE and GIS techniques. Environmental Earth Sciences, 74(6), 4649–4669. Retrieved from https://doi.org/10.1007/s12665-015-4430-7

Farhan, Y., Zregat, D., & Farhan, I. (2013). Spatial Estimation of Soil Erosion Risk Using RUSLE Approach, RS, and GIS Techniques: A Case Study of Kufranja Watershed, Northern Jordan. Journal of Water Resource and Protection, 05(12), 1247–1261. Retrieved from https://doi.org/10.4236/jwarp.2013.512134 .

Fathizad, H., Karimi, H., & Alibakhshi, S. M. (2014). The estimation of erosion and sediment by using the RUSLE model, RS and GIS techniques (Case study: arid and semi-arid regions of Doviraj, Ilam province, Iran). International Journal of Agriculture and Crop Sciences, 7(6), 304-314.

Feda, H. (2018). Assessment of Soil Erosion by R and USLE Model Using Remote sensing and GIS Techniques (Master's Thesis) : A Case Study of Huluka Watershed, Central Ethiopia. May.

Ferreira, V. L. M. (2015). Assessing Soil Erosion Due to Land Use Change at the Alqueva Reservoir Surrounding Area TT (PHD Dissertation). Faculty of Sciences and Technology, University of the Algarve.

Fenta, A. A., Tsunekawa, A., Haregeweyn, N., Poesen, J., Tsubo, M., Borrelli, P., Panagos, P., Vanmaercke, M., Broeckx, J., Yasuda, H., Kawai, T., & Kurosaki, Y. (2020). Land susceptibility to water and wind erosion risks in the East Africa region. Science of the Total Environment. Retrieved from https://doi.org/10.1016/j.scitotenv.2019.135016.

Flügel W, Märker M, Moretti S, Rodolfi G., & Sidrochuk A. (2003). Integrating geographical information systems, remote sensing, ground-truthing and modeling approaches for regional erosion classification of semi-arid catchments in South Africa. Hydrological Processes, 17: 929-942.

Foster, G. R., Yoder, D. G., Weesies, G. A., McCool, D. K., McGregor, K. C., & Bingner, R. L. (2003). User's guide: Revised Universal Soil Loss Equation. Washington DC: U.S. Department of Agriculture, Research Service.

Foster, R. H. (2006). Methods for assessing land degradation in Botswana. Earth & Environment, 1, 238–276.

Garg, P. K. and Harrison, A. R. (1992). Land Degradation and Erosion Risk Analysis in S. E. Spain: A Geographic Information System Approach. Catena, 19(5): 411-425.

Ganasri, B. P., & Ramesh, H. (2016). Assessment of soil erosion by RUSLE model using remote sensing and GIS - A case study of Nethravathi Basin. Geoscience Frontiers, 7(6), 953–961. Retrieved from https://doi.org/10.1016/j.gsf.2015.10.007.

Gemechu, A. (2016). Estimation of Soil Loss Using Revised Universal Soil Loss Equation and Determinants of Soil Loss in Tiro Afeta and Dedo Districts of Jimma Zone, Oromiya National Regional State, Ethiopia. Trends in Agricultural Economics, 9(1), 1–12. Retrieved from https://doi.org/10.3923/tae.2016.1.12.

Geomatics, P. (2016). Geomatica Training Guide. Markham, Canada. Retrieved from http://www.pcigeomatics.com/pdf/training-guides/2016/Geomatica-1.pdf.

Gis, C. E., & David, R. (2014). Soil Erosion Assessment using GIS and Revised Universal Soil Loss Equation (RUSLE).

Gitas, I.Z., K. Douros, C. Minakou, G.N. Silleos., & Karydas,C.G. (2009). Multi-temporal soil erosion risk assessment in N. Chalkidiki using a modified USLE raster model. EARSeL eProceedings 8.

Goldman, S. J., Jackson, K., & Bursztynsky, T. A. (1986). Erosion and Sediment Control Handbook. New York: McGraw-Hill, Inc.

Goudie, A. (1981). The Human Impact: Man's Role in Environmental Change. Oxford: Basil Blackwell.

GOVERNMENT OF BOTSWANA (GOB). (1975). National policy on tribal grazing land. Paper No. 2 of 1975. Gaborone: Government Printer.

GOVERNMENT OF BOTSWANA (GOB). (1991). National policy on agricultural development. Paper No. 1 of 1991. Gaborone: Government Printer.

Harrie, L. (2008). Geographic information processing: Theory, methods, and applications (In Swedish).ed Formas, Stockholm.

Hawando, T. (1995). The survey of the Soil and Water Resources of Ethiopia. UNO/Toko Chen, T., R.Q. Niu, P.X. Li, L.P. Zhang and B. Du. 2010. Regional soil erosion risk mapping using RUSLE, GIS, and remote sensing: A case study in Miyun Watershed, North China. Environmental Earth Sciences, 63(3): 533-541.

Hudson N.W. (1965). Field measurement of accelerated soil erosion in localized areas. Rhodesia Agricultural Journal, 31(3); pp.46-48.

Hudson, C.A. (1987). A regional application of SLEMSA in the Cathedral Peak area of the Drakensberg (Unpublished MSc Thesis). University of Cape Town.

Hudson, N. (1995). Soil Conservation. 3rd Edition. London: B T Batsford Limited.

Huete, A. R (1988). A Soil Adjusted Vegetation Index (SAVI). Remote Sensing of Environment, 25: 295-309.

Huete, A. R, Jackson, R D., and Post, D. F. (1985). Spectral Response of Plant Canopy with Different Soil Backgrounds. Remote Sensing of Environment, 17: 37-53.

Humberto, I. C, and Rattan, L. (2010). Principles of Soil Conservation and Management. Ohie State University, Columbus, USA.

Hurni H.(1985). Erosion-Productivity-Conservation systems in Ethopia.In.Proceedings of paper presented at the 4th conference of soil conservation, Maracay, Venezuela.

Hurni, H. (1985a). Soil Formation Rates in Ethiopia, Soil Conservation Project, Working paper 2, Ministry of Agriculture, Addis Ababa, Ethiopia.

Hurni, H. (1993). Land Degradation, famine and resource scenarios in Ethiopia. In World Soil Erosion and Conservation, ed. D. Pimentel. Cambridge University press, Cambridge. 27−62.

Igwe.P.U., Onuigbo, A.A., Chinedu, O.C., Ezeaku, I.I., & Muoneke, M.M. (2017). Soil Erosion: A Review of Models and Applications. International Journal of Advanced Engineering Research and Science, 4(12), 138–150. Retrieved from https://doi.org/10.22161/ijaers.4.12.22

IWMI (International Water Management Institute) & IGRAC(International Groundwater Resources Assessment Centre). (2017). Farmer Needs and Preference for Agriculture Water Solutions in the Ramotswa Transboundary Aquifer Area, Botswana.

Jacobs, D. E., Brown, M. J., Baeder, A., Sucosky, M. S., Margolis, S., Hershovitz, J., Kolb, L., & Morley, R. L. (2010). A Systematic Review of Housing Interventions and Health. Journal of Public Health Management and Practice, 16, S5–S10. Retrieved from https://doi.org/10.1097/phh.0b013e3181e31d09

Jain, M.K., Kothari., & Ranga Raju, K.G. (2005). GIS-based distributed model for soil erosion and rate of sediment outflow from catchments. Journal of Hydraulic Engineering, 131,755-769.

Jain, S.K., & Goel, M.K. (2002). Assessing the vulnerability to soil erosion of the Ukai Dam catchments using remote sensing and GIS. Journal of Hydrological Sciences, 47(1):31−40.

Jaramillo, F. (2007). Estimating and Modelling Soil Loss and Sediment Yield in the Maracas-St. Joseph River Catchment with Empirical Models (RUSLE and MUSLE) and a Physically Based Model (Erosion 3D) (M.Sc. Thesis). McGill University, Montrea.

Jetten, V., Govers, G., & Hessel, R. (2003). Erosion Models: Quality of Spatial Predictions. Hydrological Processes, 17(5): 887-900.

Jha, M.K., & Paudel, R.C. (2010). Erosion predictions by empirical models in a mountainous watershed in Nepal. Journal of Spatial Hydrology, 10 (1).

Kaltenrieder. V.V.J. (2007). Adaptation and Validation of the Universal Soil Loss Equation (USLE) for the Ethiopian Eritrean Highlands (MSc thesis). University of Bern. Switzerland.

Kashe, K., Kolawole, O. D., Moroke, T. S., & Mogobe, O. (2019). Dryland crop production in Botswana : Constraints and opportunities for smallholder arable farmers. Smallholder Farmers and Farming Practices: Challenges and Prospects, December.

Khare, D., Mondal, A., Kundu, S., & Mishra, P. K. (2016). Climate change impact on soil erosion in the Mandakini River Basin, North India. Applied Water Science, 7(5), 2373–2383. Retrieved from https://doi.org/10.1007/s13201-016-0419-y

Kayet, N., Pathak, K., Chakrabarty, A., & Sahoo, S. (2018). Evaluation of soil loss estimation using the RUSLE model and SCS-CN method in hillslope mining areas. International Soil and Water Conservation Research, 6(1), 31–42. Retrieved from https://doi.org/10.1016/j.iswcr.2017.11.002

Kim, H. S. (2006). Soil Erosion Modeling Using RUSLE and GIS on the Imha Watershed, South Korea (MSc Thesis). Colorado State University, Korea.

Knijff, J. M., Jones, R. J. A., & Montanarella, L. (2000). Soil erosion risk assessment in Europe. Joint Research Centre, European Commission, EUR 19044 EN.

Laker, M. C. (2000). Soil Resources: Distribution, Utilization, and Degradation. In: Fox, R. and Rowntree, K. (Editors). The Geography of South Africa in a Changing World. Cape Town: Oxford University Press. pp. 326-360.

Lal, R., & Elliot, W. (1994). Erodibility and Erosivity. In: Lal, R. (Editor). Soil Erosion: Research Methods. 2nd Edition. Florida: Soil and Water Conservation Society and St. Lucie Press. pp. 181-208.

Lal, R. (1998). Soil erosion impact on agronomic productivity and environment quality: Critical Review. Plant Science, 17: 319 – 464.

Lal, R. (2001). Soil degradation by erosion. Land Degradation & Development, 12. 519 - 539. 10.1002/ldr.472.

Lal, R. (2003). Soil erosion and the global carbon budget. Environment International, 29 (4). Retrieved from http://dx.doi.org/10.1016/S0160-4120(02)00192-7.

Lal, R. (2007). Promoting technology adoption in sub-Saharan Africa, South Asia. Crops, Soils, Agronomy News, 52:10–13.

Larney, F. J., Olson, B. M., Janzen, H. H., & Lindwall, C. W. (2000). Early Impact of Topsoil Removal and Soil Amendments on Crop Productivity. Agronomy Journal, 92(5): 948-956.

Lazzari, M., Gioia, D., Piccarreta, M., Danese, M., & Lanorte, A. (2015). Sediment yield and erosion rate estimation in the mountain catchments of the Camastra artificial reservoir (Southern Italy): A comparison between different empirical methods. Catena, 127, 323- 339.

Le Roux,J.J., Morgenthal,T.L., Malherbe, J., Sumner,P.D., & Pretorius,D.J. (2008). Water erosion prediction at a national scale for South Africa. Water SA, 34.

Le Roux, J. J., & Sumner, P. D. (2013). Water erosion risk assessment in South Africa: A proposed methodological framework. Geografiska Annaler, Series A: Physical Geography, 95(4), 323–336. Retrieved from https://doi.org/10.1111/geoa.12018

Liiri, M., Häsä M., Haimi, J., & Setälä, H. (2012). History of land-use intensity can modify the relationship between functional complexity of the soil fauna and soil ecosystem services – A microcosm study. Applied Soil Ecology. 55: 53–61. Doi:10.1016/j.apsoil.2011.12.009N.

Lillesand, T. M. & Kiefer, R. W. (1994). Remote Sensing and Image Interpretation. John Wiley & Sons. New York.

Lillesand, T. M., Keifer, R.W., & Chipman,J.W. (2004). Remote Sensing and Image Interpretation, Fifth Edition, R.R. Donnelley-Crawfordsville.United States of America.

Littleboy, M., Cogle, A. L., Smith, G. D., Rao, K. P. C., & Yule, D. F. (1996). Soil Management and Production of Alfisols in the Semi-arid Tropics. IV. Simulation of Decline in Productivity Caused by Soil Erosion. Australian Journal of Soil Research, 34(1): 127-138.

Lord, T. M., & McLean, A. (1969). Aerial photo interpretation on British Columbia rangelands. Journal of Range Management, 22(1), 3-9.

Lu, D., Mausel, P., Brondízio, E., & Moran, E. (2004). Change detection techniques. International Journal of Remote Sensing, 25(12), 2365–2401. Retrieved from https://doi.org/10.1080/0143116031000139863.

Magee, K. S. (2011). Segmentation, object-oriented applications for remote sensing land cover and land use classification (Doctoral dissertation). University of Cincinnati, USA.

Magole, L., & Thapelo, K. (2005). The Impact of Extreme Flooding of the Okavango River on the Livelihood of the Molapo Farming Community of Tubu village, Ngamiland Sub-district, Botswana. Botswana Notes and Records, 37, 125-137. Retrieved from www.jstor.org/stable/40980409

Mainam, F. (1999). Modelling soil erodibility in the semiarid zone of Cameroon: assessment of inter rill erodibility parameters for mapping soil erosion hazard by means of GIS techniques in the Gawar area. Enschede: Ghent.

Mango, L.M. (2010). Modeling the Effect of Land Use and Climate Change Scenarios on the Water Flux ofthe Upper Mara River Flow, Kenya; FIU: Miami, FL, USA.

Manrique, L. A. (1993). Technology for soil erosion assessment in the tropics: A review, Communication in Soil Science and Plant Analysis, 24: 1033-1064.

Manyiwa, T., & Dikinya, O. (2013). Using universal soil loss equation and soil erodibility factor to assess soil erosion in Tshesebe village, North East Botswana. African Journal of Agricultural Research, 8(30), 4170–4178. Retrieved from https://www.researchgate.net/publication/260000115

Marble, D. F. (1987). Geographic Information Systems: An Overview. In: Ripple, W. J. (Editor). Geographic Information Systems for Resource Management: A Compendium. USA: The American Society for Photogrammetry and Remote Sensing and the American Congress on Surveying and Mapping. pp. 2-8.

Mark, J.C. (1997). Detection and Analysis of Change in Remotely Sensed Imagery with Application to Wide Area Surveillance. IEEE Image Processing, 6, NO 1.

Marondedze, K.A., & Scutt.B. (2020). Assessment of Soil Erosion using the RUSLE model for the Epworth District of the Harare Metropolitan Province, Zimbabwe, Institute of Geographical Science, Freie Universitat Berlin, Berlin, Germany.

Mashame, G., & Akinyemi, F. (2016). Towards a Remote Sensing Based Assessment of Land Susceptibility To Degradation: Examining Seasonal Variation in Land Use-Land Cover for Modelling Land Degradation in a Semi-Arid Context. ISPRS Annals of Photogrammetry, Remote Sensing and Spatial Information Sciences, III–8 (July), 137–144. Retrieved from https://doi.org/10.5194/isprsannals-iii-8-137-2016

Matlhodi, B., Kenabatho, P. K., Parida, B. P., & Maphanyane, J. G. (2019). Evaluating land use and land cover change in the Gaborone dam catchment, Botswana, from 1984-2015 using GIS and remote sensing. Sustainability (Switzerland), 11(19). Retreived from https://doi.org/10.3390/su11195174

McCool, D.K., Foster G.R., Renard, K.G., Yoder, D.C., & Weeisies, G.A. (1995). The Revised Universal Soil Loss Equation. Department of Defense/Interagency Workshop on Technologies to Address Soil Erosion on Department of Defense Lands San Antonio, TX, June 11-15, 1995.

Mendelsohn, R., Dinar, A., Mendelsohn, R., & Dinar, A. (2019. Land Use and Climate Change Interactions, 1(2009), 309–332.

Merritt, W. S., Letcher, R. A., & Jakeman, A. J. (2003). A review of erosion and sediment transport models. Environmental Modelling and Software, 18(8–9), 761–799. Retrieved from https://doi.org/10.1016/S1364-8152(03)00078-1

Mhangara, P., Kakembo, V., & Lim, K. J. (2012). Soil erosion risk assessment of the Keiskamma catchment, South Africa using GIS and remote sensing. Environmental Earth Sciences, 65(7), 2087–2102. Retrieved from https://doi.org/10.1007/s12665-011-1190-x

Ministry of Agricultural Development and Food Security. (2019). Strategies and Goals 20018/19 Performance Report on MOA Indicator. Botswana.

Mitasova, H., Hofierka, J., Zlocha, M., & Iverson, L. R. (1996). Modelling topographic potential for erosion and deposition using GIS. International Journal of Geographical Information System, 10(5), 629-641.

MOA. (2018). Drought Management Strategy for Botswana. Botswana.

Morgan, J. L., Gergel, S. E., & Coops, N. C. (2010). Aerial photography: a rapidly evolving tool for ecological management. BioScience, 60(1), 47-59.

Moisa, M. B., Negash,D.A., Merga,B.B., & Gemeda,D.O. (2020). Impact of Land Use and Land Cover Change on Soil Erosion Using Rusle Model And Gis : A Case of Temeji Watershed, Western Ethiopia. Retrieved from https://doi.org/10.21203/rs.3.rs-100340/v1.

Moore, I. D., & Burch, G. J. (1986). Physical basis of the length slope factor in the universal soil loss equation. Soil Science Society of America, 50, 1294-1298.

Morgan, K. M., Lee, G. B., Kiefer, R. W., Daniel, T. C., Bubenzer, G. D., & Murdock, J. T. (1978). Prediction of Soil Loss on Cropland with Remote Sensing. Journal of Soil and Water Conservation, 33(6): 291-293.

Morgan, R.P.C. (1986). Soil erosion and conservation. Blackwell, London.

Morgan, R. P. C., & Davidson, D. A.(1991), Soil Erosion and Conservation, Longman Group, UK.

Morgan, R.P.C. (1995). Soil Erosion and Conservation, second edition, Longman Group Limited, London.

Morgan, R.P.C. (2005). Soil Erosion and Conservation.Third edition.Wiley-Blackwell. ISBN: 978-1- 4051-1781-4.

Morgan, R.P.C. (2009). Soil Erosion and Conservation; John Wiley & Sons: Hoboken, NJ, USA

Mullan, D. (2013). Soil erosion under the impacts of future climate change: Assessing the statistical significance of future changes and the potential on-site and off-site problems. Catena, 109, 234–246. Retrieved from https://doi.org/10.1016/j.catena.2013.03.007.

Murayama, Y., Estoque, R.C., Subasinghe, H., Hou, H. & Gong, H. (2015). Land-use/land-cover changes in major Asian and African cities. Annual Report on the Multi Use Social and Economic Data Bank. Scientific Research Publishing Inc.USA 92, pp.11-58.

Mutowa, G & Chikodzi, D. (2013).Erosion Hazard Mapping in the Runde Catchment:Implication for Water Resources Management. Journal of Geosciences and Geomatics, 1.No.1,22-28.

Naqvi, H. R., Mallick, J., Devi, L. M., & Siddiqui, M. A. (2013). Multi-temporal annual soil loss risk mapping employing Revised Universal Soil Loss Equation (RUSLE) model in Nun Nadi Watershed, Uttrakhand (India). Arabian Journal of Geosciences, 6(10), 4045–4056. Retrieved from https://doi.org/10.1007/s12517-012-0661-z

National Development Plan 11, Volume 1, April 2017- March 2023. (2016, December, 20). Retrieved from https://Botswana.un.org

Olson,C.E.(1960). Elements of Photographic Interpretation Common to several sensors,Photogrammetric Engineering, 26,no 4,pp.651-656.

Ostovari, Y., Ghorbani, D, S., Bahrami, H., Naderi, M., & Damatte, J. A. M. (2017). Soil loss estimation using RUSLE model, GIS and remote sensing techniques: a case study from the Dembecha watershed, northwestern Ethiopia. Geoderma Regional, 11, 28-36.

Pande, L.M., Prasad, J., Saha, S.K., & Subramanyam, C. (1992). Review of Remote Sensing applications to soils and agriculture. Proc. Silver Jubilee Seminar, IIRS, Dehra Dun.

Panditharathne, D. L. D., Abeysingha, N. S., Nirmanee, K. G. S., & Mallawatantri, A. (2019). Application of revised universal soil loss equation (RUSLE) model to assess soil erosion in "Kalu Ganga" River Basin in Sri Lanka. Applied and Environmental Soil Science, 2019, Article ID 4037379, 15. Retrieved from https://doi.org/10.1155/2019/4037379.

Panagos, P., Borrelli, P., Meusburger, K., Alewell, C., Lugato, E., & Montanarella, L. (2015). Estimating the soil erosion cover-management factor at the European scale. Land Use Policy, 48, 38-50.

Paris, S. (1990). Erosion Hazard Model (modified SLEMSA), Field Document No. 13, second version, Land Resources Evaluation Project, Malawi, Pp 17.

Patil R. J., & Sharma S. K. (2013, 29-30 December). Remote Sensing and GIS based modeling of crop/ cover management factor (C) of USLE in Shakker river watershed. Proceedings of International Conference on Chemical, Agricultural and Medical Sciences (CAMS-2013). Kuala Lumpur, Malaysia.

Parveen, R., & U. Kumar. (2012). Integrated Approach of Universal Soil Loss Equation (USLE) and Geographical Information System (GIS) for Soil Loss Risk Assessment in Upper South Koel Basin, Jharkhand. Journal of Geographic Information System, 4: 588-596.

Pham, T. G., Degener, J., & Kappas, M. (2018). Integrated universal soil loss equation (USLE) and Geographical Information System (GIS) for soil erosion estimation in A Sap basin: Central Vietnam. International Soil and Water Conservation Research, 6(2), 99–110. Retrieved from https://doi.org/10.1016/j.iswcr.2018.01.001

Phinzi, K., & Ngetar, N. S. (2017). Mapping soil erosion in a quaternary catchment in Eastern Cape using geographic information system and remotes sensing. South African. Journal of Geomatics, 6(1), 11-29.

Phinzi, K. (2018). Spatio-Temporal Appraisal of Water-Borne Erosion Using Optical Remote Sensing and GIS in the Umzintlava Catchment (T32E), Eastern Cape, South Africa (Master's Thesis). University of KwaZulu-Natal, South Africa.

Phinzi, K., & Ngetar, N. S. (2019). The assessment of water-borne erosion at catchment level using GIS-based RUSLE and remote sensing: A review. International Soil and Water Conservation Research, 7(1), 27–46. Retrieved from https://doi.org/10.1016/j.iswcr.2018.12.002.

Pimentel, D., Harvey, C., Resosudarmo, P., Sinclair, K., Kurz, D., MnCair, M., Crist, S., Shpritz, L., Fitton, L., Saffouri, R., & Blair, R. (1995). Environmental and economic costs of soil erosion and conservation benefits. Science, 267, 1117–1123.

Pimentel, D. (2006). Soil erosion, a food and environmental threat. Environment, Development and Sustainability, 8, 119–137.

Pimentel, D., & Burgess, M. (2013). Soil erosion threatens food production. Agriculture (Switzerland), 3(3), 443–463. Retrieved from https://doi.org/10.3390/agriculture3030443

Popp, J.H., Hyatt, D.E., & Hoag, D. (2000). Modelling environmental condition with indices: a case study of sustainability and soil resources; Ecol. Model, 130(1-3):131−143.

Qi, J., Chehbouni, A., Huete, A. R., & Kerr, Y. H. (1994). Modified soil adjusted vegetation index (MSAVI). Remote Sensing of Environment, 48, 119-126.

Quora.com. (2019). Retrieved from https://www.quora.com/What-are-various-types-of-soil-erosion.

Rahman, M. R., Shi, Z. H., & Chongfa, C. (2009). Soil erosion hazard evaluation-An integrated use of remote sensing, GIS and statistical approaches with biophysical parameters towards management strategies. Ecological Modelling, 220(13–14), 1724–1734. . Retrieved from https://doi.org/10.1016/j.ecolmodel.2009.04.004.

Reed, M. S., Stringer, L. C., Dougill, A. J., Perkins, J. S., Atlhopheng, J. R., Mulale, K., & Favretto, N. (2015). Reorienting land degradation towards sustainable land management: Linking sustainable livelihoods with ecosystem services in rangeland systems. Journal of Environmental Management, 151, 472–485. . Retrieved from https://doi.org/10.1016/j.jenvman.2014.11.010.

Renard, K., Foster, GR, Wessies, G.A., & Porter J.P. (1994). RUSLE Revised universal soil loss equation. Journal of Soil and Water Conservation, 46:30−33.

Renard, K. G., Foster, G. R., Weesies, G. A., McCool, D. K., & Yoder, D. C. (1997). Predicting soil erosion by water: a guide to conservation planning with the Revised Universal Soil Loss Equation (RUSLE), 703. Washington, DC: United States Department of Agriculture.

Renard, K. G., Yoder, D. C., Lightle, D. T., & Dabney, S. M. (2011). Universal soil loss equation and revised universal soil loss equation. Handbook of erosion modelling, 8, 135- 167.

Reusing, M., Schneider, T., & Ammer, U. (2000). Modelling soil erosion rates in the Ethiopian highlands by integration of high resolution MOMS-02/D2-stereo-data in a GIS. International Journal of Remote Sensing, 21, 1885-1896.

Ritchie, J. C. (2000). Soil Erosion. In: Schultz, G. A. and Engman, E. T. (Editors). Remote Sensing in Hydrology and Water Management. Berlin: Springer. pp. 271-286.

Roose, E.J. (1977). Use of the Universal Soil Loss Equation to Predict Erosion in West Africa. In Soil erosion: Prediction and control. Soil Conservation Society of America, Special Publication no. 21. Ankeny, Iowa.

Rosewell, C. J. (1993). Soil Loss: a program to assist in the selection of management practices to reduce erosion. Technical handbook no. 11 (2nd ed.), Sydney: Conservation Services of New South Wales, Department of Conservation and Land Management.

Saavedra, C. (2005). Estimating spatial patterns of soil erosion and deposition in the Andean region using geo-information techniques: a case study in Cochabamba, Bolivia (Ph.D. dissertation). Wageningen University, The Netherlands.

Schultze, R.E. (1979). Soil loss in the Key Area of the Drakensberg – a regional application of the 'Soil Loss Estimation Model for Southern Africa' (SLEMSA). In, Hydrology and Water Resources of the Drakensberg, Pp. 149-167, Natal Town and Regional Planning Commission, Pietermaritzburg, South Africa.

Schulze R.E.(1995). Hydrology and Agro-hydrology. A text to accompany the ACRU 3.00 Agro hydrological modeling system. Department of Agricultural Engineering. University of Natal. Pietermaritzburg, South Africa

Sebego, R. J., Atlhopheng, J. R., Chanda, R., Mulale, K., & Mphinyane, W. (2019). Land use intensification and implications on land degradation in the Boteti area: Botswana. African Geographical Review, 38(1), 32–47. Retrieved from https://doi.org/10.1080/19376812.2017.1284599.

Seboka, G. N. (2016). Spatial Assessment of NDVI as an Indicator of Desertification in Ethiopia using Remote Sensing and GIS (Master's Thesis). Lund University, Sweden.

Sefe, F., Ringrose, S., & Matheson, W. (1996). Desertification in north-central Botswana: causes, processes, and impacts. Journal of Soil & Water Conservation, 51(3), 241–248.

Shahram, K, P.E., Leroy, F., Heitz, P.E., Yuming, W., Michael, P. (2007). Developing a GIS-based Soil Erosion Potential Model of the UGUM Watershed. Water & Environmental Research Institute of the Western Pacific, University of GUAM, 117.

Shaikh, M. S., & Shetkar, R. V. (2018). Soil Erosion Estimation Modelling by Revised Universal Soil Loss Equation and Soil and Water Assessment Tool on Geographic Information System Platform. Journal of Water Resource Engineering and Management,5(2).

Shougang, Z., Na, L., & Ruishe, Q. (2014). The Application and Study of GIS in Soil Erosion Model. Advances in Sciences and Engineering, 6(2):31-34.

Simms A.D, Woodroffe C.D., & Jone B.G. (2003). Application of RUSLE for erosion management in a coastal catchment, southern NSW.

Smith, S. V., Bullock, S. H., Hinojosa-Corona, A., Franco-Viscaíno, E., Escoto-Rodríquez, M., Kretzschmar, T. G., Farfan, L. M., & Salazar-Cesena, J. M. (2007). Soil erosion and significance for carbon fluxes in a mountainous Mediterranean-climate watershed. Ecological Applications, 17(5), 1379-1387.

H. J. Smith (1999) Application of Empirical Soil Loss Models in southern Africa: a review. South African Journal of Plant and Soil, 16:3, 158-163. Retrieved from https://doi.org/10.1080/02571862.1999.10635003

Snyman, H.A. (1999). Soil erosion and conservation. In: Tainton NM (ed.) Veld Management in South Africa. University of Natal Press: Scottsville, South Africa. pp. 355-380.

Sourlamtas, K. (2019). Soil erosion estimation for the Göta Älv river using remote sensing, GIS and the Revised Universal Soil Loss Equation (RUSLE) model (Master's thesis). Stockholm University, Sweden.

Statistics Botswana. (2011). South East District. Population and Housing Census 2011. Selected Indicators for Villages and Localities. Botswana.

Statistics Botswana. (2015). Population and Housing Census 2011. National Statistics Tables. Botswana

Statistics Botswana. (2020). Cities/Town and Villages. Projections 2020. Botswana.

Stocking, M. A. (1994). Assessing Vegetative Cover and Management Effects. In: Lal, R. (Editor). Soil Erosion: Research Methods. 2nd Edition. Florida: Soil and Water Conservation Society and St. Lucie Press. pp. 211-232.

Stocking, M.A. (1980). Soil loss estimation for rural development: a position for geomorphology. Geomorphology, 36, Pp. 264-273.

Stone, R.P., & Hilborn, D. (2012). Universal soil loss equation (USLE) factsheet. Ministry of Agriculture, Food and Rural Affairs, Ontario.

Tamene, L., Adimassu, Z., Aynekulu, E., & Yaekob, T. (2017). Estimating landscape susceptibility to soil erosion using GIS-based approach in Northern Ethiopia. International Soil and Water Conservation Research, 5, 221-230.

Tefera, B. G. Ayele, Y. Atnafe, M.A. Jabbar., & P. Dubale. (2002). Nature and causes of land degradation in the Oromiya Region: A review. International Livestock Research Institute (ILRI), Socio- economics and Policy research. Working Paper 36.

Telkar, S. (2018). Soil Erosion : Types and Their Mechanism Soil Erosion : Types and Their Mechanism. Biomolecule Reports, ISSN:2456-8759.

Tesfamichael, S. G. (2004). Mapping Potential Soil Erosion Using Rusle, Remote Sensing and Gis : The Case Study of Weenen Game Reserve (Master's Thesis). University of KwaZulu-Natal, South Africa.

Tesfaye, G., Debebe, Y., & Fikirie, K. (2018). Soil Erosion Risk Assessment Using GIS Based USLE Model for Soil and Water Conservation Planning in Somodo Watershed, South West Ethiopia. International Journal of Environmental & Agriculture Research (IJOEAR), 4(5), 35–43. Retrieved from https://doi.org/10.13140/RG.2.2.15774.79682.

Thomas, J., Joseph, S., & Thrivikramji, K. P. (2018). Assessment of soil erosion in a tropical mountain river basin of the southern Western Ghats, India using RUSLE and GIS. Geoscience Frontiers, 9(3), 893–906. Retrieved from https://doi.org/10.1016/j.gsf.2017.05.011.

Thornes, J. B. (1985). The Ecology of Erosion. Geography, 70(1): 222-235.

Tiessen, H. J., & Moir.O. (1993). Total and organic carbon. In: Soil Sampling and Methods of Analysis, M.E. Carter, Ed. Lewis Publishers, Ann Arbor, MI. pp. 187-211.

Toy, J.T., Foster,G. R., & Renard, K.G. (2002). Soil Erosion:Processes, Prediction, Measurement and Control.J ohn Wiley & Sons. New York.

Troeh, F. R, Hobbs, J. R., & Donahue, R L. (1980). Soil and Water Conservation for Productivity and Environmental Protection. N. 1.: Prentice Hall, Inc.

Uddin, K., Murthy, M. S. R., Wahid, S. M., & Matin, M. A. (2016). Estimation of soil erosion dynamics in the Koshi basin using GIS and remote sensing to assess priority areas for conservation. PLoS ONE, 11(13), 1-19.

UN. (2007). Natural Resource Aspects of Sustainable Development in Botswana. Retrieved from http://www.un.org/esa/agenda21/natlinfo/countr/botswana/natur.htm#desert.

UNCCD. (1997). United Nations Convention to Combat Desertification. Retrieved from http://www.unccd.int.

United States Department of Agriculture (USDA). (1972). Sediment sources, yields, and delivery ratios. National Engineering Handbook, Section 3 Sedimentation.

University of British Columbia. (2020). Retrieved from https://www.landfood.ubc.ca.

Vijith, H., Seling, L. W., and Dodge-Wan, D. (2017). Effect of cover management factor in quantification of soil loss: case study of Sungai Akah sub-watershed, Baram River basin Sarawak, Malaysia. Geocarto International, 1-17.

Vongsy, K. M. (2007). Change detection methods for hyper spectral imagery (Master's Thesis) Department of electrical engineering, Wright state university.

Wachal, D., & Banks, K. (2007). Modeling Erosion and Sediment Control Practices: A Management Approach for Disturbed Sites. World Environmental and Water Resources Congress 2007, pp. 1-14.

Walling, D.E., & Probst, J.L.(1997). Human Impact on Erosion and Sedimentation, IAHS Publication Nº 245. IAHS, Wallingford, Oxfordshire, UK., 311 pp.

Wang, L., Huang, J., Du, Y., Hu, Y., & Han, P. (2013). Dynamic Assessment of Soil Erosion Risk Using Landsat TM and HJ Satellite Data in Danjiangkou Reservoir Area, China. Remote Sensing, 5, 3826-3848.

Warren, A., & Agnew, C. (1988). An assessment of desertification and land degradation in arid and semi-arid areas. Dry lands Paper No. 2, IIED, London, 38 pp.

Wener, C. G. (1981). Soil Conservation In Kenya, Nairobi. Ministry of Agriculture, Soil Conservation Extension Unit.

Williams, J. R. (1975). "Sediment yield prediction with universal equation using runoff energy factor." Agricultural Research Service report ARS-S-40. U.S. Department of Agriculture.

Wischmeier, W.H. and Smith, D.D. (1978). Predicting rainfall erosion losses, a guide to conservation planning. Agric. Hand B. No. 537, US Department of Agriculture, Washington DC.

Wordofa, G. (2011). Soil Erosion Modeling Using Gis and Rusle on the Eurajoki Watershed Finland (Bachelor´s Thesis). Department of Environmental Engineering, Tampere University of Applied Sciences.

Worku, R. D. (2018). Assessment of Soil Erosion Risk using GIS and RUSLE in Meja Watershed, West Shewa, Ethiopia (Master's Thesis). Hawassa University, Ethiopia.

Yazidhi, B. (2003). A Comparative Study of Soil Erosion Modeling in Lom Kao-Phetchabun (Master's Thesis). ITC, Netherlands.

Yimer, F., Ledin, S., & Abdelkadir, A. (2008). Concentrations of exchangeable bases and cation exchange capacity in soils of cropland, grazing and forest in the Bale Mountains, Ethiopia. Forest Ecology and Management, 256: 1298–1302.

APPENDICES

Appendix 1: LULC of the study area

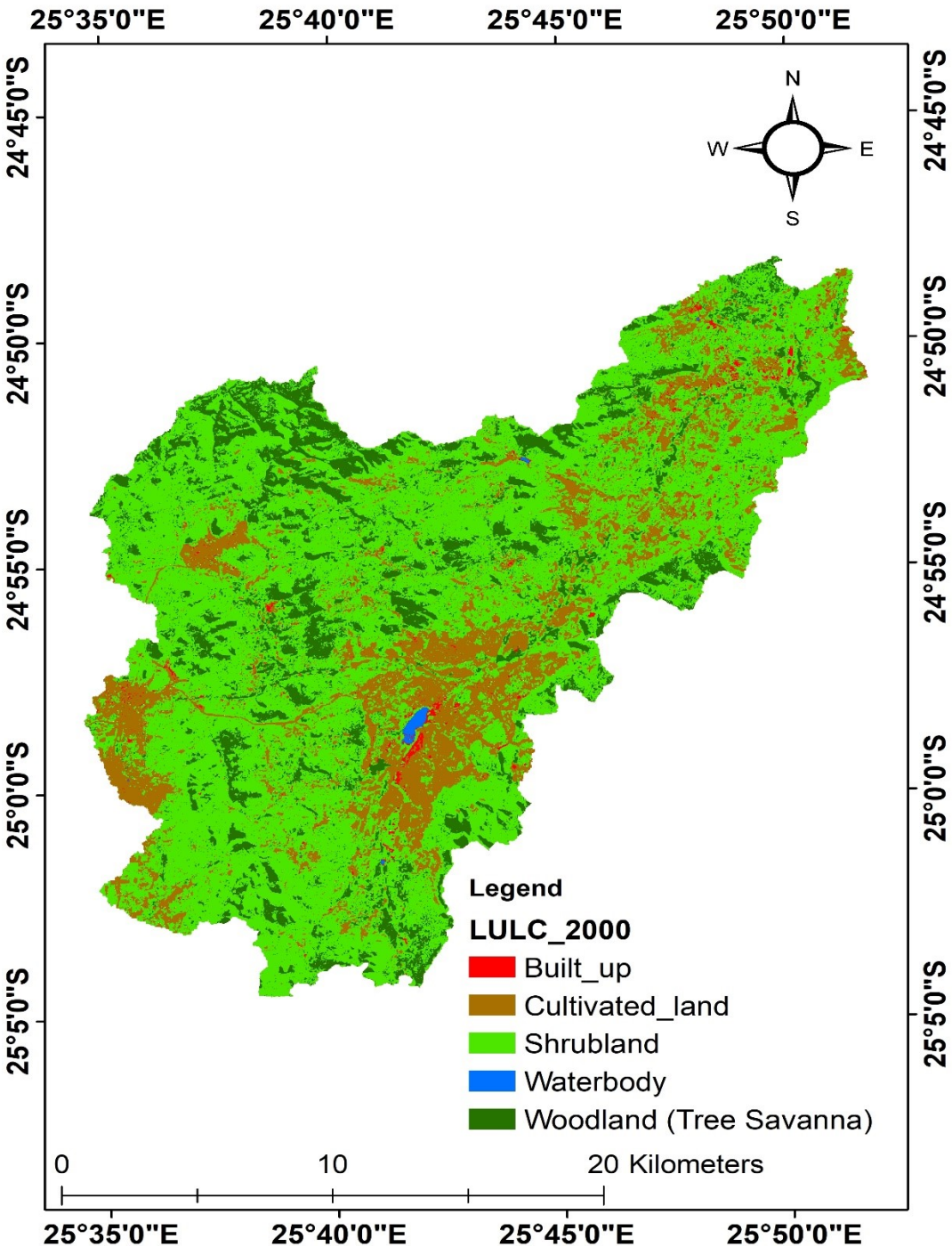

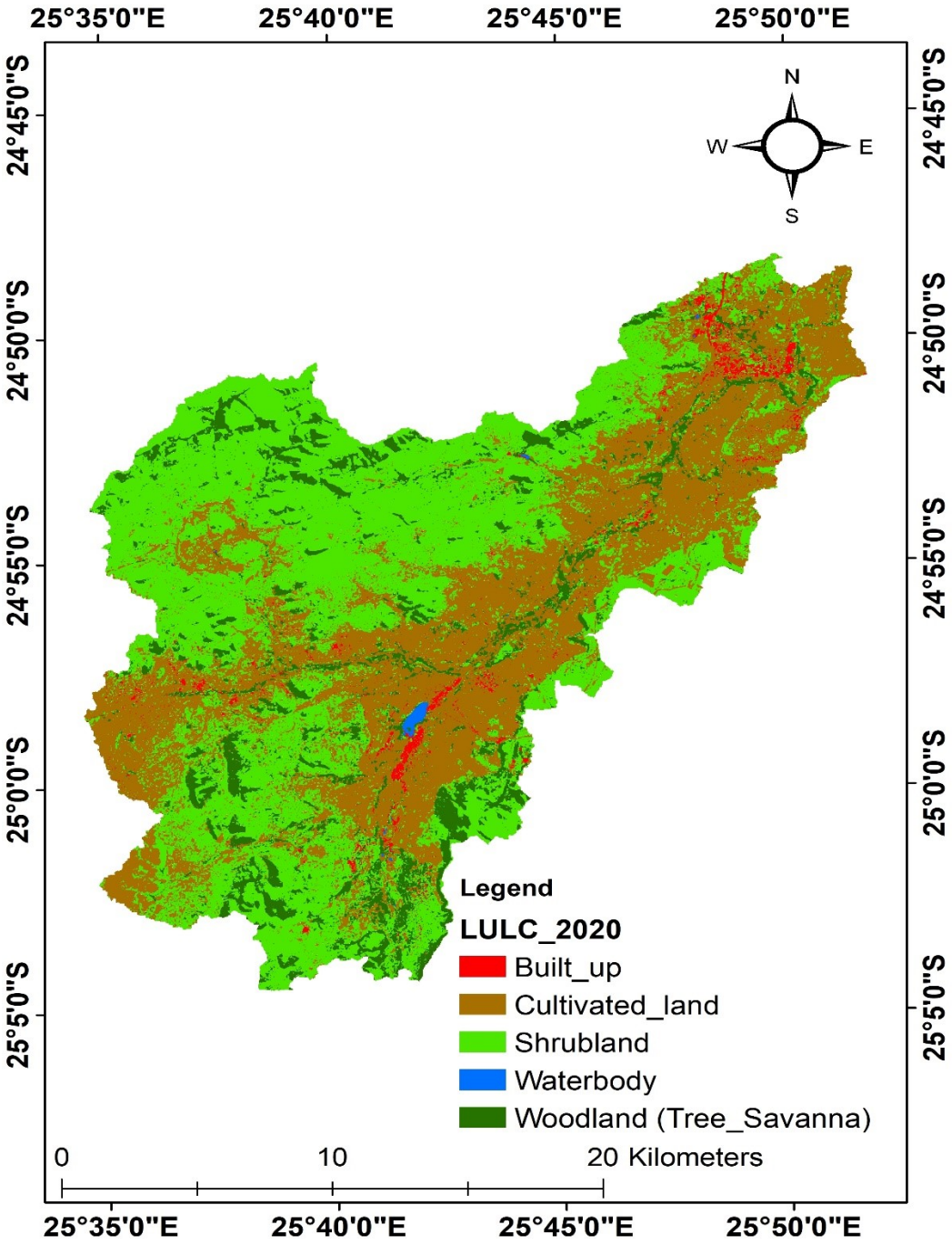
25°35'0"E
25°40'0"E
25°45'0"E
25°50'0"E
24°45'0"S
24°50'0"S
24°55'0"S
25°0'0"S
25°5'0"S
N
W
E
S
Legend
LULC_2020
Built_up
Cultivated_land
Shrubland
Waterbody
Woodland (Tree_Savanna)
0
10
20 Kilometers

Appendix 2: LULC Confusion Matrix

2000								
Land Use/Land Cover	Waterbody	Woodland (Tree Savanna)	Shrubland	Cultivated land	Built_up	Total	UA	Kappa
Waterbody	**9**	0	1	0	0	10	0.90	
Forest	0	**16**	6	1	0	23	0.70	
Shrubland	0	5	**62**	8	1	76	0.82	
Cultivated_Land	0	0	2	**28**	1	31	0.90	
Built_up	2	0	1	1	**6**	10	0.60	
Total	11	21	72	38	8	**150**	0.00	
PA	0.82	0.76	0.86	0.74	0.75	0.00	**0.81**	
Kappa								**0.71**

PA=Producer Accuracy, UA=User Accuracy

2020								
Land Use/Land Cover	Built_up	Waterbody	Woodland (Tree Savanna)	Shrubland	Cultivated land	Total	UA	Kappa
Built_up	**9**	0	0	0	1	10	0.90	
Waterbody	0	**10**	0	0	0	10	1.00	
Forest	0	0	**14**	1	0	15	0.93	
Shrubland	1	0	3	**64**	7	75	0.85	
Cultivated_land	0	0	0	6	**33**	40	0.83	
Total	10	10	17	71	41	**150**	0.00	
PA	0.90	1	0.82	0.90	0.80	0.00	**0.87**	
Kappa								**0.80**

Appendix 3: Soil erosion Confusion matrix

SLEMSA

Erosion status	No Erosion	Erosion	Total	UA	Kappa
No erosion	3	2	5	0.6	
Erosion	1	4	5	0.8	
Total	4	6	10		
PA	0.75	0.67		**0.7**	
Kappa					**0.4**

RUSLE

Erosion status	No Erosion	Erosion	Total	UA	Kappa
No erosion	3	1	4	0.75	
Erosion	0	6	6	1	
Total	3	7	10		
PA	1	0.86		**0.9**	
Kappa					**0.78**